University of Bath

UNIVERSITY OF BATH

PHD

An investigation into the design and performance of base station antenna diversity in digital mobile radio networks

Hollis, J. B.

Award date:
1994

Awarding institution:
University of Bath

[Link to publication](#)

An Investigation into the Design and
Performance of Base Station Antenna
Diversity in Digital Mobile Radio Networks.

Submitted by

J B Hollis

for the degree of Ph.D

of the University of Bath

1994

COPYRIGHT

UMI Number: U071161

UMI

Dissertation Publishing

UMI U071161

ProQuest

CONTENTS

ii

SUMMARY

An investigation has been undertaken to examine the viability of implementing base station antenna diversity in UHF digital mobile radio networks and to produce a means of predicting the benefits of its use. The cross correlation between signal envelopes received via base station antennas separated both vertically and horizontally have been both theoretically predicted and measured in the field.

It has been shown that with antennas spaced vertically rather than horizontally the signals become correlated more quickly as the mobile moves away from the base station. This has been verified by the field measurements and in certain situations it places a limitation on the usefulness of this form of diversity. Another constraint in the performance with antennas spaced vertically is that there is a trade off between the achievable envelope cross correlation and the branch strength. It has been shown that optimum antenna separations exist which are dependent on the effective base station antenna height "seen" by the mobile and the spread in arrival angle of the multi-path waves at the base station.

A computer simulation model of the narrow-band mobile data diversity channel is presented. This has been demonstrated to be a useful tool in examining the effects of different antenna position and spacing on the received data bit error rates. The results of simulation are shown to correspond well with field measurements of 8000 bits/ sec GMSK data transmission transmitted from a UHF mobile radio in an urban environment to a base station 2km away.

General conclusions are made to summarise the circumstances under which diversity gain can be achieved from the spatial separation of base

station antennas.

ACKNOWLEDGEMENT

Nomenclature

c_f	Correlation factor
d	Antenna separation
d'	Effective antenna separation
d_V	Vertical antenna separation
d_H	Horizontal antenna separation
D	Length of flat ground (Figure 2.9)
$E_Z(f)$	Power spectra of the z directional electric field component
$F(\ )$	Cumulative distribution
F_c	Carrier frequency
F_d	Maximum Doppler frequency
F_D	Peak deviation of FM signal
F_n	Doppler frequency
F_s	Shaddowing frequency
h	Elevation of base station with respect to the mobile.
H	Height difference between flat ground and mobile (Figure 2.9)
H_1, H_2	Base station antenna heights above ground level.
H'_1, H'_2	Effective base station antenna heights above ground level.
m	Mean value of sequence
n	Mean power of Gaussian noise level
N	Number of samples
N_r	Level crossing rate
N_s	Data sequence length
N_{sh}	Number of shaddowing components
ρ	Complex cross correlation
ρ_{env}	Cross correlation coefficient of two signal envelopes
$p(\ )$	Probability distribution
Pe	Probability of bit error
Pe_{IBER}	Probability of irreduceible bit error
q	Magnitude of the line of sight component
$r_0, r_1, r_2,$	Received signal levels
r_a	Area mean of r
r_j	Autocorrelation of sequence X(nT)
r_V	Effective distance of the scatterers from the mobile for multipath waves received in the vertical plane
r_H	Effective distance of the scatterers from the mobile for multipath waves received in the horizontal plane
R	Distance between mobile and base station
T_a	Time interval
T_i	Duration of the i th fade
v	Mobile speed
x	Mean value of X(i)
x_n	Mean power of signal r_n
$X(nT)$	Discrete signal sequence
y	Mean value of Y(i)
β	Random phase

α_H	Arrival angle of the multipath wave in the horizontal plane
α_v	Arrival angle of the multipath wave in the vertical plane
γ	Instantaneous signal to noise ratio
γ_0	Mean signal to noise ratio
λ	Carrier wavelength
θ_n	Angle of arrival between the direction of the n th wave and direction of vehicle motion.
σ_r	Standard deviation of r
ϕ	Sector of signal arrival angle at the base station.
ϕ_H	ϕ for horizontally spaced antennas
ϕ_V	ϕ for vertically spaced antennas

CHAPTER 1

Introduction.

The ability to access, manipulate and transfer digital information is an essential part of commercial, public service and industrial life in the developed world. Whilst normal access to data bases and the transfer of digital data is made directly or via a fixed digital link increasingly there is a requirement to provide such service to people in vehicles or elsewhere away from their normal place of work where access to a physical connection is not readily available. This requirement is met by the use of mobile data; the transmission by radio of digital information to and from devices that move. These devices could for example be data terminals in vehicles, hand-held terminals and lap top computers. Mobile data allows people to transmit and receive digital data where they find it most convenient.

In the past use of PMR and public cellular radio have been used to verbally request or provide information via another person with access to a data terminal in turn connected to a data base. Such procedures are clearly inefficient in the use of human resource, prone to misinterpretation, insecure and slow. The benefit of

providing direct access to remote data bases has been recognised for some time particularly by closed user groups usually operating over limited geographical areas. These have included emergency services and public utilities[1-5]. In addition to replacing routine speech traffic messages such as status reporting, data base interrogation and updating and mobilising information. The provision of mobile data allows the implementation of new services such as Automatic Vehicle Location[6-7] and fax transmission[8].

A significant advance to the implementation of mobile data has been brought about by the granting of licences for national public networks. Such licences now exist in the USA, Australia and several European countries. This provided the opportunity for companies to implement mobile radio systems utilising hardware and protocols designed specifically for data-only transmission. Until then many mobile data systems had to be implemented on what were analogue speech radio systems and the addition of data transmission necessarily involved restrictions and compromise in their design[9] . The installation of public mobile data networks over the last two years has allowed a cost-effective means of providing mobile data communications to a wide range of organisations and user groups without the large expenditure for the construction, operation and maintenance of their own network infra-

structures[10-11]. The more recent European national networks operate at UHF and use radio base stations networked via exchanges[12-15]. They operate with data transmission rates of between 8 and 9.6 Kbits/sec using Gaussian filtered Minimum Shift Keying (GMSK) or similar variants.

Propagation in UHF mobile radio systems is characterised by the fact that a line-of-sight signal seldom exists and received signals are a composite of scattered and reflected waves. The interactions of these waves at a moving vehicle causes rapid fading to be experienced. By reciprocity similar fading is experienced at the base station. When signals are modulated with data the effect is to generate bit errors in the received data[16-17].

The successful operation of public mobile data networks is dependent on them being able to control and transfer data packets reliably and to minimise the occurrence of corrupt information being presented to the user. Furthermore, competition between the network providers and the need to attract users, provides incentive to ensure that reliable data communication is available over a large an area as possible even in places where signals are weak.

Public mobile data networks use strategically placed radio base station to provide radio coverage. Base station transmitters are usually licensed to radiate

around 25 W effective radiated power (erp) and
subscriber equipment is normally limited to ten watts
erp. A growing part of the subscriber equipment market
is that of portable terminals where constraints on
physical size, antenna position, EMC and health and
safety issues necessarily constrain the radiated erps
to around one watt. This can create an imbalance in
link budget of typically 10 to 12 dB.

If the base station erp is not reduced then in some
geographic areas subscriber equipment may receive and
successfully decode signals from a base station but not
be able to communicate because its messages will not be
received and successfully decoded by the base station.
Special techniques are used to prevent the subscriber
trying to communicate in these circumstances[18]. This
effectively means that the radio coverage of a portable
subscriber is reduced compared with that of a mobile
subscriber. It was considered that diversity reception
implemented at the base station could be a means of
increasing the communication range of such subscribers.

This thesis reports on an investigation into the
viability of using base station antenna diversity in
UHF digital mobile radio networks. Diversity
reception[19-20] is an effective method of reducing the
influence of fading by utilising a number of
transmission paths with independent fades but carrying

the same information. By combining or selecting the signals received over the different paths (or branches) the probability of deep fades is reduced and the average fade duration is shortened hence reducing bit error rates associated with the channel and the minimum usable signal level of the base station.

In Chapter 2 the theoretical cross correlation of the envelopes of signals received via spatially separated antennas is presented. It is shown that the antenna spacing, the distance of the mobile transmitter from the base and the distance of the scatterers from the mobile will quite significantly affect the performance of base station diversity schemes.

The published literature on base station diversity is fairly limited but is reviewed in Chapter 3. This work has generally been with antennas spaced horizontally, vertically or a combination of the two with the purpose of determining the spacing requirements to yield de-correlated signals. Measurements have generally been restricted to 800/900 MHz and usually within a range of between one and five kilometres of the base station. Public mobile data systems operating at 450 MHz use larger radius cells typically six kilometres in cities. The larger wavelength also places more constraints on the achievable antenna spacing because for a given value of cross correlation the required spacing is inversely proportional to the wavelength. Horizontal spacing of antennas has received most interest and it

has been shown that the cross correlation is dependent on the incoming signal's azimuthal arrival angle. Vertical spacing of antennas offers the advantage of providing signal cross correlation that is independent of azimuthal arrival angle but generally greater spacing is required for a given value of cross correlation. Little attention has been paid to the fact that with vertical spacing the signal level in the lower branch will be reduced and this will reduce the benefits of the signal cross correlation.

Measurements of signal cross-correlation and relative strength have been made with a variety of different base station antenna configurations and with mobiles operating in different environmental locations. These results are presented, analysed and discussed in Chapter 4.

In order to assess the benefits of such strategies it is necessary to predict the behaviour of the radio channel including the diversity receiving system. The behaviour can be expressed in terms of mathematical expressions into which a range of different parameters can be inputted. From these expressions it is possible to predict the probability of bit errors. This approach is unsatisfactory for two reasons; firstly it will be shown that practical diversity systems are often non-ideal in that the branch (transmission path) signal strengths may be unequal and the individual branches

may be partially correlated. It becomes mathematically intractable to analyse this. Secondly mathematical analysis usually assumes the bit errors are randomly distributed; it is well understood that on mobile radio channels the probability of bit errors being generated is dependent on past channel behaviour and errors tend to occur in bursts[21].

Attempts have been made to model the generation of bit errors directly from a statistical model of the mobile radio channel in terms of its probability density function and average fade duration[22-23]. These techniques whilst providing more realistic bit error distributions produce pessimistic predictions of bit error probabilities.

An alternative method of providing bit error statistics involves recording bit-error patterns occurring during mobile radio data transmission and storing these patterns on computer discs for future analysis [21-22]. Such empirical models are derived from measurements and consequently all environmental influences are implicit in the result even if they cannot be separated or recognised. The validity of this modelling is limited only by the accuracy with which the initial measurements were made and by the extent to which the operational parameters represent the physical environment in which the model is applied. Such an approach provides realistic data for examining coding strategies but does not lend itself to analysis under

different operational parameters.

In order to predict the behaviour of the narrow band diversity radio channel a computer model has been developed and is presented in Chapter 5. Since the fading experienced on a mobile radio channel is inherently a random process it is well suited to computer simulation. The computer model is able to generate selectably correlated signals with the statistical properties of those experienced in the field. By simulating the bit errors that occur when data is transmitted over the simulated channel it has been possible to examine and quantify the benefits of implementing diversity reception in mobile data systems. This computer model has been termed the DMRCS – Data Mobile Radio Channel Simulator. Such simulation of the mobile radio channel is shown to offer several benefits compared with other methods of estimating the performance of digital mobile radio channels. The most obvious benefit from computer simulation is its flexibility. A host of input parameters can be varied and the resultant changes on channel behaviour can be readily determined without recourse to extensive field or bench measurements.

Field measurements were made to demonstrate the possible benefits of base station antenna diversity in improving the performance of mobile to base data transmission from areas of marginal radio coverage.

Both vertical and horizontally spaced base station antennas were used. The measurements were undertaken at UHF using 8Kbits/sec GMSK data modulation and the bit errors of the selectively combined signal were stored for subsequent analysis. Computer simulations of the received bit error distributions were undertaken with the DMRCS and these are compared with the measured results. Results presented in Chapter 6 show the predictions to correlate well with the results obtained from field measurements. Base station antenna diversity utilising physical separation of antennas is shown, in certain circumstances, to offer a useful enhancement to the performance of UHF digital mobile radio networks particularly at the fringes of radio coverage.

CHAPTER 2

The Mobile Radio Channel and the Application of Base
Station Antenna Diversity.

2.1 Multipath Fading.

In many mobile radio systems the received signal exhibits
fast fluctuations superimposed on relatively slow
variations of a local mean signal level. The rapid
fluctuations are due to multipath propagation caused by
reflections from and diffractions around buildings and
other structures in the vicinity of the mobile receiver.
These interfering signals produce a complex standing-
wave pattern of varying field strength, with maxima being
approximately a quarter wavelength apart. A mobile moving
through this standing wave pattern receives a signal with
random variations in amplitude and phase. In the absence
of a direct wave the envelope distribution of the
received signal has been shown to be mathematically
tractable in that it often approximates to the Rayleigh
probability distribution if it is first normalised to the
local mean signal averaged over a distance which is long
compared with the distance between fades but short
compared with the size of topographical features[24-27]. The

phase of the signal is uniformly distributed from 0 to 2π radians. The probability distribution of the received signal level r_o, having mean power x_o, is given by:-

$$p(r_0) = \frac{r_0}{x_0} e^{\frac{-r_0^2}{2x_0}} \qquad 2.1$$

From which the cumulative distribution $F(r_0)$ can be shown to be:-

$$F(r_0) = 1 - e^{\frac{-r_0^2}{2x_0}} \qquad 2.2$$

When the signal falls below its statistical mean a fade occurs and depending on its depth and duration, will cause bit errors in received data. Although significant departures from a Rayleigh distribution are not unusual, the departures have a smaller fading range. Because of the deleterious effect of rapid fading on the transmission of data, the more severe Rayleigh distributed model is generally used and will form the basis of propagation modelled for this work. The length of the fade is dependent on its defined depth and on the Doppler frequency. This latter figure discussed later being dependent on the vehicle speed and RF carrier

frequency. At higher speeds the fades occur more often but are of shorter average duration compared with those at lower speeds.

The depth and duration of the fades encountered in signals exhibiting a Rayleigh distribution are of interest because of the effect such fades have on the number and distribution of bit errors in the received signal. In such analysis a quantitative expression of the expected rate at which the envelope crosses a specified level r_L in the positive direction is of interest. If N_r is the level crossing rate (LCR) it can be shown to be given by[28-29]:-

$$N_r = \int_0^\infty \dot{r} \; p(r_L, \dot{r}) \, d\dot{r} \qquad\qquad 2.3$$

Where $\dot{r}$ is the time derivative of r, $p(r_L, \dot{r})$ is the joint probability function of r and $\dot{r}$ at $r=r_L$.

In a mobile radio environment the transmitted signals are usually vertically polarised and it is thus the electric field component of the electro-magnetic wave that is significant and for such it can be shown that the LCR is given by[30]:-

$$N_r = \sqrt{2\pi} F_d \, p e^{-p^2} \qquad\qquad 2.4$$

Where $p = r_L/r_{rms}$, r_{rms} = rms value of r and F_d = maximum Doppler frequency.

Having found the LCR the average fade duration can readily be calculated. If T_i is the duration of the i th fade then the probability that $r < r_L$ over a time interval T_a is given by:-

$$p(r \leq r_L) = \frac{1}{T_a} \sum T_i \qquad\qquad 2.5$$

Where the average fade duration is given by:-

$$\overline{T} = \frac{1}{T_a N_r} \sum T_i = \frac{1}{N_r} p(r \leq r_L) \qquad\qquad 2.6$$

and

$$p(r \leq r_L) = \int_0^{r_L} p(r) \, dr = 1 - e^{-p^2} \qquad\qquad 2.7$$

Therefore the average fade duration for the electric field component can be shown to be

13

$$\overline{T} = \frac{e^{p^2} - 1}{pF_d\sqrt{2\pi}} \qquad 2.8$$

Although as shown it is relatively easy to determine the average fade duration an analytical fade duration distribution appears mathematically intractable[31]. In order to ascertain the probability distribution of the fade (and interfade) durations, measurements have been made on recorded signals that exhibit Rayleigh fading[32-36]. In the computer simulation undertaken statistics of fade and interfade durations have been compiled and compared with both those measurements and the average fade duration as defined in equation 2.8.

Whenever the receiver or transmitter is in motion, each received scattered wave experiences a Doppler shift F_n given by:-

$$F_n = \frac{v\cos\theta_n}{\lambda} \qquad 2.9$$

Where v is the vehicle speed, λ is the carrier wavelength and θn is the angle between the direction of arrival of the n th wave and the direction of the vehicle motion.

14

The maximum Doppler shift experienced is clearly given by:-

$$F_d = \frac{V}{\lambda} \qquad 2.10$$

The power spectra of the z - directional electric field component for a uniform angular distribution of scattered signals can be shown to be given by:-

$$E_z(f) = \frac{1.5}{\pi F_d} (1 - (\frac{F - F_c}{F_d})^2)^{-\frac{1}{2}} \qquad 2.11$$

Where F_c is the carrier frequency.

2.2 Frequency selective fading.

An important consideration with multipath propagation is that the constituent waves of a transmitted signal will experience different propagation time delays. Typical values range from a fraction of a microsecond to many microseconds depending on the type of environment. The larger spreads occur in heavily built-up areas. Measurements made in New York City at 910 MHz have yielded excess delays of typically 2 us though values of

15

9 to 10 us were measured in some locations[37-39]. Bajwa and Parsons have reported similar measurements in the city of Birmingham[40-41]. If the spread of time delays is of similar order of magnitude to that of the symbol period then intersymbol interference can result. Reported values of time delay spread are of no significance at the data transmission rates used in this work and are not considered further.

The existence of the different time delays in the various waves causes the statistical properties of two signals of different frequencies to become independent at sufficient frequency separation. The coherence (or correlation) bandwidth is the range of frequencies that fade together or with high correlation. Correlation bandwidths have been reported in New York City to be greater than 55 KHz and 20 KHz for correlation coefficients of 0.5 and 0.9 respectively[42]. Correlation bandwidths of 250 KHz have been reported in suburban environments. It can generally be expected that the correlation bandwidth is greater than the data transmission bandwidth used in this work and will therefore not be considered further.

2.3 Log-normal fading

The multipath fading experienced in land mobile radio and discussed in section 2.1 is usually superimposed on relatively slow variations of the local mean level. This local mean, measured every few tens of wavelength and expressed logarithmically is usually found to be normally distributed[44-49] having a power distribution function given by:-

$$p(f) = \frac{1}{\sigma_r \sqrt{2\pi}} e^{\frac{-(f-r_a)^2}{2\sigma_r^2}} \qquad 2.12$$

where $r' = 20\log_{10}r$, σ_r is the standard deviation of the local mean r and r_a is the area mean. From which the cumulative distribution of r' can be shown to be:-

$$F(f) = \frac{1}{2} + \frac{1}{2} erf \left(\frac{f-r_a}{\sqrt{2}\sigma_r} \right) \qquad 2.13$$

where the error function $erf(x)$ is defined as:-

$$erf(x) = \frac{2}{\sqrt{\pi}} \int_0^x e^{-z^2} dz \qquad 2.14$$

The standard deviation of the local mean has been shown to be independent of range and base station elevation but dependent on transmission frequency, degree of local clutter and the size of the area considered as "local".

17

The standard deviation is higher for increased transmission frequency, proportion of high buildings and size of local area.

2.4 Ricean fading.

In some mobile radio situations, particularly in open areas or near the base station, the received signal comprises a significant line-of-sight signal in addition to the scattered signal. The presence of this line of site component effectively reduces the fading range of the signal. The resultant envelope fading statistics are those of a sine wave plus additive Gaussian noise and have been analysed by Rice[29]. He showed that the probability distribution of the signal is given by:-

$$p(r) = \frac{r}{x_0} e^{\frac{-r^2+q^2}{2x_0}} Io(\frac{rq}{x_0}) \qquad 2.15$$

where q is the magnitude of the line-of sight component and Io is the Bessel function of the first kind defined as:-

$$Io(z) = \frac{1}{2\pi} \int_0^{2\pi} e^{z\cos\theta} d\theta \qquad 2.16$$

Clearly when q=0 the Ricean distribution reduces to that for a Rayleigh signal given in equation 2.1.

2.5 Diversity

Diversity reception is an effective method of reducing the influence of fading by utilising a number of transmission paths with independent fades but carrying the same information. By combining or selecting the signals received over these different paths (or branches) the probability of deep fades is reduced. Practical diversity systems for mobile radio generally employ only two branches. It can readily be shown that as the number of branches increases the incremental improvement decreases and the system becomes more complex. Various diversity schemes have been described in the literature including space, frequency, time and polarisation[19-20]. Space diversity utilises receiving antennas separated in space such that signals are received over paths with independent fading characteristics. Frequency diversity requires the simultaneous transmission of identical data on two or more frequencies sufficiently separated so that the fading is uncorrelated. This form of diversity is not suitable for mobile radio because of its inefficient

utilisation of the frequency and the requirement for additional mobile radio transmitters. Time diversity requires that data is transmitted several times. If the data packets are separated sufficiently in time the fading associated with the individual packets will be uncorrelated. A majority voting can be made on the stored data packets to reduce the bit error rates. Whilst time diversity offers the benefit of requiring only one antenna and radio receiver it does so at the expense of reducing the information throughput because of the need to transmit identical information several times. Polarisation diversity requires the simultaneous transmission of both horizontally and vertically polarised waves which are found to remain relatively independent over scattering paths. Reception of both polarisations by separate antennas can therefore yield a useful diversity gain.

Although diversity reception can be implemented at the mobile[50-52] or base station[53-57] it is clearly more economical at the latter. Furthermore the need for diversity reception is usually greater at the base station due to the lower ERP's of the mobiles compared with those of the base station. The field measurements and computer simulations to be described later are with base station diversity using spatially separated antennas.

A review of published literature on base station antenna diversity is provided in Chapter 3.

2.6 Base Station Diversity with Spaced Antennas.

Consider the transmission from a moving vehicle a distance R from the base station receiver. Assuming no significant line of sight component exists and the waves received at the base station come from scatterers surrounding the mobile. The sector of arrival angles ϕ at the base station will be as shown in Figures 2.1 and 2.2 for vertical and horizontal separation of antennas respectively.

For vertical separation of antennas it is clear that:-

$$\phi_v = \theta_2 - \theta_1$$

$$\tan(\theta_2) = \frac{R + r_v}{h}$$

$$\tan(\theta_1) = \frac{R - r_v}{h}$$

and $h = R \tan\alpha_v$ 2.17

where   R= the distance between the mobile and base station.

r_v= the effective distance of the scatterers from the mobile for multipath waves received in the vertical plane.

21

h=the elevation of the base station with respect to the mobile.

α_v=arrival angle of the multipath wave in the vertical plane.

ϕ_v= the spread of arrival angle at the base station.

θ_2 and θ_1 are the angles shown in Figure 2.1

Using the identity

$$\tan(\phi) = \frac{\tan\theta_2 - \tan\theta_1}{1 + \tan\theta_2 \tan\theta_1} \qquad 2.18$$

it follows that

$$\tan(\phi_v) = \frac{2r_v \, h \, \tan\alpha_v}{R^2 \tan^2\alpha_v + (R^2 - r_v^2)} \qquad 2.19$$

now ϕ_v *is very small therefore* $\phi_v \sim \tan\phi_v$

also $R^2 > h^2 - r^2$

therefore

22

$$\phi_V \sim \frac{2r_V R \tan\alpha_V}{R^2(1+\tan^2\alpha_V)} \qquad 2.20$$

$$\phi_V = \frac{2r_V \sin(\alpha_V)\cos(\alpha_V)}{R} \qquad 2.21$$

For horizontal separation of antennas it is clear from Figure 2.2 that:-

$$\tan\left(\frac{\phi_H}{2}\right) = \frac{r_H}{R} \qquad 2.22$$

where r_H = the effective distance of scatterers from the mobile for multi-path waves received in the horizontal plane.

because $R > r_H$ then $\phi_H \sim \tan\phi_H$

$$\phi_H = \frac{2r_H}{R} \qquad 2.23$$

The complex cross-correlation between two signals received via spatially separated antennas can be shown to be given by:-

$$\rho = \left| \int_{-\pi}^{\pi} e^{-j2\pi d \sin(\alpha_i - \alpha)} p(\alpha_i) \, d\alpha_i \right| \qquad 2.24$$

where α_i = arrival angle of the i th multipath wave.

$\alpha = \alpha_H$ for horizontal spacing and α_V for vertical spacing.

d'= effective antenna spacing measured in wavelengths,= d_H sin α_H for horizontal spacing and d_V cos α_V for vertical separation.

d_H =horizontal spacing.

d_V =vertical spacing.

If it is assumed that α_i is normally distributed then:-

$$p(\alpha_i) = \frac{1}{\sigma_a \sqrt{2\pi}} e^{\left(\frac{-(\alpha_i - \alpha)^2}{2\sigma_a^2} \right)} \qquad 2.25$$

Where the standard deviation σ_a of arrival angle $\approx \phi/2$. $P(\alpha_i)$ is illustrated in Figure 2.3.

Numerical integration has been undertaken to evaluate this equation. A look up table being used to convert the

24

squared magnitude of the complex cross-correlation (p^2) to envelope cross-correlation (p_{env}). The computed results for vertical separation are shown in Figure 2.4 and for horizontal separation in Figure 2.5 to 2.6 for a range of values of ϕ_V and ϕ_H.

Since ($\alpha_1-\alpha$) is small $\sin(\alpha_1-\alpha) \approx (\alpha_1-\alpha)$ also $p^2 \approx p_{env}$ therefore:-

$$p_{env} \sim e^{-(\pi \dot{\alpha} \phi)^2} \qquad 2.26$$

using 2.21 and 2.23 we get:-

$$p_{env} \sim e^{-(\frac{2\pi d_V \sin\alpha_V \cos\alpha_V}{R})^2} \qquad 2.27$$

for vertical separation
and

$$p_{env} \sim e^{-(\frac{2\pi d_H r_H \sin\alpha_H}{R})^2} \qquad 2.28$$

for horizontal separation.

It is clear for a given antenna separation and base to mobile range that the received signals will be less

25

correlated if scatterers are in close proximity (e.g. urban environment) rather than in longer proximity (e.g. rural environment). Also for a given type of antenna separation and mobile environment the signal cross correlation will increase with increasing base to mobile range. With horizontal separation of antennas, equation 2.28 indicates that the cross correlation is dependent on the orientation α_H of the mobile with respect to the base station antennas. The cross correlation being minimum for the broadside case and equal to unity for the in-line case. No such limitation exists with the antennas spaced vertically; however the degree of correlation increases more rapidly as the mobile moves away from the base because of the resultant reduction in arrival angle in the vertical plane.

2.7 Signal selection and combining.

Having obtained two or more signals with uncorrelated or partially correlated envelopes a means of either combining or selecting the signal is required[58-59]. Combining can take place prior to demodulation - this yields higher SNR's compared to that obtained with post detection combining[60] but at the expense of requiring the signals to be co-phased.

If a signal with the Rayleigh probability density function given in 2.1 is received in the presence of Gaussian noise of mean power=n, then it follows that the instantaneous SNR is given by:-

$$\gamma = \frac{r^2}{2n} \qquad\qquad 2.29$$

and the mean SNR is given by:-

$$\gamma_o = \frac{\gamma^2}{n} \qquad\qquad 2.30$$

If the noise power is constant then it can readily be shown that the PDF of the SNR is given by:-

$$P(\gamma) = \frac{1}{\gamma_o} \, e^{-\frac{\gamma}{\gamma_o}} \qquad\qquad 2.31$$

Kahn[61] proposed what is now referred to as maximal ratio combining whereby the signals are co-phased weighted in proportion to their SNR and then summed. The output of the maximal ratio combiner has a SNR of:-

$$\gamma_r = \sum_{i=1}^{m} \gamma_i = \frac{1}{2n} \sum_{i=1}^{m} r_i^2 \qquad 2.32$$

where m is the number of branches.

It can be shown that assuming the noise voltage contribution from the various branches are uncorrelated, the best possible output SNR is obtained by such additive combining. When the noise sources are correlated (for example with ignition interference) the correlated noise appears as signal and the performance of the combiner is degraded. In order to avoid the inherent complexities of providing variable weighting capabilities equal gain combining has been reported where no weighting is applied to the individual branches[62-63]. The output of an equal gain combiner is given by:-

$$\gamma_r = \frac{1}{m} \left(\sum_{i=1}^{n} \sqrt{\gamma_i} \right)^2 = \frac{1}{2mn} \left(\sum_{i=1}^{m} r_i \right)^2 \qquad 2.33$$

The major limitation of these combining techniques is that the signals need to be added in phase, in pre-detection combining schemes necessitating the use of specialised circuitry[64-65]. Other forms of combining are based on switching between branches[66-68]. In selection

28

combining the branches are scanned and the one with the highest SNR is selected. Other forms of switched combining operate such that if the signal on one branch falls below some predetermined threshold level, another branch is selected if this is above the threshold then switching ceases otherwise the switching is continued until a signal above the threshold is found[69-70]. The possible rapid switching that can arise if all branches are below a threshold is avoided in switch-and-stay where if, for example in a two branch system, branch 1 is initially selected and then falls below the threshold then branch 2 will be switched in. If this too is below the threshold the combiner will stay on the second branch until branch 1 is above the threshold.

2.8 Performance of diversity schemes

The effectiveness of diversity can be assessed in different ways. In mobile radio it is the increase in the reliability brought about by reducing the depth and duration of fading. The analysis of diversity combining schemes is often premised on either or both the assumptions of independence between the fading on the individual branches and equal mean signal levels on those branches. The measurements of branch cross correlation

and signal strength for base station antenna diversity schemes, presented in Chapter 4 show that neither premise is necessarily justified. It becomes increasingly difficult to mathematically determine the probability distribution (and hence the LCR and average fade duration) of a combined signal when the branches are both partially correlated and of unequal mean signal level. The probability distribution of a selection diversity scheme is presented below.

Consider two signals r_1 and r_2 with a Rayleigh distribution given by:-

$$p(r_n) = \frac{r_n}{x_n} e^{\frac{-r_n^2}{2x_n}} \qquad 2.34$$

Where r_n and x_n are the amplitude and mean power of the nth signal.

The amplitude of the signals are composed of two normally distributed quadrature variables y_n and z_n each of the form:-

$$p(y_n) = \frac{1}{\sqrt{2\pi x_n}} \; e^{\frac{-y_n^2}{2x_n}} \qquad 2.35$$

If the two signals r_1 and r_2 have components y_1, z_1 and y_2, z_2 respectively then the individual quadrature components are correlated as follows:-

$$y_2 = py_1 + c_1 \qquad z_2 = pz_1 + c_2 \qquad 2.36$$

Where p is the complex cross-covariance and c_1 and c_2 are the uncorrelated portions of y_2 and z_2 respectively.

It has been shown that the correlation coefficient, p_{env}, of r_1 and r_2 is related to the complex cross covariance as follows[71]:-

$$p_{env} = \frac{\pi}{4(4-\pi)} \left(p^2 + \frac{p^4}{16} + \frac{p^6}{64} + \dots \right) \qquad 2.37$$

This relationship has been tabulated by Pierce[72].

Rice[28] has shown that the joint distribution of two correlated complex Gaussian processes are a Rayleigh variate with a joint distribution given by:-

31

$$p(r_1, r_2) = \frac{r_1 r_2}{x_1 x_2} \, I_0 \left(\frac{p r_1 r_2}{(1-p^2)\sqrt{x_1 x_2}} \right) \, e^{-\frac{1}{2(1-p^2)}\left(\frac{r_1^2}{x_1}+\frac{r_2^2}{x_2}\right)} \qquad 2.38$$

For selection diversity the probability of the selected signal, r, is above some value, r_t, is given by:-

$$Prob(r > r_t) = Prob(r_1 > r_t, \ r_2 > r_t)$$
$$= Prob(r_1 > r_t) + Prob(r_2 > r_t) - Prob(r_1 > r_t, \ r_2 > r_t) \qquad 2.39$$

From which it can be deduced that:-

$$Prob(r > r_t) = e^{\frac{-r_t^2}{2x_1}} Q(a, pb) + e^{\frac{-r_t^2}{2x_2}} (1 - Q(ap, b)) \qquad 2.40$$

where

$$a = \sqrt{\frac{r_t^2}{x_2(1-p^2)}} \qquad b = \sqrt{\frac{r_t^2}{x_1(1-p^2)}} \qquad 2.41$$

and Q(c,g) is Marcum's Q function defined as

$$Q(c,g) = \int_c^\infty e^{-\frac{g^2+x^2}{2}} Io(gx) x \, dx \qquad 2.42$$

and Io( ) is the Bessel function of the first kind defined
in 2.16

Equation 2.40 has been evaluated using numerical
integration techniques to yield values of CDF at
different correlation co-efficients and mean signal
ratios. Figures 2.7 and 2.8 show the probabilities of the
instantaneous combined signal being greater than (mean
signal-20dB) and (mean signal-40dB) respectively. In the
design of some base station antenna diversity systems
there is often a trade-off to be made between the
correlation of the two branches and their respective mean
signal levels.

It has been shown elsewhere[70] that the performance of
selection combiners is only slightly inferior to
equal-gain and maximal ratio combiners and is slightly
better than switch-and-stay and switch-and-examine
combiners. It is therefore considered that since the
generalised probability distribution of these combiner
outputs are mathematically intractable or unwieldy
equation 2.40 for selection diversity provides a useful
approximation for other combiners.

2.9   Height-gain   characteristics   in   mobile   radio   propagation.

It is well known that a base station antenna height gain of 6dB per octave has been predicted for propagation over flat ground[73].

$$g_H = 20 \log H_1 \qquad 2.43$$

Where g_H = antenna height gain

H_1 is the antenna height above ground level.

Clearly doubling the base station antenna height doubles the signal received at the mobile.

Measurements in flat suburban and urban environments have supported this[74]. Where the terrain between the base station and the mobile is not flat 2.43 is no longer valid and a revised height-gain figure is given by:-

$$g_H = 20 \log \acute{H}_1 \qquad 2.44$$

Where H'_1 is the effective base station antenna height determined by the terrain contour between the base and

mobile; it will therefore change in value as the mobile moves.

Lee[75] has investigated the effective base antenna height over *non obstructive direct paths* (i.e. where the path is unobstructed by the terrain contour). He considered the two general terrain profiles shown in Figure 2.9 with the base station antenna being either above (i) or below (ii) the mobile. In these situations the effective base station antenna heights approximate to:-

$$i) \; \acute{H_1} = H_1 + \frac{DH}{R-D} \qquad ii) \; \acute{H_1} = H_1 + H \qquad 2.45$$

Where R is the distance between base and mobile antennas and the other symbols are as shown in Figure 2.9.

The determination of effective base antenna height in the obstructive path is more complex because the propagation paths cannot be so clearly described. Okumura[73] calculated the effective base station antenna height as the average height of the base antenna above ground level calculated over the range 3 to 15 Km (or the range of the mobile from the base if less) in a direction towards the mobile as illustrated in Figure 2.10. Other expressions of effective base station antenna height have been presented[76].

If we consider a vertical spaced antenna diversity scheme with the top antenna at a height H_1 and a second antenna lower down at a height H_2 then the signal received via the second antenna relative to that received by the upper antenna is given by:-

$$\bar{r}_1 - \bar{r}_2 = 20\log\frac{H_2'}{H_1'} \qquad 2.46$$

Where H_1' and H_2' are the effective height of the upper and lower antennas.

Since the difference between two actual antenna heights is the same as the difference between the corresponding effective antenna heights then 2.46 is given by:-

$$\bar{r}_1 - \bar{r}_2 = 20\log(1 - \frac{d_v}{H_1'}) \qquad 2.47$$

Where d_v is the antenna separation ($=H_1 - H_2$)

If antenna 1 is fixed at the highest allowable position on the mast and antenna 2 is located below it then it is

clear that increasing the separation reduces the
correlation of the two received signals but at the
expense of reducing the signal strength in the lower
branch. Clearly there is a trade-off in the achievable
performance.

Using equations 2.40 and 2.43 the probability that a
combined signal exceeds specific values has been computed.
These calculations have been undertaken for a range of
upper effective antenna heights between 40 and 100
wavelengths above ground. For each set of calculations the
signal strength in the upper antenna is normalised to 0dB.
The computation has been undertaken with the assumption
that the signal strength received in the lower branch
reduces by 6dB per octave of effective antenna height.

The results are shown in Figures 2.11 to 2.20 for a
selection of values of ϕ_v typical of those likely to be
encountered in UHF mobile radio systems.

Figure 2.21 provides a summary of optimum antenna
separation for different values of ϕ_v and upper antenna
position. The results show that the optimum antenna
separation increases with the height of the uppermost
antenna and with decreasing ϕ_v .
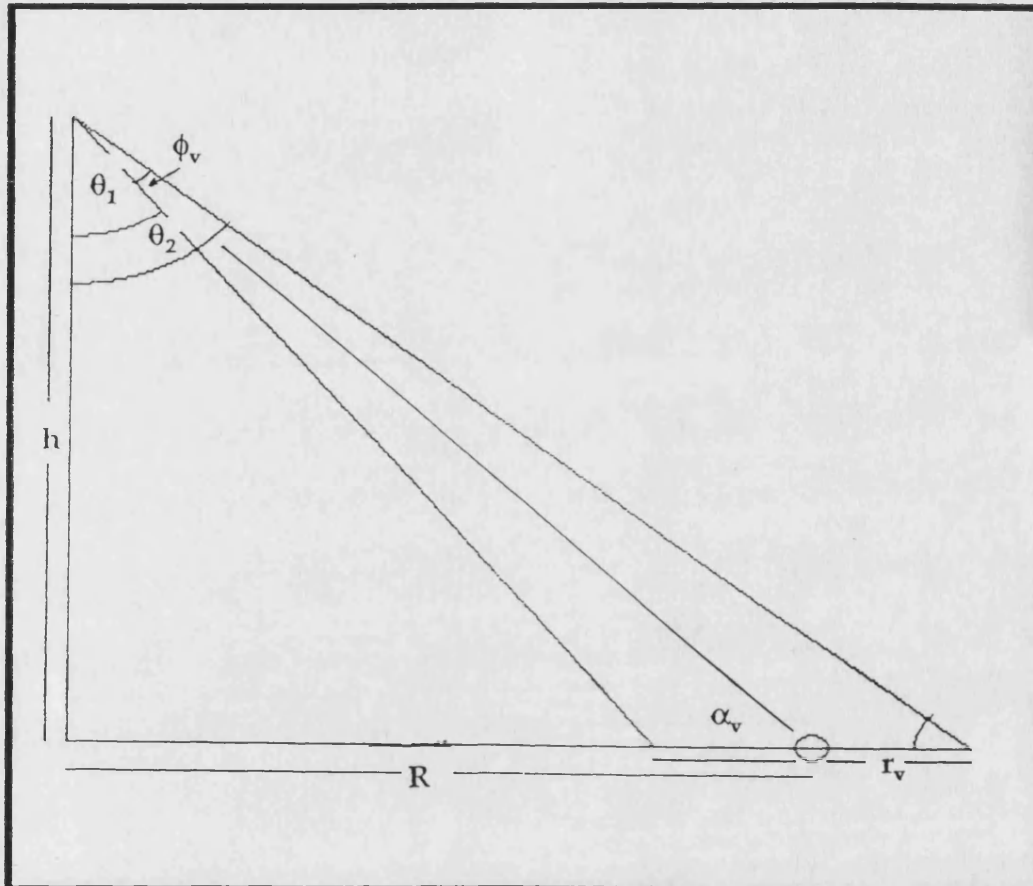
Figure 2.1   Spread of arrival angles ϕ_v at the base station for vertically spaced antennas.
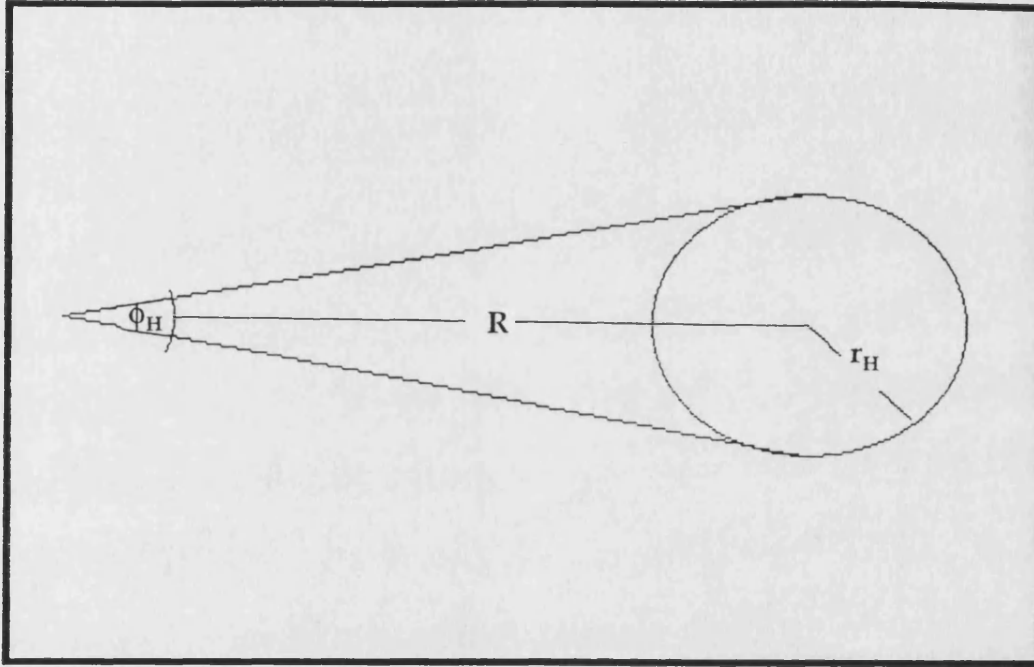
38

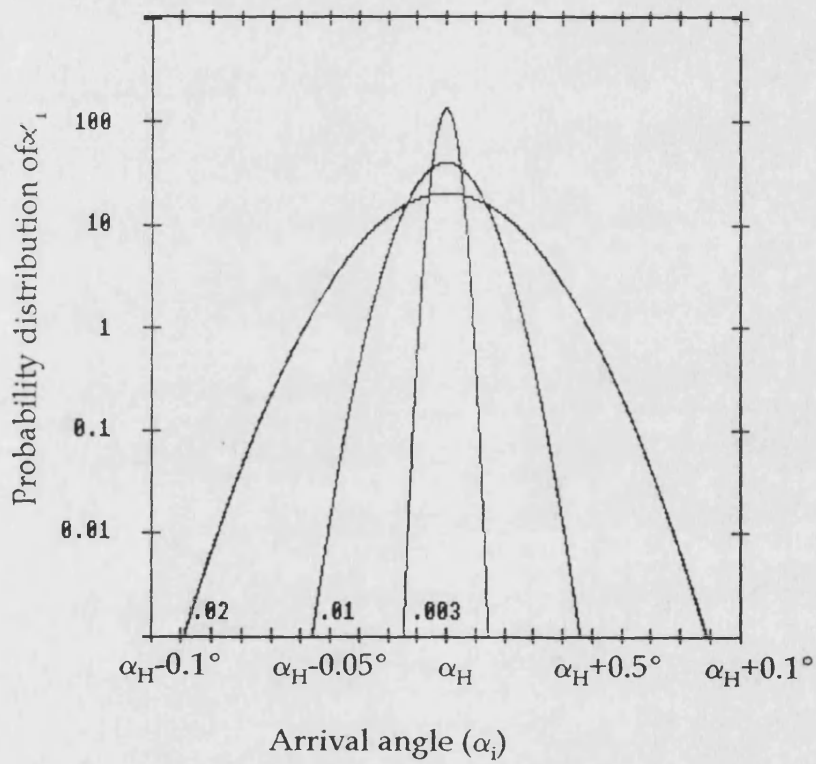Figure 2.2 Spread of arrival angles ϕ_H at the base station for horizontally spaced antennas.

39

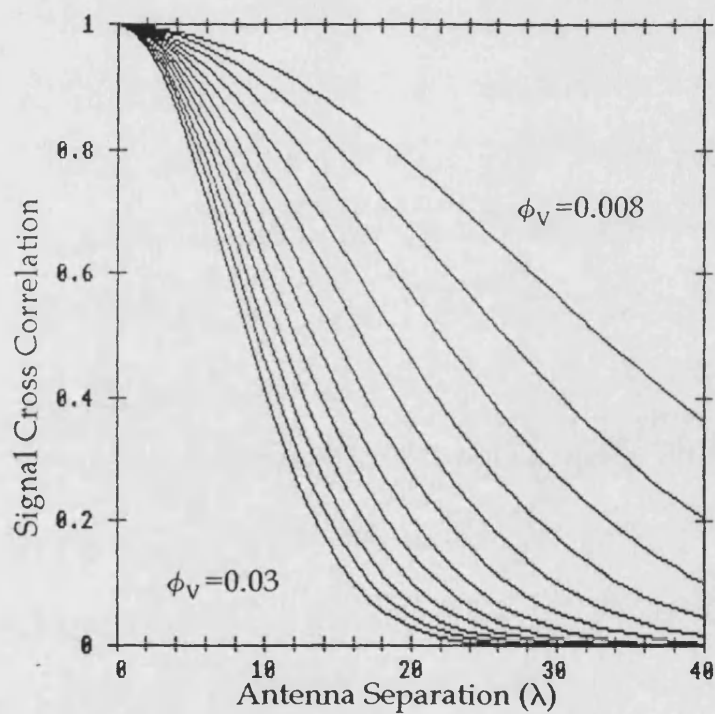Figure 2.3   Probability distribution of α_i based on a normal distribution for different values of σ.

Figure 2.4   Curves showing the relationship between
vertical antenna separation and signal correlation for
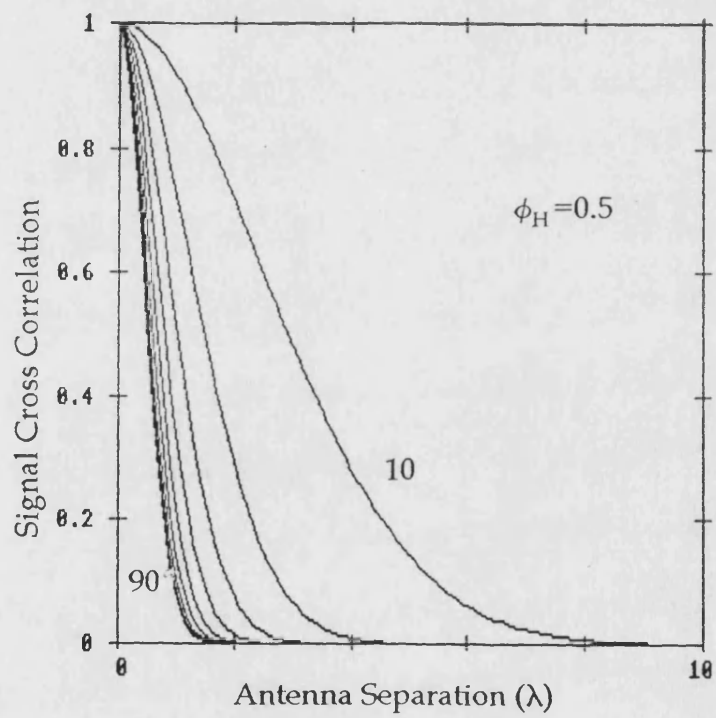values of ϕ_v from .008 to .03 radian in steps of .002.

41

Figure 2.5 Curves showing the relationship between horizontal antenna separation and signal correlation for value of ϕ_H = 0.5 radian.
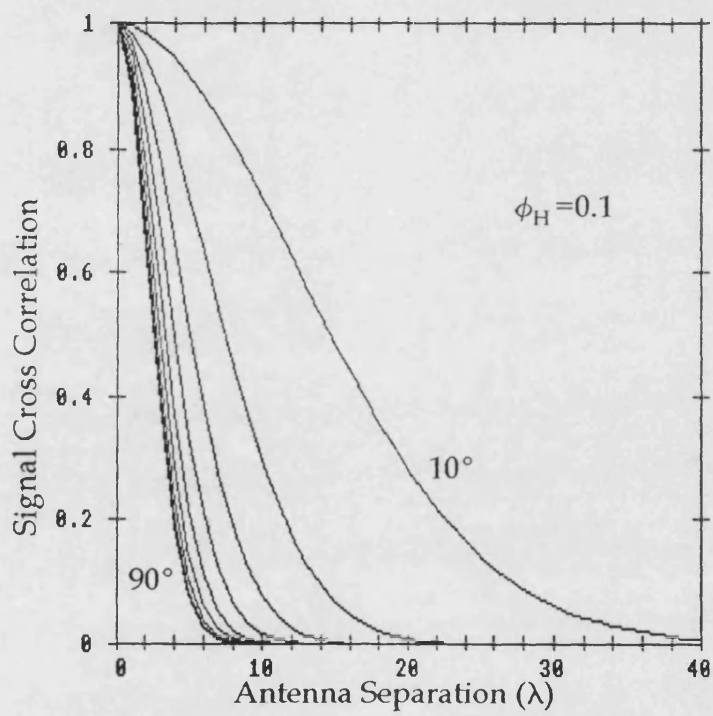
42

Figure 2.6   Curves showing the relationship between horizontal antenna separation and signal correlation for value of ϕ_H =0.1 radian.
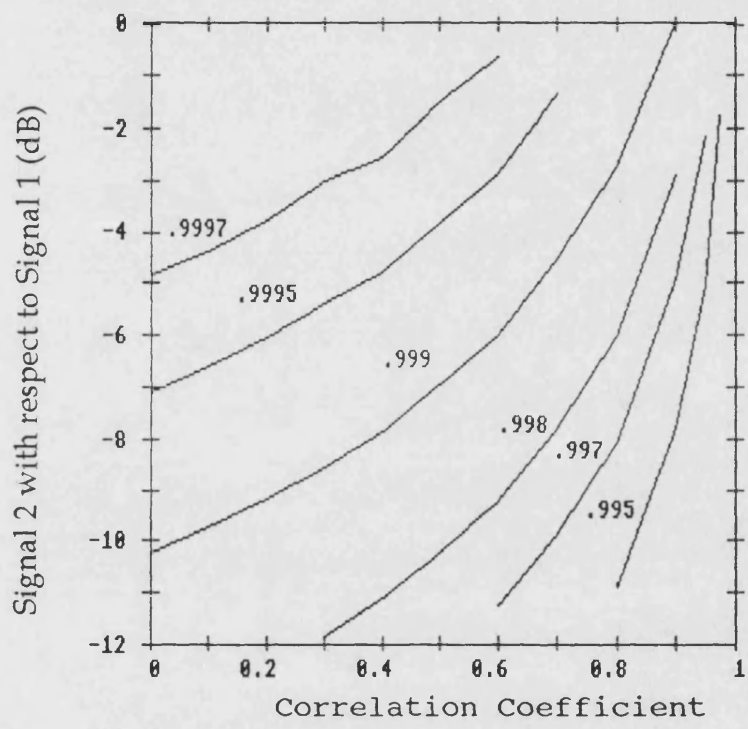
43

Figure 2.7   Probability of the instantaneous selected
diversity signal being greater than (mean-20dB) for
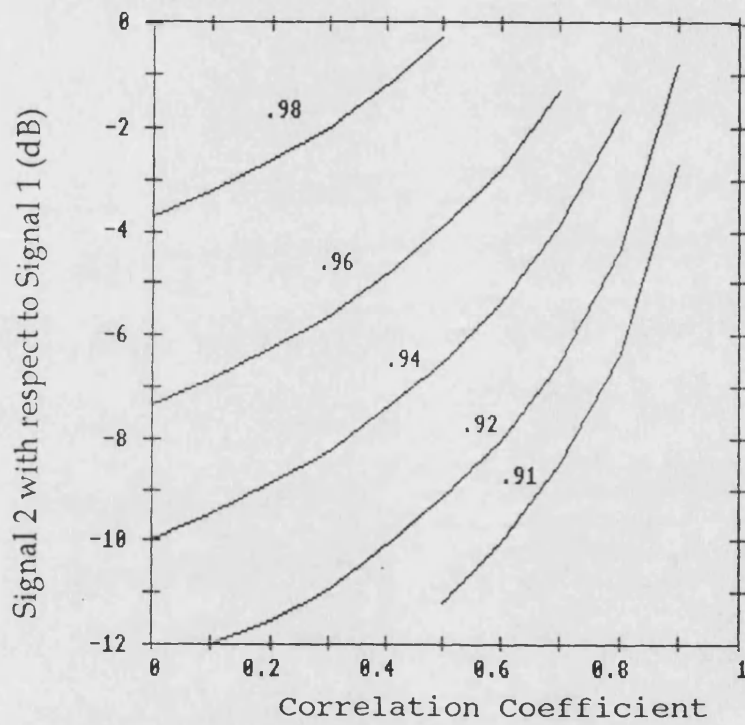different signal correlations and relative strengths.

Figure 2.8   Probability of the instantaneous selected
diversity signal being greater than (mean-10dB) for
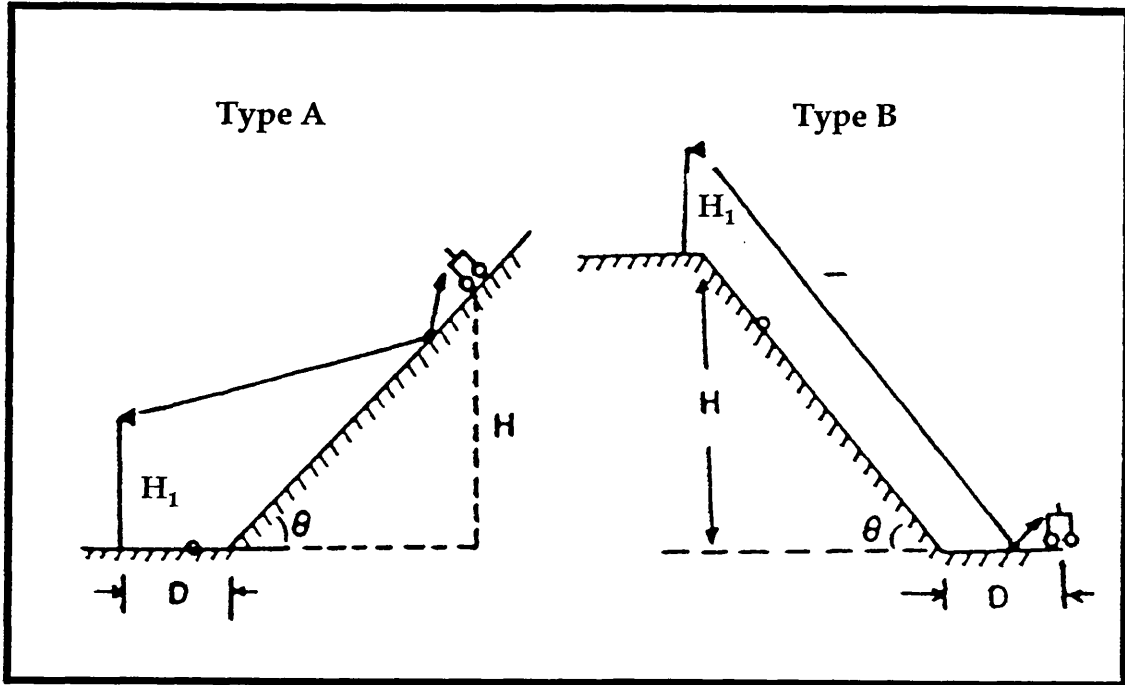different signal correlations and relative strengths.

Figure 2.9 Estimate of effective base station antenna height for a non obstructive path with the mobile antenna being on

Type A:- a slope higher than the base station.

Type B:- flat ground lower than the base station
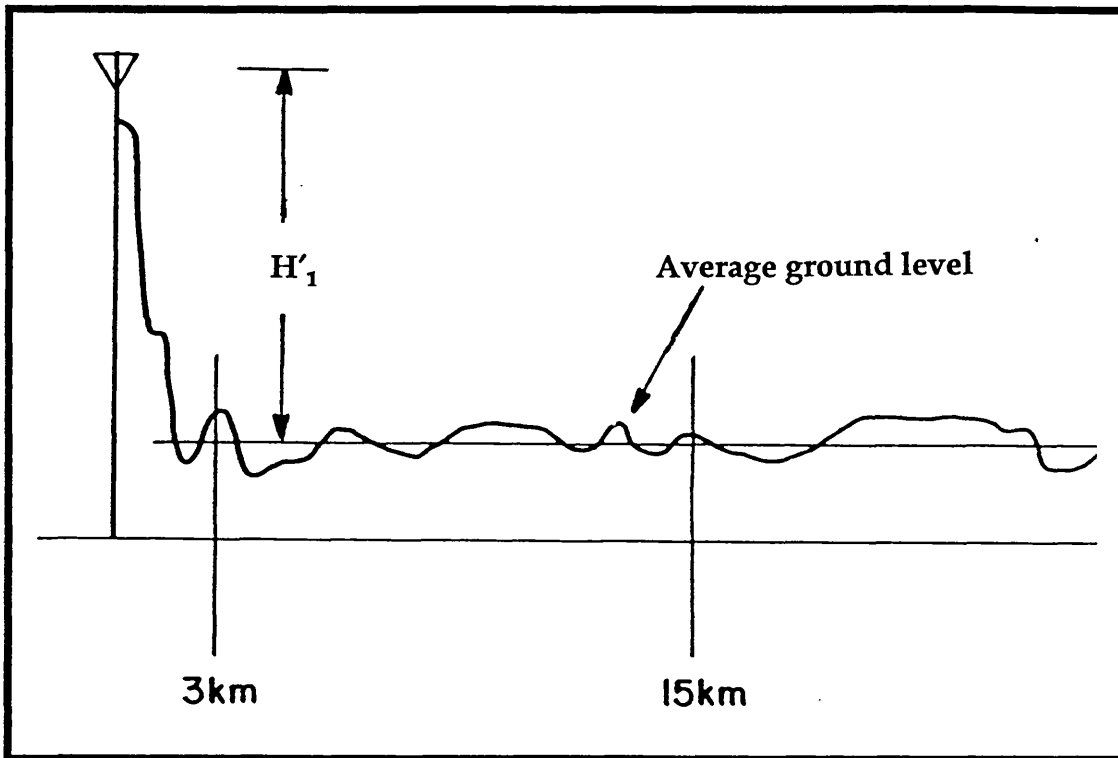
46

Figure 2.10   Estimate of effective base station antenna
height for an obstructive path.

Figure 2.11 Probability of the instantaneous selected diversity signal being greater than (mean-20dB) for different antenna positions and with spread of arrival angle (ϕ_v)=.04 radian.

Figure 2.12 Probability of the instantaneous selected diversity signal being greater than (mean-20dB) for different antenna positions and with spread of arrival angle (ϕ_v)=.02 radian.
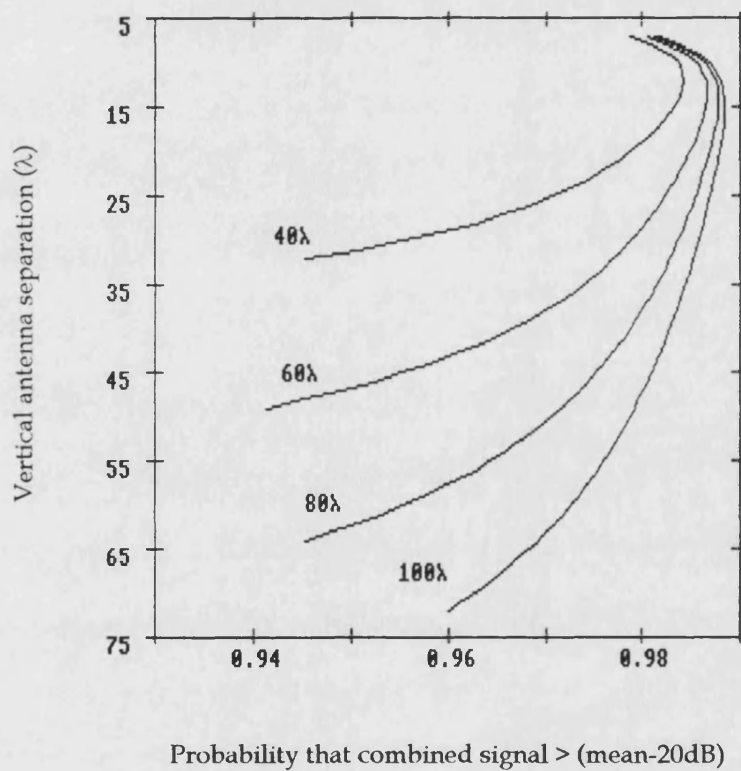
Figure 2.13 Probability of the instantaneous selected diversity signal being greater than (mean-20dB) for different antenna positions and with spread of arrival angle (ϕ_v)=.014 radian.

50

Figure 2.14   Probability of the instantaneous selected
diversity signal being greater than (mean-20dB) for
different antenna positions and with spread of arrival
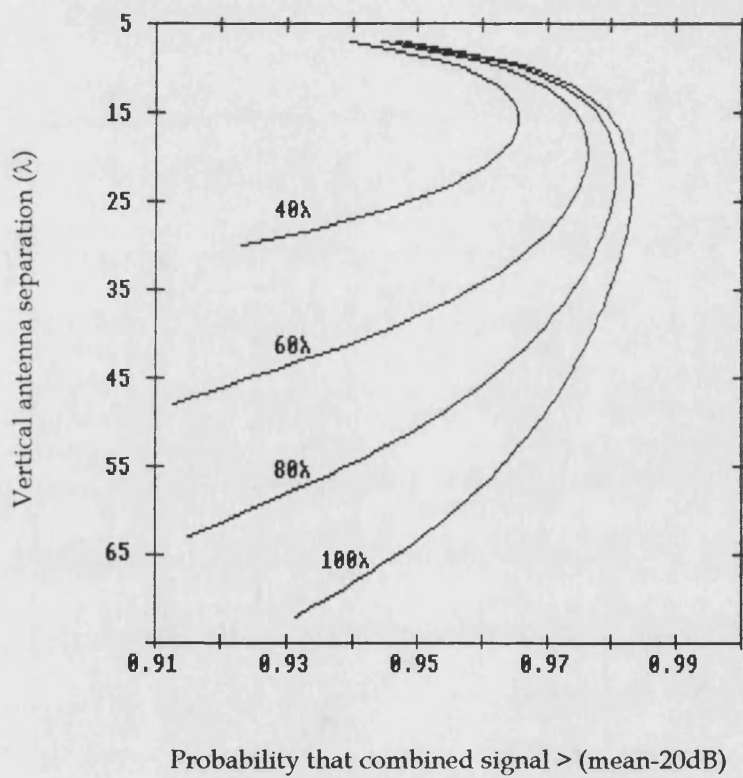angle (ϕ_v)=.01 radian.

51

Figure 2.15 Probability of the instantaneous selected diversity signal being greater than (mean-20dB) for different antenna positions and with spread of arrival angle (ϕ_v)=.006 radian.

52

Figure 2.16   Probability of the instantaneous selected diversity signal being greater than (mean-40dB) for different antenna positions and with spread of arrival angle (ϕ_v)=.04 radian.
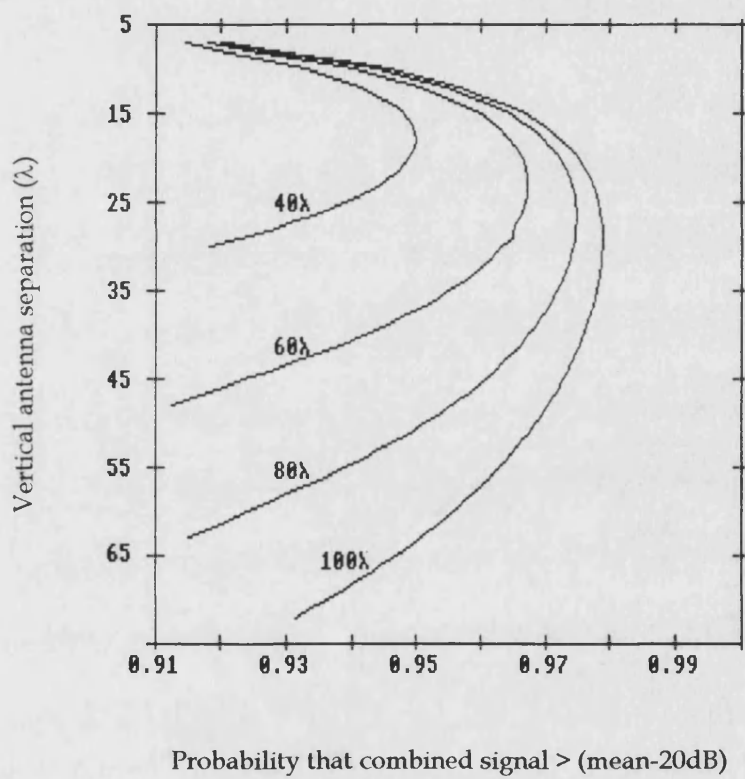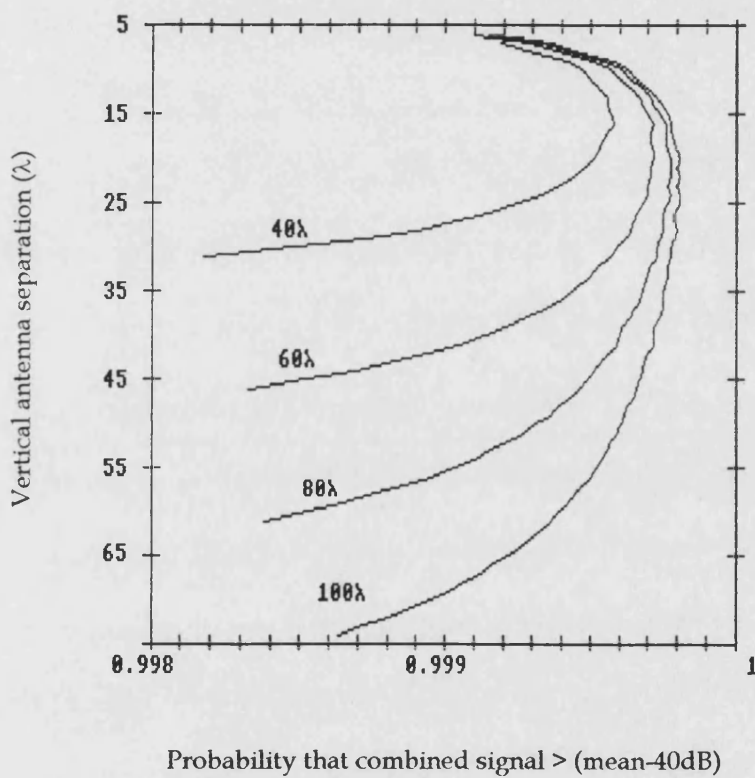
Figure 2.17 Probability of the instantaneous selected diversity signal being greater than (mean-40dB) for different antenna positions and with spread of arrival angle (ϕ_v)=.02 radian.

54

Figure 2.18 Probability of the instantaneous selected diversity signal being greater than (mean-40dB) for different antenna positions and with spread of arrival angle (ϕ_v)=.014 radian.
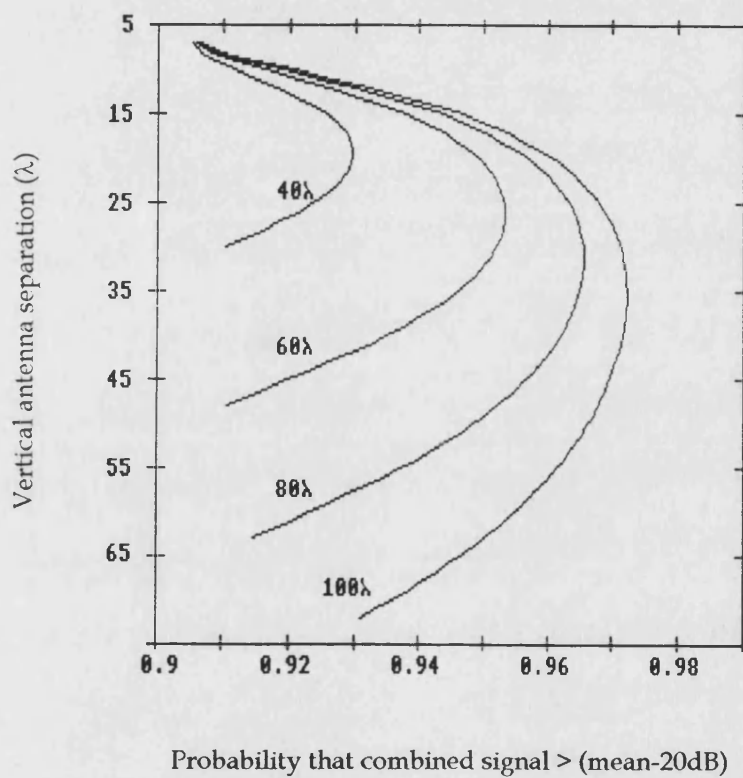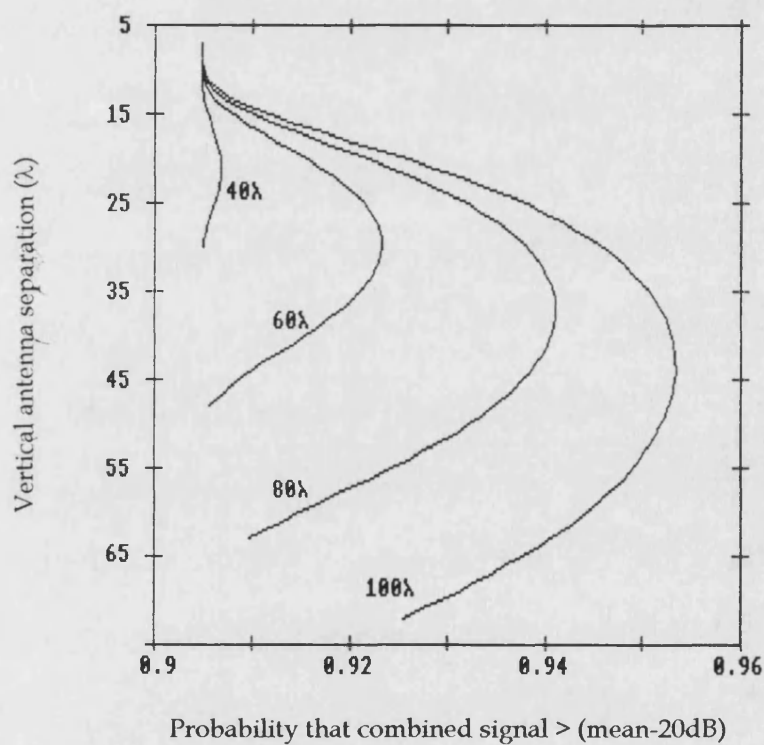
55

Figure 2.19 Probability of the instantaneous selected diversity signal being greater than (mean-40dB) for different antenna positions and with spread of arrival angle (ϕ_v)=.01 radian.
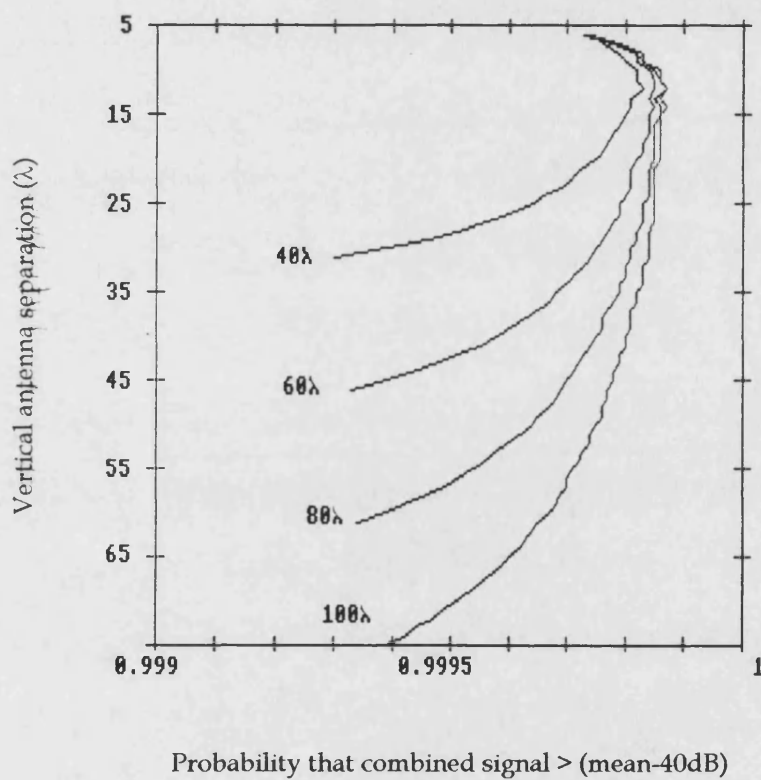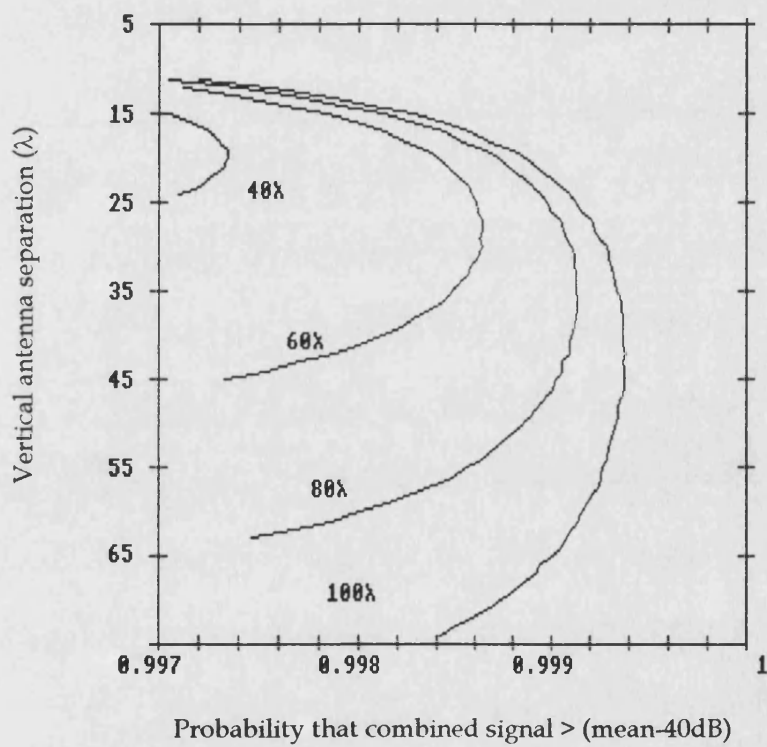
Figure 2.20 Probability of the instantaneous selected diversity signal being greater than (mean-40dB) for different antenna positions and with spread of arrival angle (ϕ_v)=.006 radian.

57

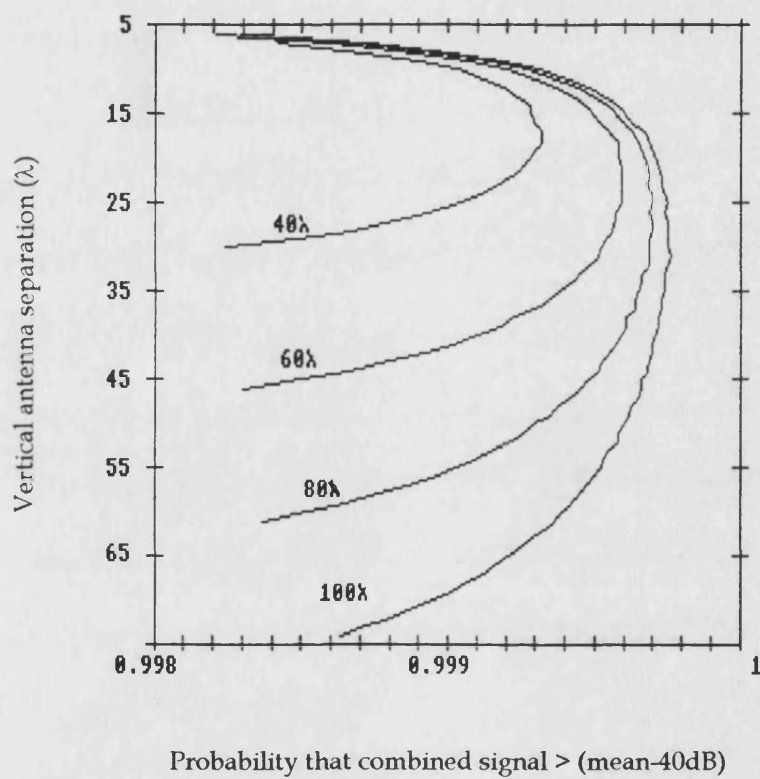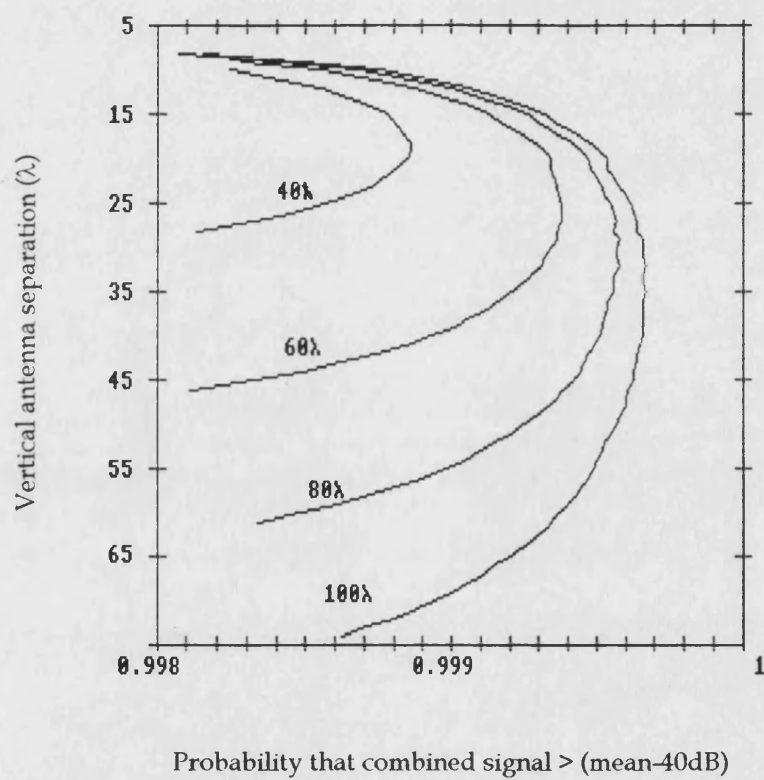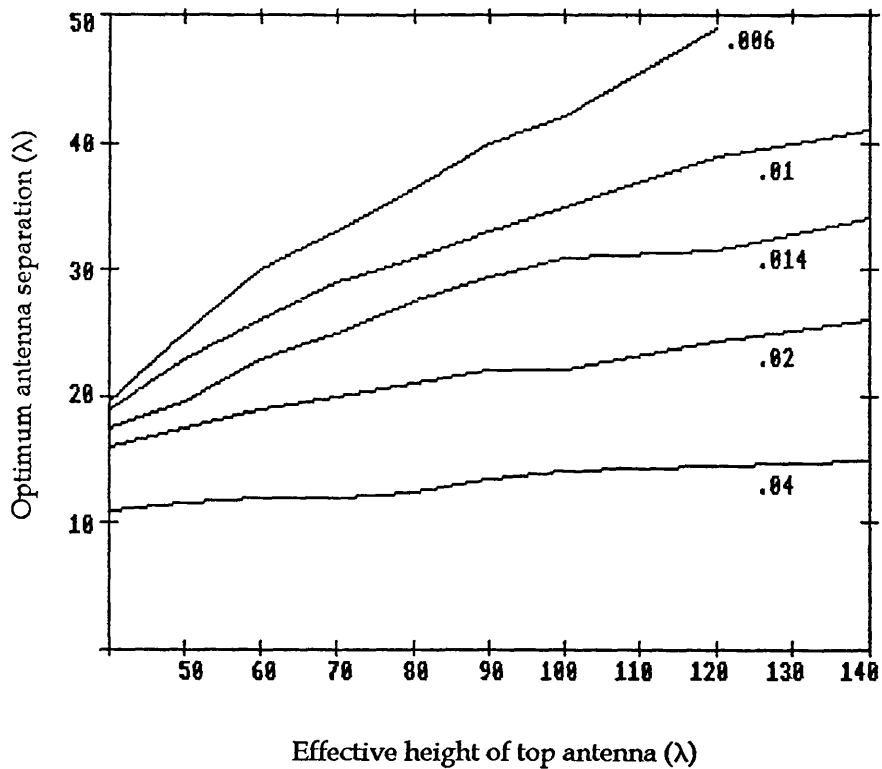Figure 2.21   Curves showing the optimum vertical antenna spacing for different values of top antenna heights and values of spread of arrival angle (ϕ_v). These figures are based on an effective antenna height gain relationship of 6dB per octave.

CHAPTER 3

Review of Published Work on Base Station Antenna Diversity.

3.1 Introduction.

It is well understood that there is spatial uncorrelation of the field components received in a mobile radio environment[25]. This uncorrelation can be used to implement diversity both at the mobile and base station by suitably combining signals received via two (or more) spatially separated antennas. It has been shown that at the mobile, surrounded by local scatterers, antenna separations of 0.2λ are sufficient to yield uncorrelated signals[27]. Base station antennas are usually deliberately located clear of local scatterers and received signals are from scatterers in the vicinity of the mobile. The assumption of isotropic scattering does not hold at the base station, instead signals are received over a narrow spread of arrival angles.

3.2 Spatial diversity with horizontal separation of antennas.

A number of workers have reported on the horizontal spacing requirements of base station antenna diversity.

Lee reported on measurements undertaken in Holmdel, New Jersey at 836 MHz using horizontal spaced horns having a 24° beamwidth in the horizontal plane[53]. These antennas were mounted at a range of heights around 4 metres; at this low level, local scattering was inevitable and directional antennas were used to simulate the condition where the antennas were mounted well clear of nearby objects. The antennas were directed towards a test run some 5km away. Lee showed that in order to achieve correlation of <0.7 the minimum antenna spacing was 15-20λ in the broadside case (incoming signals perpendicular to the axis of the base station antennas) and 70-80λ for the on-line case (incoming signals in-line with the axis of the base station antennas). Lee observed little dependence of height on the correlation of signals for a given separation. In a later paper Lee presented further measurements at 836 MHz using the same base station and test run but the horn antennas were oriented at different angles between the broadside and in-line cases[54]. He showed that for an arrival angle of 10° from the in-line the spacing requirement reduced to 30λ. Lee's measurements were made from a hilltop in a rural area with narrow beam width antennas to reduce the effect of local scattering. The elevation difference between the base station and mobile antennas was typically 100 to 130 metres. These factors contributed to high levels of correlation between the received

signal and perhaps provide an upper bound to the minimum required horizontal antenna spacing.

Rhee and Zysman have reported on measurements made at 821 MHz at the Bell Laboratories at Whippany New Jersey using horizontal antenna spacing[55]. They used antennas with a 6 dB beamwidth of 80°. By contrast to Lee's measurements, theirs were made in a suburban area with less elevation between base and mobile and increased antenna beamwidth. Various test runs were undertaken at distances of between 2 and 8 km from the base. Horizontal antenna separations of $6-7\lambda$ yielded correlation coefficients of <0.7 for arrival angles of 0 to 60° from the broadside. They also observed that adjusting both the antenna height and spacing can achieve a given correlation. For example a correlation of circ 0.55 was obtained with an antenna separation of 3.4λ at 15m and 6.6λ at 30m. The theoretical calculations indicate that the correlation to be independent of antenna height. Unlike earlier work[53-54] Rhee and Zysman's measurements were undertaken in a suburban area with relatively low antenna heights of 15 and 30 metres and with less directional antennas. At these heights in this environment there are more likely to be local scatterers and the lower the antennas are down the mast the lower the signal correlation will be for a given separation.

Lee used his own experimental data and that of Rhee

and Zysman[55], indicating that both antenna height and horizontal spacing could be adjusted to achieve a given correlation, to introduce a new design parameter η defined as[56]:-

$$\eta = \frac{H_1}{d_H} \qquad 3.1$$

Where H_1 is the antenna height and d_H is the antenna spacing.

Lee plotted the distribution of experimental data points on a scatter diagram and drew a linear regression line to fit the highest data points. The line represented the upper limits of correlation for a selected value of η.

More recently Adachi et al reported on measurements at 896 MHz in the Everton district of Liverpool[57]. They presented measurements with horizontal spacing at a fixed height but with a wide range of antenna spacing and arrival angles. The test runs were approximately radial and circumferential and were 1.3km from the base. Their results were in broad agreement with the trends found by Lee[53-54]. Because their work was limited to antennas at a fixed height they did not ascertain any dependence of height and spacing. They found lower values of correlation and attributed this to the larger

spread in multi-path arrival angles due to the closer proximity of the mobile to the base station. Their results would indicate that a horizontal separation of 20 - 30λ would yield signals sufficiently de-correlated for much of the time. Such a separation can be readily achieved at 900 MHz where the separation is 7 - 10 metres. Indeed the UK cellular operators are implementing horizontally spaced antenna diversity on their radio masts. At lower frequencies the spacing would necessitate the use of separate masts which practically and economically usually precludes its use at many sites. The increasing use of high rise buildings as radio sites does allow this antenna separation to be more readily implemented. Even so horizontal separation of two antennas has the disadvantage that the cross correlation is dependent on the horizontal arrival angle of the multi-path waves.

3.3 Spatial diversity with vertical separation of antennas

With regard to vertical antenna spacing Rhee and Zysman observed a "standing wave" pattern in cross correlation for vertically spaced and vertically polarised signals but not for horizontally polarised signals[55]. This effect was also reported by Lee and Brandt[77]. Other published work and theoretical formulation shows a monatomic reduction of cross correlation with increased

antenna separation. Rhee and Zysman concluded that this standing wave pattern was most probably generated by the interaction of signal components arriving at the base from a number of discrete, rather than uniformly distributed, angular directions in the vertical plane.

Adachi et al presented results at 896 MHz in the Everton district of Liverpool with vertical spacing using vertical dipoles and approximately radial and circumferential test routes about 1.3km from the base[57]. In both cases their results showed a clear monotonic reduction in cross correlation with increased antenna separation. Cross correlations were generally slightly lower with the radial route, probably resulting from a slightly larger spread in arrival angles in the vertical plane compared with the circumferential route.

CHAPTER 4

FIELD MEASUREMENTS

4.1 Introduction

Measurements have been undertaken to determine the degree of envelope cross correlation and the relative power levels between UHF mobile radio signals received via various combinations of antenna location and orientation. These results help determine under what conditions extra useful information is likely to be available to any proposed signal combining system connected to the base station receivers.

4.2 Antenna configurations.

Measurements have been undertaken using the following two categories of antenna configuration:-

i) Vertically separation of vertically polarised antennas mounted on a transportable mast in the university car park.

ii) Horizontally separated vertically polarised antennas on the roof of the main university building.

For the first category use was made of a transportable 30 metre telescopic mast. During erection five telescopic sections were gradually extended to allow

the positioning of antennas at five distinct locations at the top of each section as illustrated in Figure 4.1. These locations were easily accessible when the mast was in its unerrected state and luffed over on its side. At the top of the uppermost telescopic section a single pole was attached thus providing an extra antenna location. Measurements were performed using the top four of these locations.

In order to achieve horizontal separation of antennas use was made of the roof of the university building. Practical limitations prohibited varying the orientation of the antennas but by using a third antenna perpendicular to one of the other antennas it was possible to get measurements with two arrival angles (α_H) for each type of test run; this is illustrated in Figure 4.2.

The antennas used for the spatial diversity were eight-element yagis providing a beamwidth of 50° as shown in Figure 4.3. In all cases the antennas were oriented towards the individual test routes. By using directional antennas oriented this way we reduced the possibility of receiving locally scattered signals and increased the received signal levels.

4.3 Hardware configuration

The antennas were each connected via equal lengths of low loss co-axial cable to base station receivers. These 25KHz channel receivers were modified by the inclusion of an I.F. logarithmic amplifier and detector to generate a d.c. voltage proportional to signal strength expressed in dB. These two signal strengths were recorded on a multi-channel instrumentation tape recorder for later computer analysis in order to determine the strength and cross correlation coefficients of the two branches. Because these two signals had to be played back and analysed separately a means of providing synchronisation was necessary. To provide this a marker tone was directly input into the tape recorder at the instant when measurement commenced and was removed when measurements were completed. Figure 4.4 provides an overview of the base station. The relationship between the receiver signal input and the dc voltage from the IF logarithmic amplifier and detector is shown in Figure 4.5

A UHF mobile radio was modified to provide an external transmitter keying input and a continuous rated output power of 10 watts. A magnetically mounted quarter wave antenna was mounted on the centre of the roof of a small saloon car.

4.4 Measurement procedures

In each run the mobile stopped well in advance of the run geographical start marker. The tape recorder was set in motion and the mobile commanded to start over the two-way radio link. The driver announced the precise moment at which he crossed the start marker so that the operator at the base station could switch the marker tone. A reverse operation occurred at the end of each run.

4.5 Test runs

Information on the two base sites and the three test routes is given in Tables 4.1-2 and their location illustrated in Figures 4.6 to 4.9.

Mobile Location	Environment	Grid Ref	Height (m) ASL	α_v	Distance from base (R).
Dunkerton Hill	Rural	ST719607	138	0.57°	6.5km
Twerton - High St	Suburban	ST725647	23	1.70°	4.8km
Bath - Bathwick St	Urban	ST755655	23	4.68°	2.2km
Base Location :- University car park (ST773643 178m asl)					

Table 4.1 Summary information of vertical spaced diversity measurements.

Mobile Location	Environment	Grid Ref	α_H	Distance from base (R).
Dunkerton Hill	Rural	ST719607	55°, 35°	6.6km
Twerton - High St	Suburban	ST725647	88°, 2°	4.8km
Bath - Bathwick St	Urban	ST755655	61°, 29°	2.1km
Base location:- University building (ST773645 180 m asl)				

Table 4.2   Summary information of horizontal spaced antenna diversity measurements

The routes were chosen because firstly they were in different classification of environment. Secondly no significant line of site paths existed, (as shown in the base to mobile terrain profiles in Figures 4.10 to 4.15), in order to ensure significant multipath propagation. Thirdly, a mobile travelling along the routes provided mean signal levels at the base station that were sufficiently strong to ensure that the signal levels could still be measured during fades that could be 20dB below the mean level. The urban route was a one way passage along Bathwick Street near the centre of Bath. The suburban route consisted of a one way passage through Twerton High Street and the rural route of two circuits of a triangle on Dunkerton Hill.

4.6 Analysis of recorded branch signal strengths.

The recorded branch logarithmic signal strength outputs were individually sampled and digitised with a 16 bit A to D converter at a rate of 1k bit/s and stored in data files for subsequent analysis. In each case the presence of the marker tone indicated that sampling and digitising should be undertaken. The signal strength outputs varied between -120 dBm to -70 dBm and this enabled a resolution of ($50dB/2^{16}$) .00092 dBm in the stored data. Each file represented 40 seconds of measurement.

The analysis of these files was undertaken with an Archimedes A310 computer with 4Mbytes of RAM. The computer operated with an ARM3 32 bit RISC (*Reduced Instruction Set Chip*) processor running at 25MHz and utilising a 4Kbyte cache. The RISC OS 3.10 operating system was used with programs written in BASIC V or BASIC VI for applications requiring greater accuracy. BASIC VI utilises 8 bytes to store floating point numbers rather than the 5 bytes used in BASIC V.

Separation of the fast and slow fading components.
The digitised recorded received signal level R(mT) was composed of both fast and slow fading components.

$$R(mT) = F(mT) + S(mT) \qquad 4.1$$

where T is the sampling period.

The slow fading component S(mT) being due to variations in local mean. In order to calculate the cross correlation of the fast fading component F(mT) it was necessary to remove the slow fading component by normalising R(mT) to the local mean. This was done by sampling and averaging the received signal over a short time. If this time is too short then the local mean will be inaccurate due to the presence of the fast fading; conversely if chosen too long then the slow fading variations will be lost. This issue has been addressed by Lee[78] who justified a length of time corresponding to between 20 and 40 wavelengths.

Measurements had been undertaken at a speed as close as possible to 40 Km/hr (11.1 m/s) and at 450 MHz the wavelength is 0.66 metres. Averaging samples over thirty wavelengths (20 metres) therefore corresponded to averaging over two seconds.

In order to separate S(mT) from the R(mT) the digitised signal was converted into linear form and a moving average was generated.

$$\acute{S}(mT) = \frac{1}{(2K+1)} \sum_{j=-K}^{j=+k} \acute{R}(mT+j) \qquad 4.2$$

$$\textit{for } m=-K \textit{ to } Ns-K$$

Where

Ns=overall sequence length (40,000 bits)

2K+1= duration of the sequence over which the signal is averaged (2000 bits)

S' and R' = linear forms of S and R respectively

This moving average was then converted to logarithmic form and subtracted from the original sequence to yield the fast fading component. Figure 4.16 shows an example of the removal of the slow fading component from the received signal.

Samples of some of the fast fading components are shown in Figures 4.17 to 25 for a selection of antenna configurations. Although not conveying numeric information they do provide a useful insight into the general form of the fading of the received signals.

Distribution of the fast fading component

The fast fading components were analysed to see how closely they fit a Rayleigh distribution. The cumulative distribution of the fast fading component received from the three test routes has been computed and is plotted in Figures 4.26 to 28 along with the theoretical cumulative Rayleigh distribution function defined in equation 2.2. The results illustrated are from signals received by one of the antennas on the university building but similar cumulative

distributions were obtained from signals received on the transportable mast in the car park. The data generally shows a reasonable fit to the Rayleigh distribution except for where there is insufficient data (signals above mean +5dB).

The data for Twerton High Street suggests that a small line-of-sight component may be present. The path profile shown in Figure 4.13 indicates that this path was the least obstructed path; the only obstructions being local non-terrain clutter (buildings and other structures).

4.7 Computing signal cross correlation and relative strength.

For each test run the cross correlation of the two branches has been calculated using the following:-

$$\rho_{env} = \sum_{n=1}^{Ns} \frac{(\acute{R}_1(nT) - \overline{R}_1)(\acute{R}_2(nT) - \overline{R}_2)}{Ns\sigma_1\sigma_2} \qquad 4.3$$

Where R'_1 and R'_2 are the signal levels received from the upper and lower antennas respectively.

and the individual; branch means are given by:-

$$\overline{R_1} = \frac{1}{Ns} \sum_{n=1}^{Ns} \acute{R}_1(nT) \quad \text{and} \quad \overline{R_2} = \frac{1}{Ns} \sum_{n=1}^{Ns} \acute{R}_2(nT) \qquad 4.4$$

and the individual standard deviations of the branch signal strengths are given by:-

$$\sigma_1 = \sqrt{\frac{\sum_{n=1}^{Ns} (\acute{R}_1(nT) - \overline{R_1})^2}{Ns}} \quad \text{and} \quad \sigma_2 = \sqrt{\frac{\sum_{n=1}^{Ns} (\acute{R}_2(nT) - \overline{R_2})^2}{Ns}} \qquad 4.5$$

The mean difference between the signal strengths received via the vertically separated antennas has also been computed using the following.

$$\delta s = \overline{R_1} - \overline{R_2} \qquad 4.6$$

4.8 Results

The measurements are summarised in Tables 4.3 -4.5.

Antenna Separation (λ)	Cross Correlation/Relative signal strength		
	Urban	Suburban	Rural
9	0.75 -0.677dB	0.99 -1.50dB	0.90 -0.78dB
18	0.28 -1.412dB	0.95 -3.31dB	0.77 -1.63dB
27	0.09 -2.214dB	0.90 -5.60dB	0.58 -2.58dB
36	0.03 -3.098dB	0.82 -8.72dB	0.36 -3.66dB

Table 4.3 Summary of signal cross correlation and relative strength for different vertical separation of antennas.

75

Antenna Separation (λ)	Cross Correlation			
	Urban		Suburban	
	$\alpha_H=61°$	$\alpha_H=29°$	$\alpha_H=88°$	$\alpha_H=2°$
1	0.63	0.86	0.83	-
2	0.16	0.55	0.54	0.999
3	0.018	0.27	0.23	-
4	0.001	0.12	0.08	0.999
5	0	0.03	0.04	-
6	-	0.012	0.004	0.99
7	-	0.001	0.0005	-
8	-	0	0	0.989
10	-	-	-	0.98
12	-	-	-	0.97
14	-	-	-	0.96
16	0	0	0	0.955
18	0	0	0	0.94

Table 4.4 Summary of cross correlation for different horizontal antenna separation for signals received from mobile in urban and suburban test routes.

Antenna Separation (λ)	Cross Correlation			Antenna Separation (λ)	Cross Correlation	
	$\alpha_H = 55°$	$\alpha_H = 35°$			$\alpha_H = 55°$	$\alpha_H = 35°$
$\lambda/4$	0.87	0.94		$7\lambda/4$	0.0012	0.03
$\lambda/2$	0.56	0.76		2λ	0.0002	0.0124
$3\lambda/4$	0.28	0.49		$9\lambda/4$	0	0.004
λ	0.10	0.35		$5\lambda/2$	0	0.0011
$5\lambda/4$	0.029	0.19				
$3\lambda/2$	0.0075	0.081				

Table 4.5   Summary of cross correlation for different horizontal antenna separation for signals received from mobile in the rural test run.

4.9 Analysis of results

i Results with vertically spaced antennas.

The cross correlation figures in Table 4.3 have been plotted along with the theoretical formulation of equation 2.26 and the results are shown in Figure 4.29. The best fits to the measured data occurred with values of arrival angle spread, ϕ_v, shown in Table 4.6.

Test Run	Urban	Suburban	Rural
ϕ_v (radians)	0.0184	0.0038	0.008

Table 4.6 Estimated values of arrival angle spread at the base station.

Of the three test runs the suburban one is the easiest to analyse because the mobile to base path was a non obstructive direct path with all scatterers in the immediate vicinity of the mobile. Using the values of R and α_v from Table 4.1 in equation 2.21 it is calculated that the effective distance of the scatterers from the mobile for multipath waves received in the vertical plane, r_v is approximately 300 metres. Quite significant changes in cross correlation were observed over distances of several wavelengths as different scatterers contributed to the multi-path propagation.

The analysis of the results from the urban and rural test routes is less clear. In both cases the mobile to base path is obstructed by terrain as shown in Figures 4.30 - 31. Consequently it is reasonable to assume that the principal scatterers are not in the immediate vicinity of the mobile but some distance removed particularly in the rural environment. This has contributed to the lower values of ϕ_v and has produced greater cross correlation of the signals received at the base station.

The average signal strength received via the lower antenna relative to the signal received via the upper antenna are shown in Table 4.3. Using these figures and equation 2.47 has yielded estimates of effective base station height for the three test runs as shown in Table 4.7

Test Run	Urban	Suburban	Rural
Effective Antenna Height	80m	38m	70m

Table 4.7 Estimates of effective antenna height for the top antenna used in the measurements with vertically spaced antennas.

The relative strength of the signal received via the lower antenna is plotted against effective antenna height ratios in Figures 4.32 to 34 for the three test runs. In all cases the antenna gain follows a 6dB increase per octave in effective antenna height.

ii Results with horizontally spaced antennas.

The cross correlation figures in Table 4.4 have been plotted along with the theoretical formulation of equation 2.26 and the results are shown in Figure 4.35-37. The best fits to the measured data occurred with values of arrival angle spread, $\phi_H \sin \alpha_H$ shown in Table 4.8.

$\phi_H \sin \alpha_H$					
Urban		Suburban		Rural	
$\alpha_H=61°$	$\alpha_H=29°$	$\alpha_H=88°$	$\alpha_H=2°$	$\alpha_H=55°$	$\alpha_H=35°$
0.21°	0.16°	0.12°	0.0044°	0.47°	0.33°

Table 4.8 Estimated values of arrival angle spread at the base station.

The results shown in Figures 4.35-37 clearly illustrate the dependence of the arrival angle α_H on the achievable cross correlation. This is particularly apparent in the results for the suburban test run where the arrival

angle was either virtually broadside or virtually in line. Clearly for horizontal spacing the dependence on arrival angle is a disadvantage when the arrival angle is small however at other values much lower cross correlation for given antenna spacing is possible compared to that achieved with vertical spacing. The comments made earlier in this section concerning the path profiles and location of the principal scatters apply equally to the measurements with horizontally spaced antennas. For the suburban test run the application of equation 2.23 with the data in Table 4.8 indicates that the effective distance of the scatterers from the mobile for multipath waves received in the horizontal plane, r_H, is approximately 300 metres.
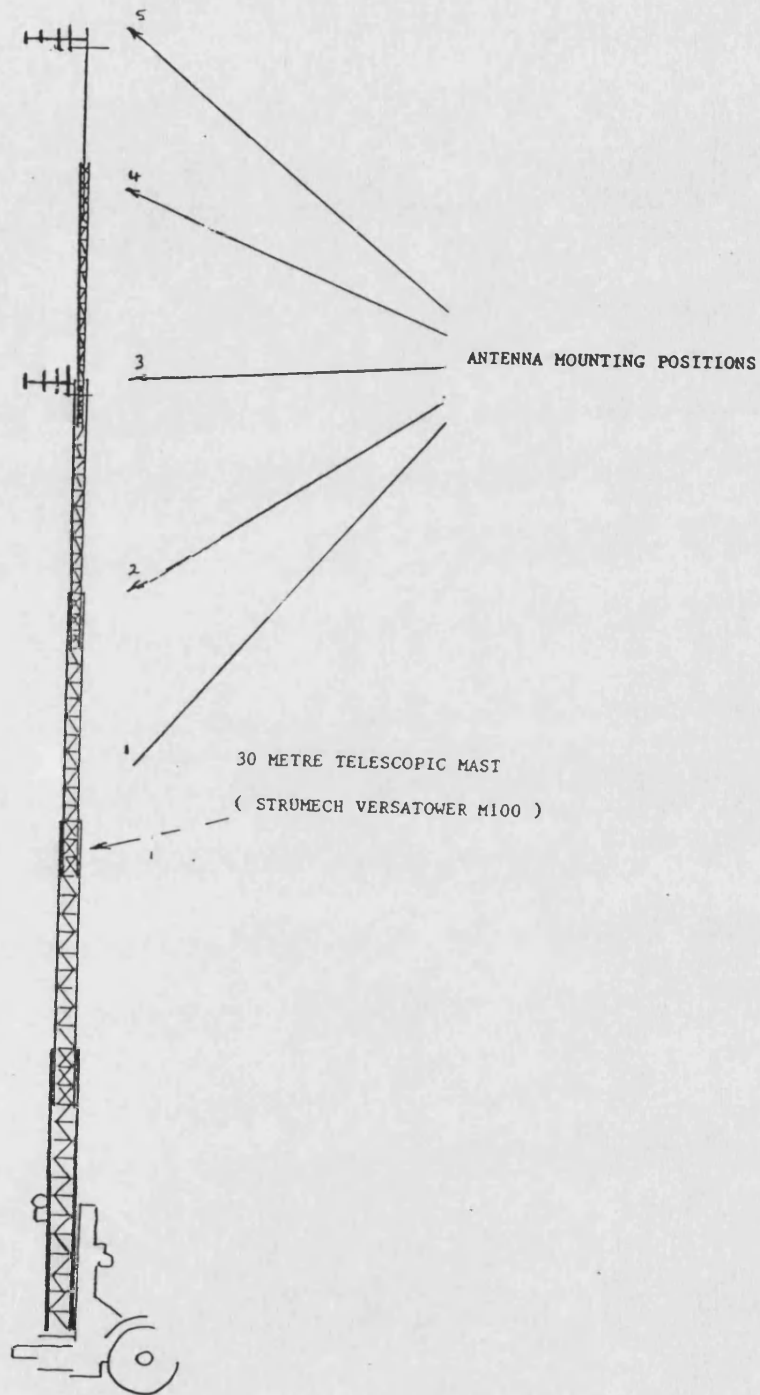
Figure 4.1   Transportable telescopic mast used in the measurements showing the different antenna positions.

Position of antennas

Position of
antennas

Incoming wave

a

α_1

α_2

$\alpha_2 = 90° - \alpha_1$

c

b

Corner of building

$\alpha_H = \alpha_1$ for antennas a&b
$\alpha_H = \alpha_2$ for antennas b&c
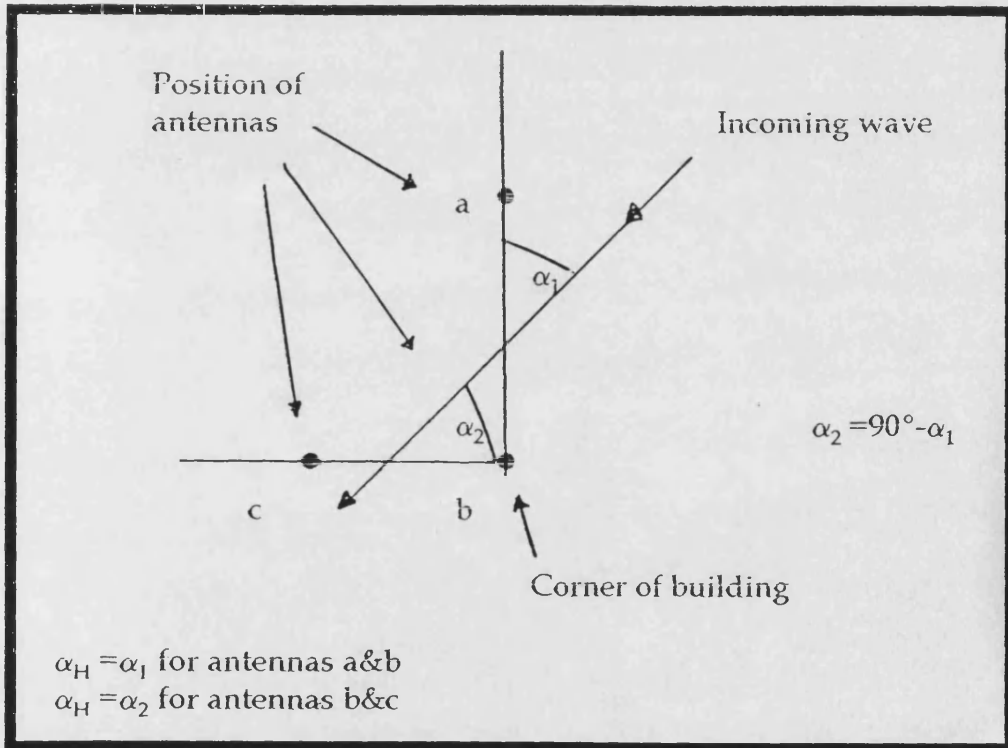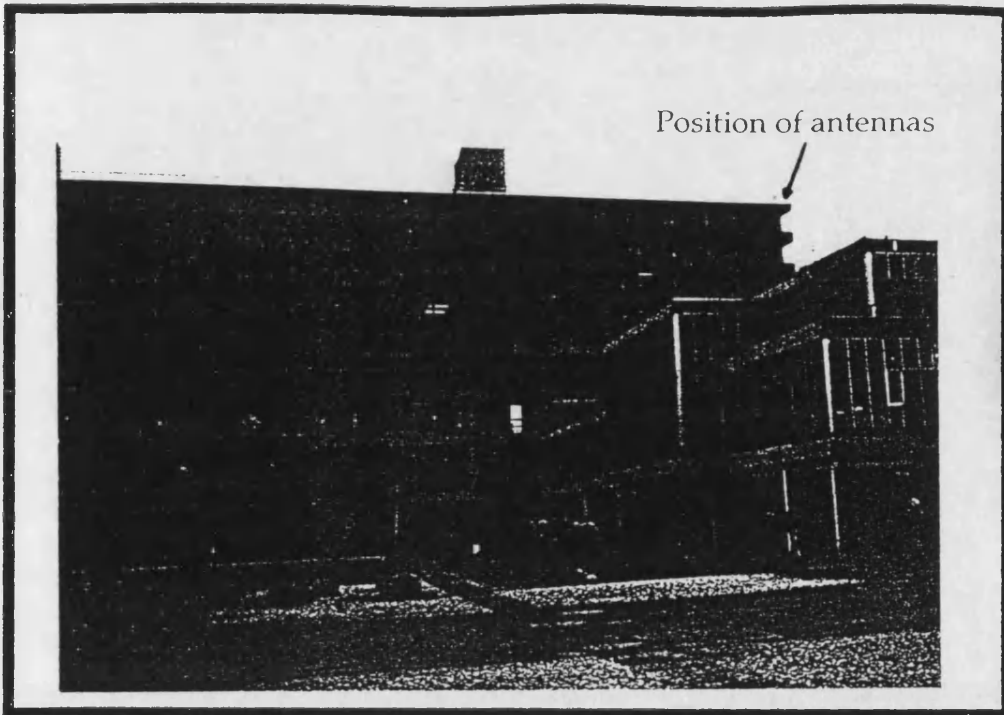
Figure 4.2 Orientation of horizontally spaced
antennas.
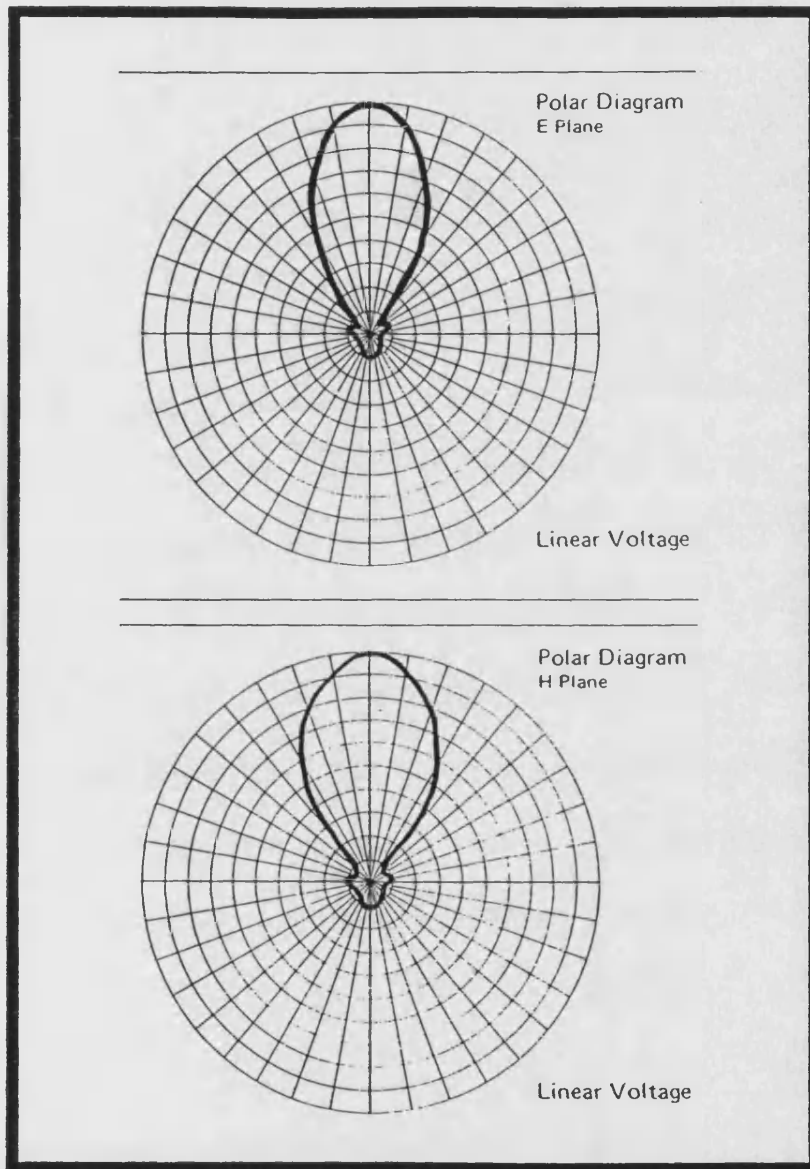
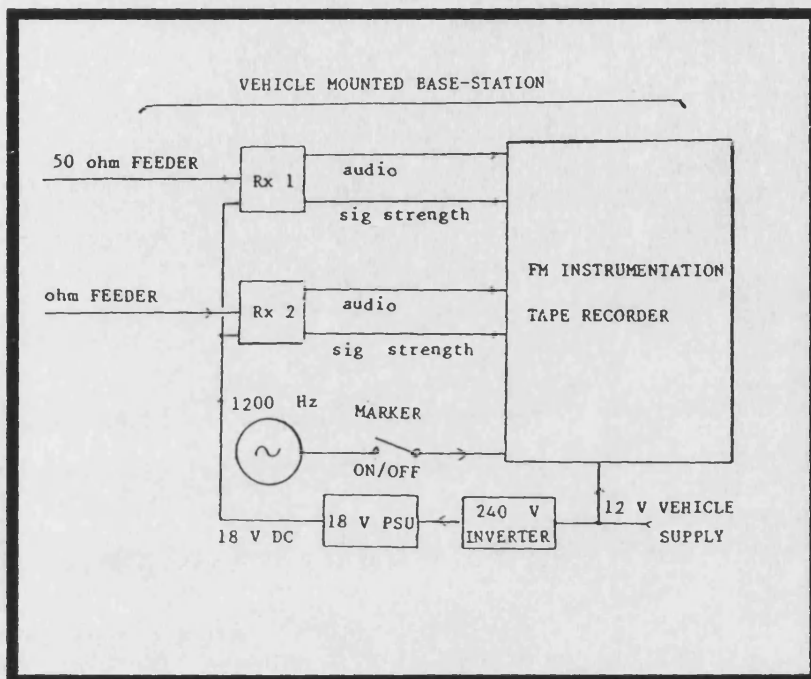Figure 4.3   Polar diagrams of E and H planes of 8 element yagis used in the measurements.

Figure 4.4 Configuration of hardware used to record signals at the base station.
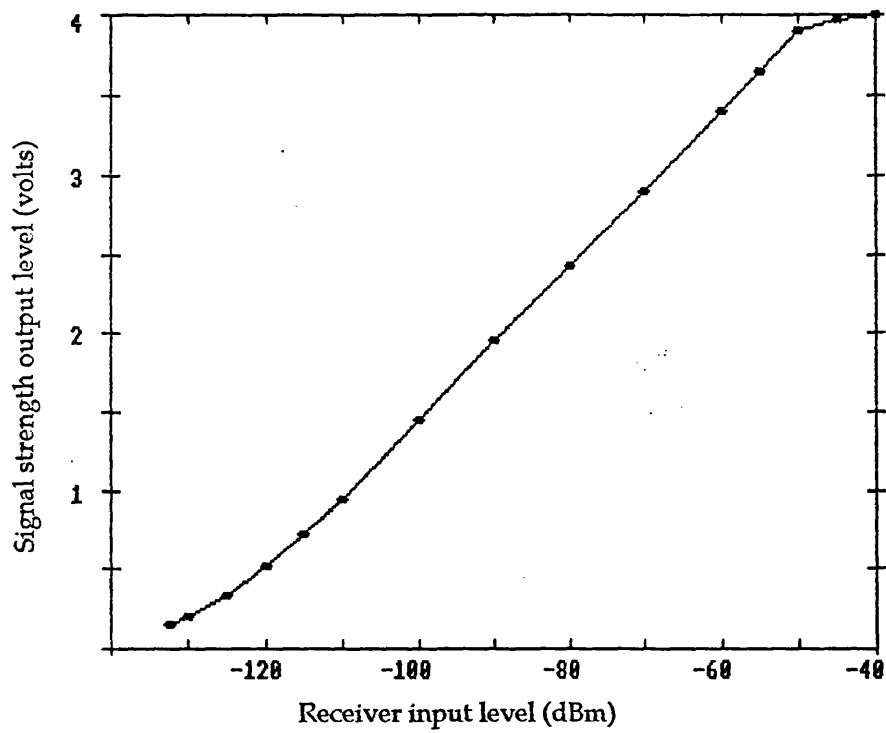
Figure 4.5 Relationship between the base station
input and the dc voltage from the IF logarithmic
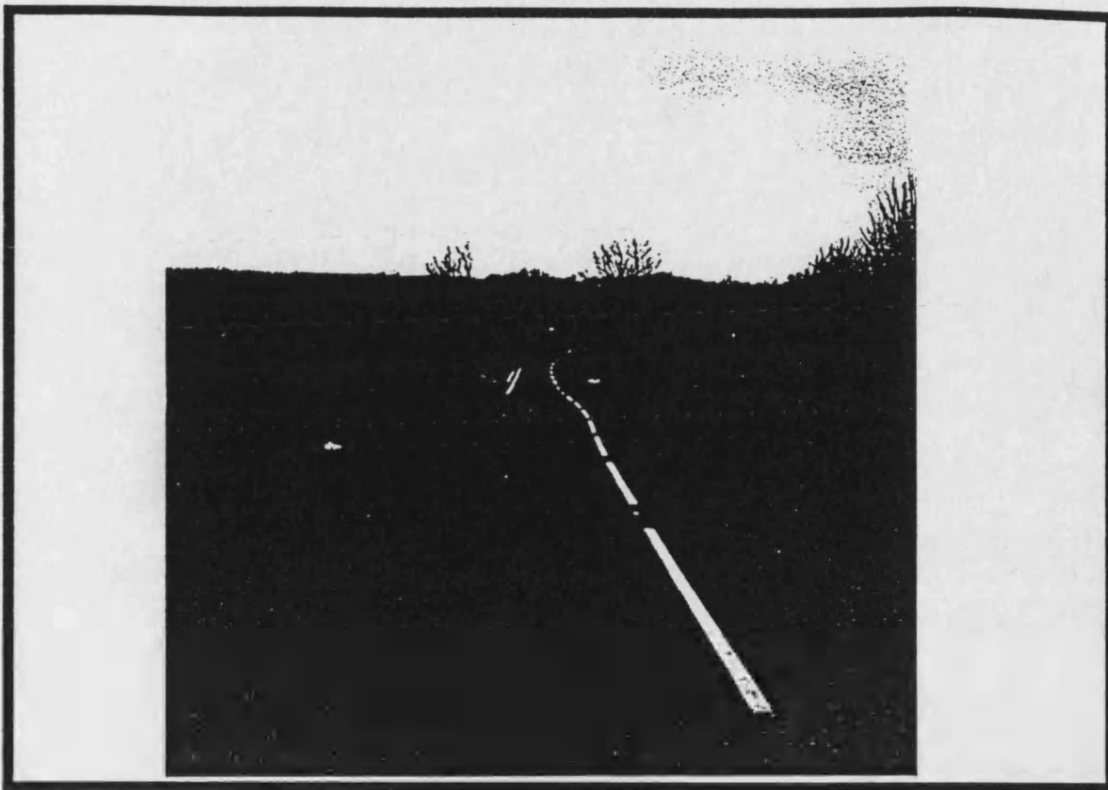amplifier and detector.
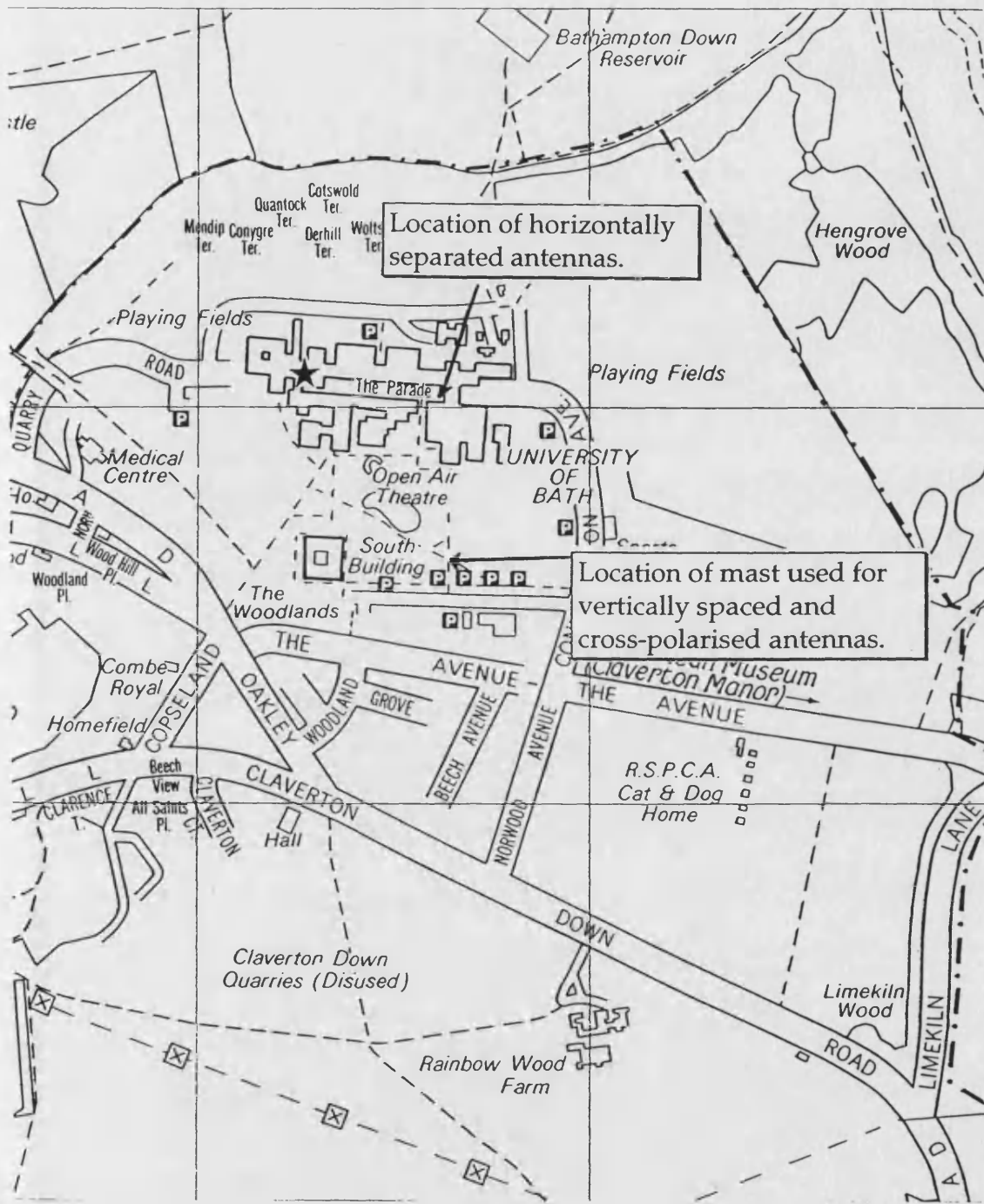
Figure 4.6   Location of base station sites.
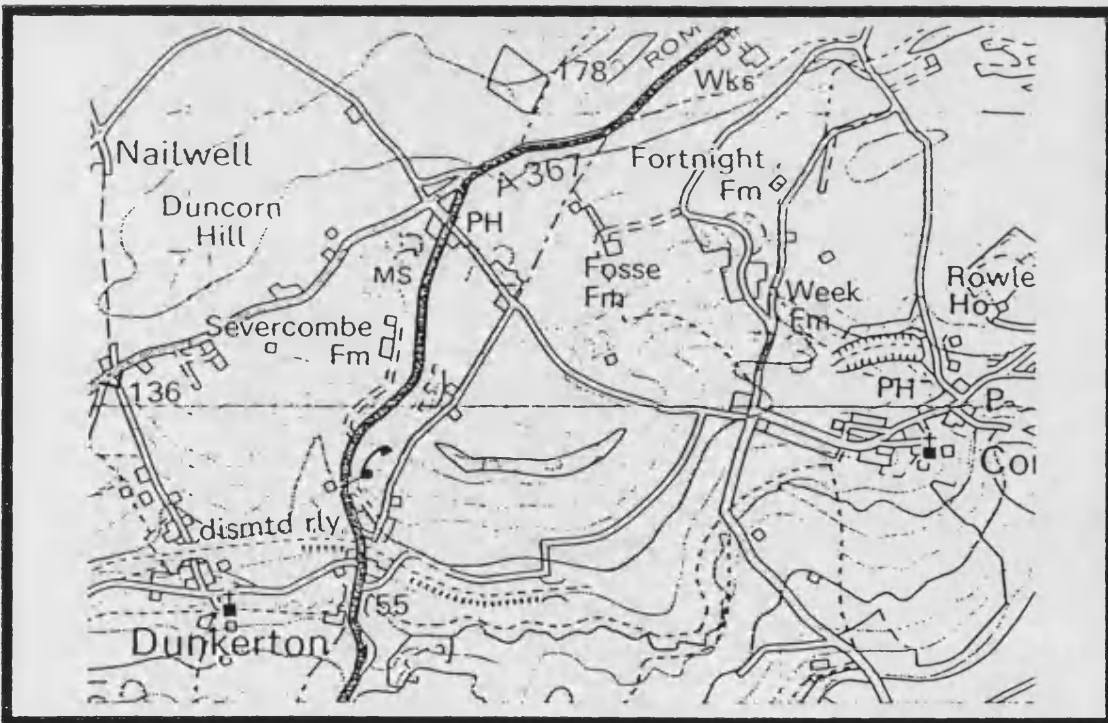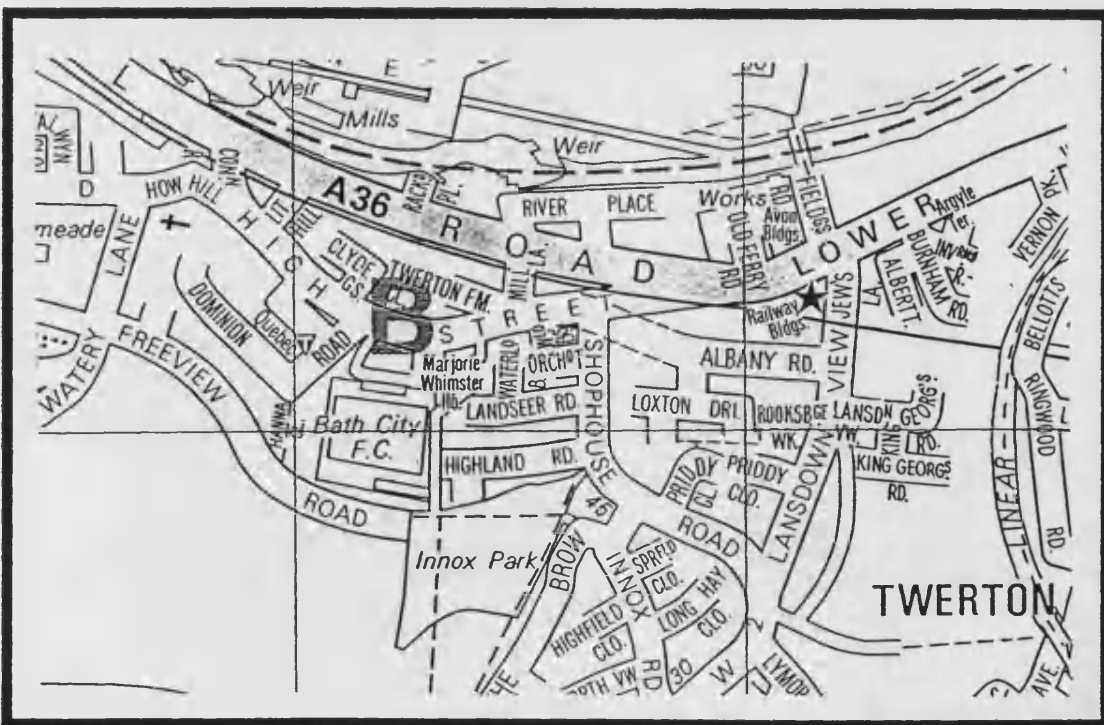
Figure 4.7   Rural test run:- Dunkerton Hill

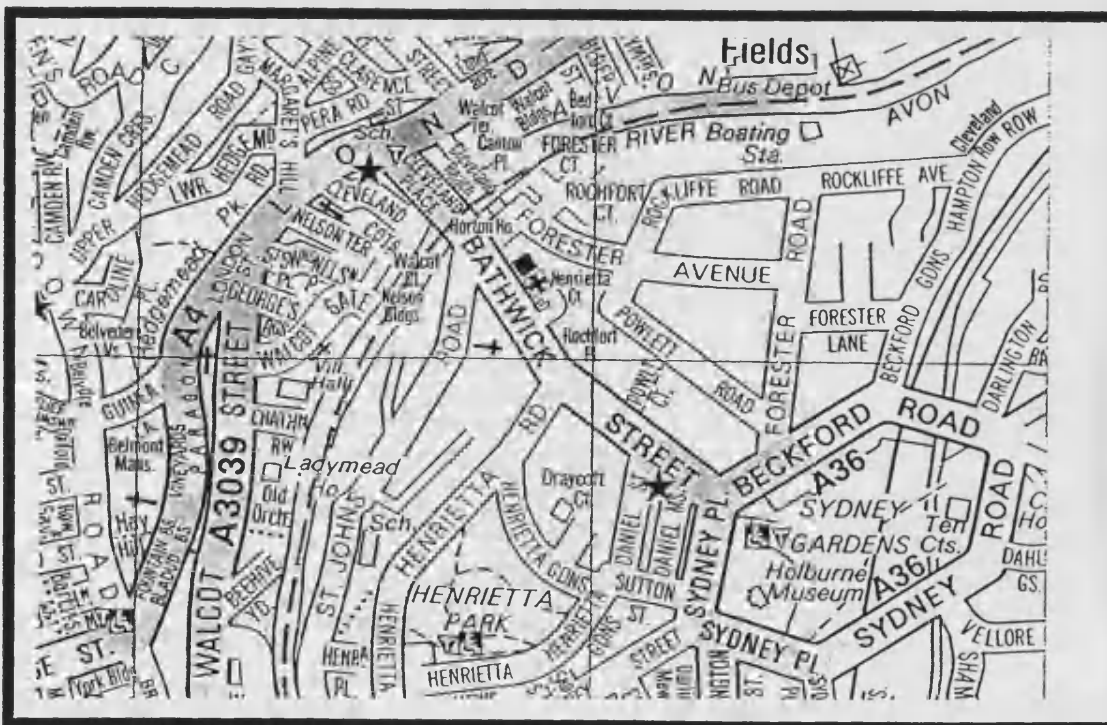Figure 4.8   Suburban test run:- High Street, Twerton.

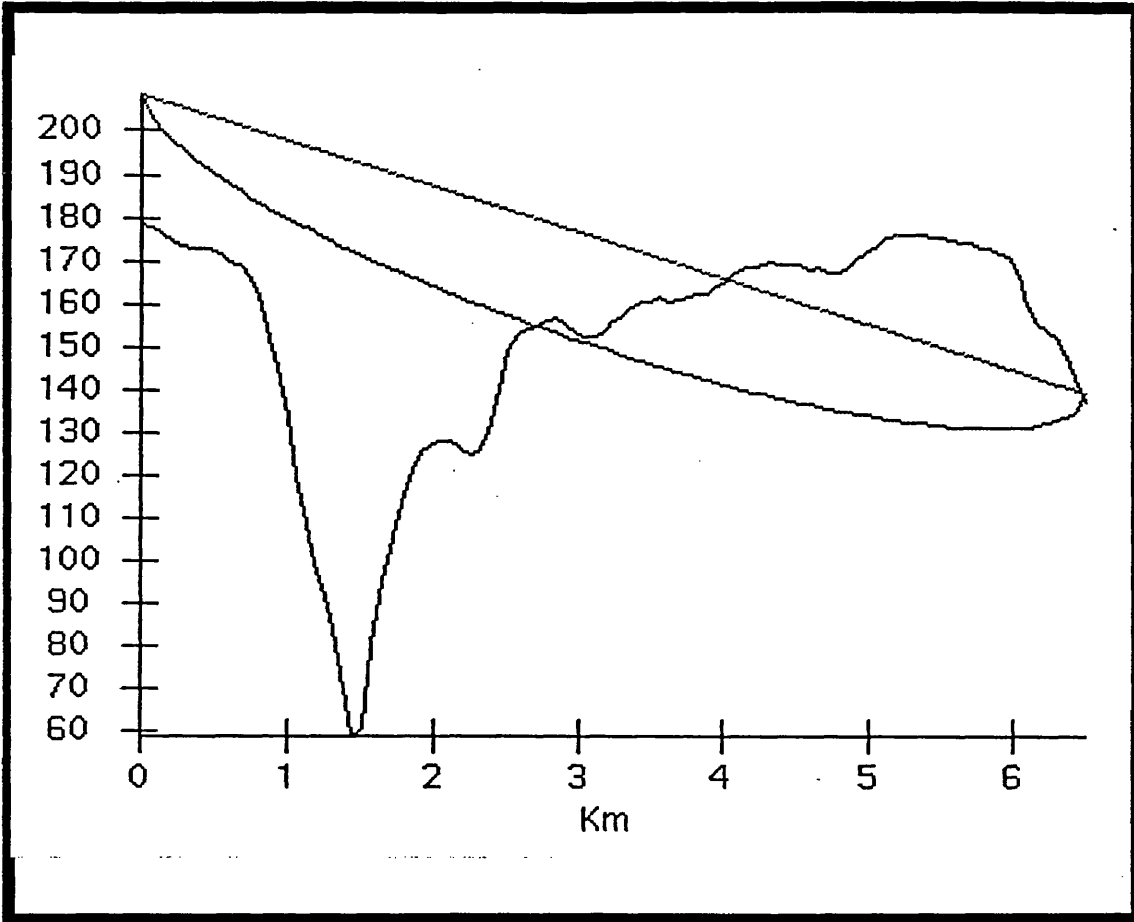Figure 4.9   Urban test run:- Bathwick Street, Bath.

Figure 4.10   Path profile:- University car park to Dunkerton Hill.
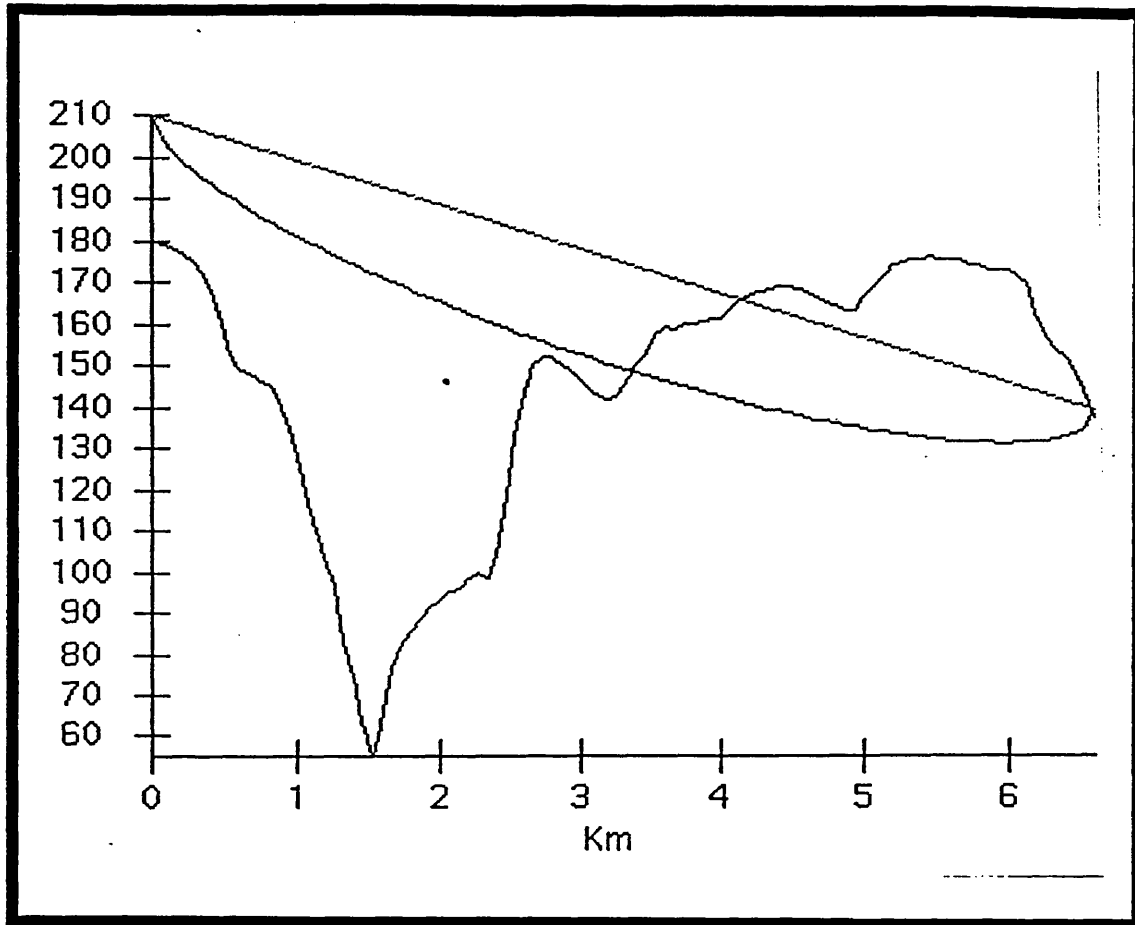
Figure 4.11 Path profile:- University Building to
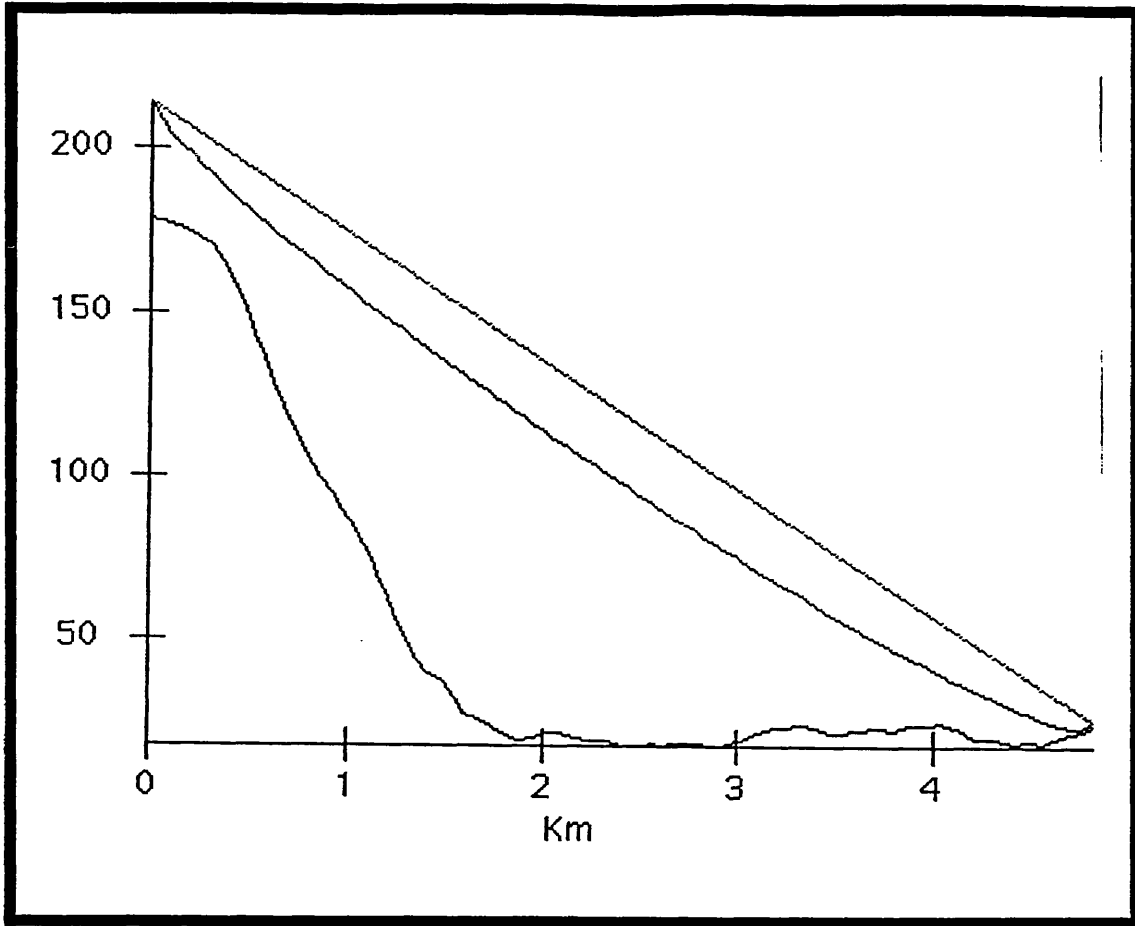Dunkerton Hill.

Figure 4.12   Path profile:- University car park to
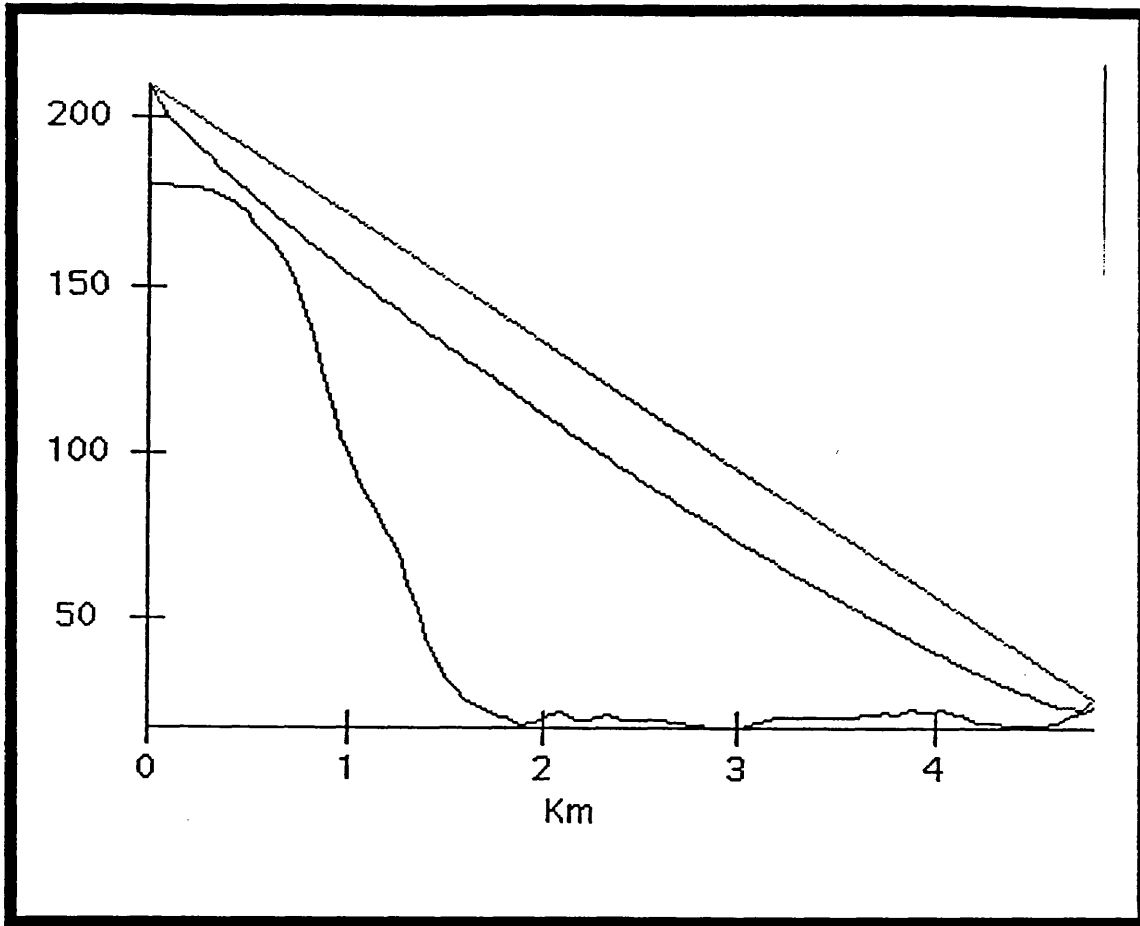High Street, Twerton.

Figure 4.13   Path profile:- University Building to
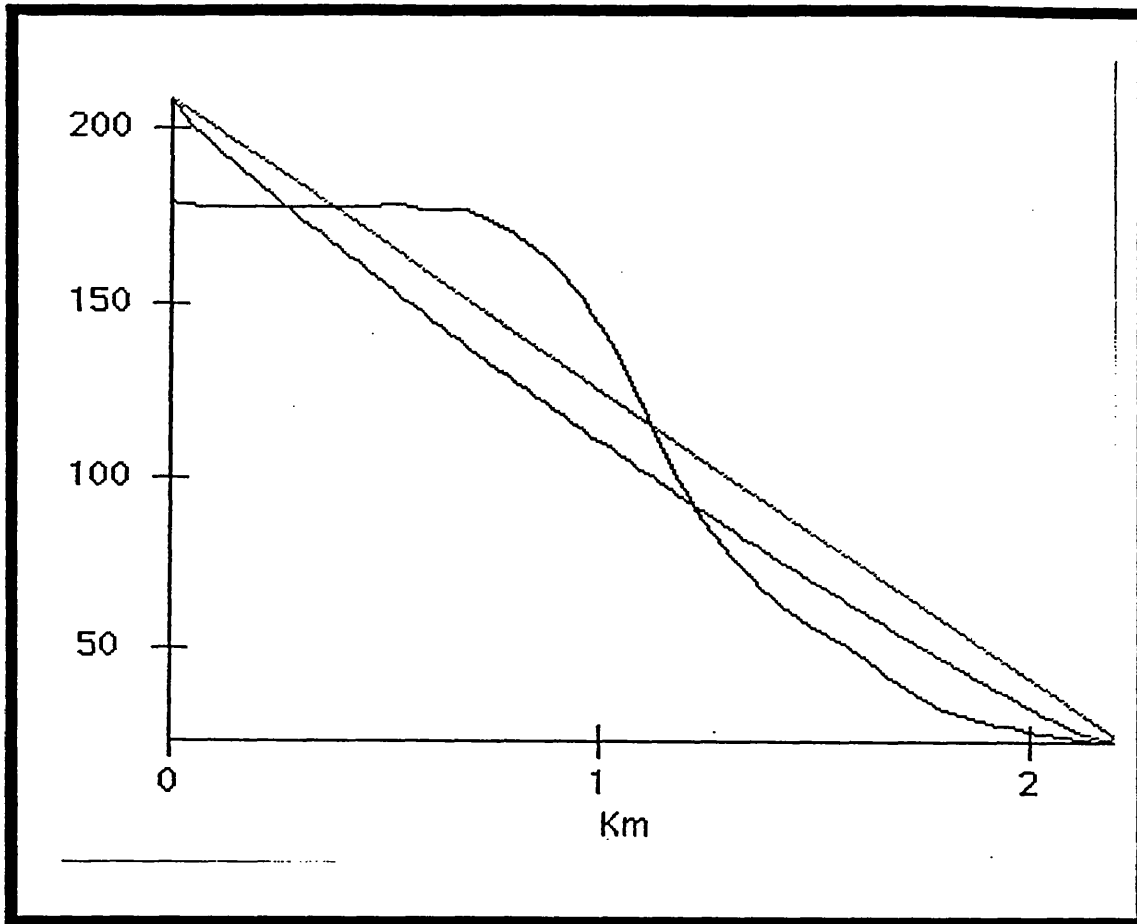High Street, Twerton.

Figure 4.14 Path Profile:- University car park to
Bathwick Street, Bath
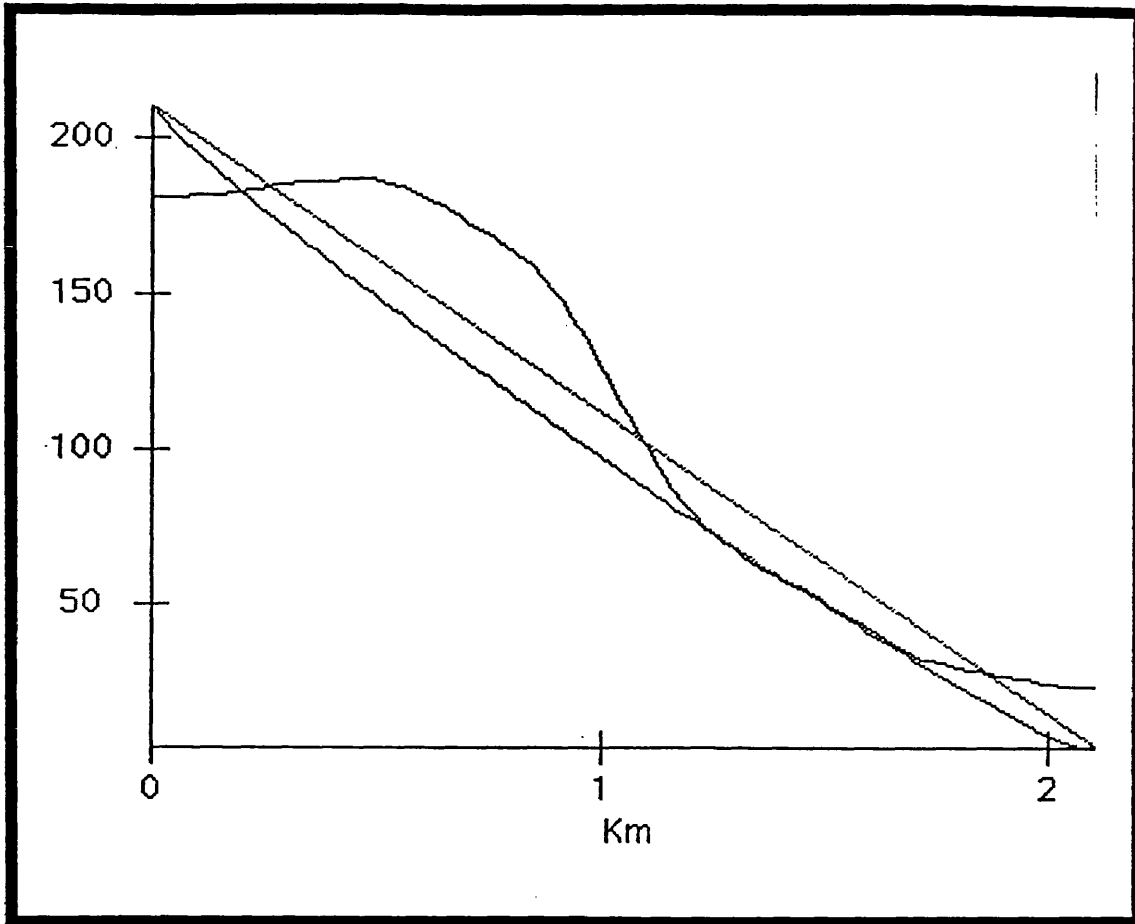
Figure 4.15   Path Profile:- University building to
Bathwick Street, Bath
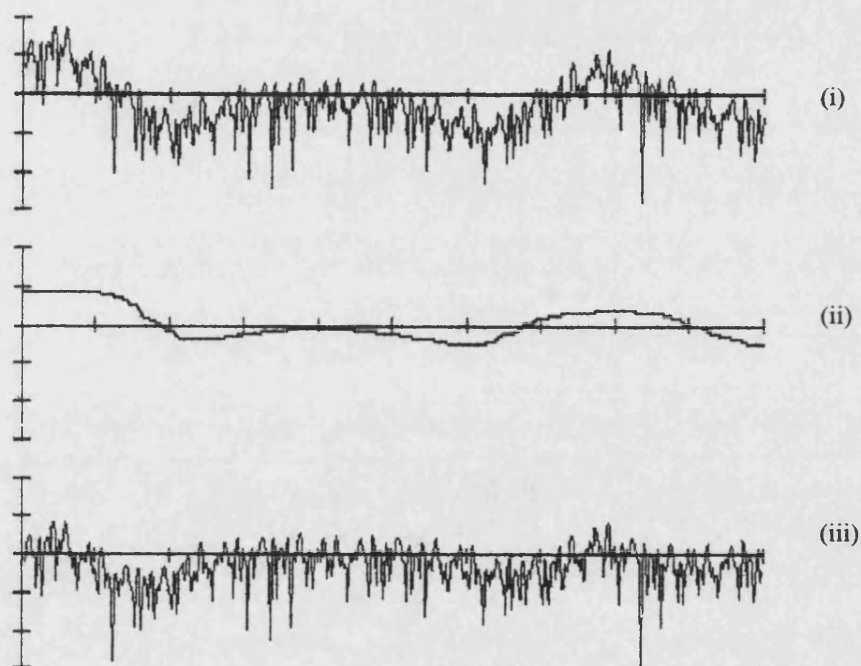
Figure 4.16 Sample of results of removing the slow
fading component (ii) from the received signal (i) to
yield the fast fading component (iii). (Vertical
increments are 10dB, horizontal increments are 1
second).
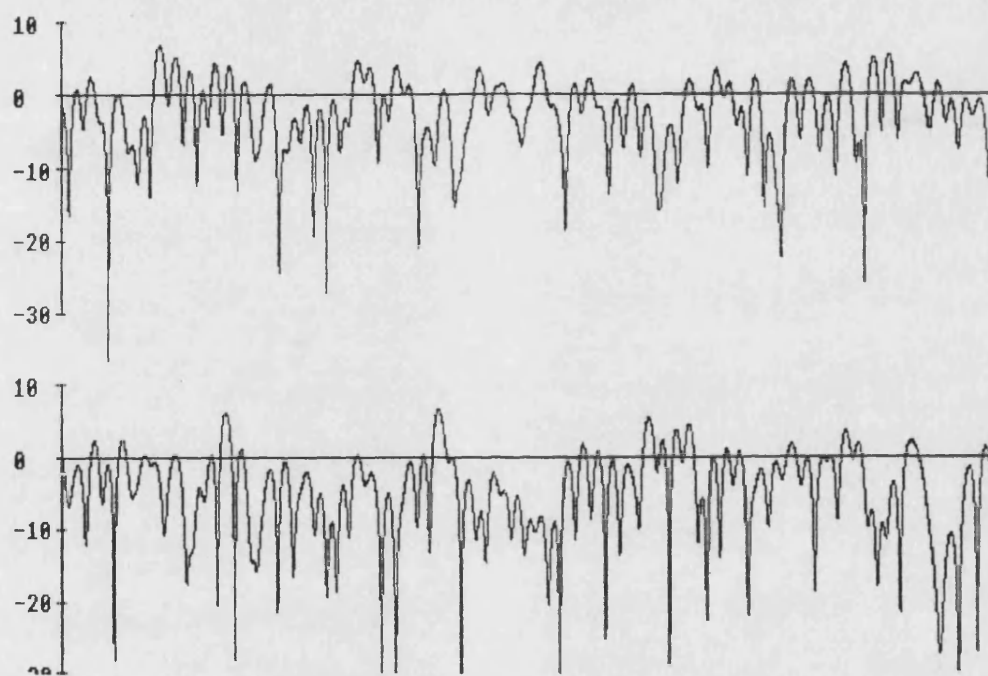
Antenna spacing =27λ

Cross correlation coefficient =0.09

δs =-2.21dB

Figure 4.17   Sample of signal strength data with slow
fading removed received via vertically spaced
antennas from the urban route in Bathwick Street.
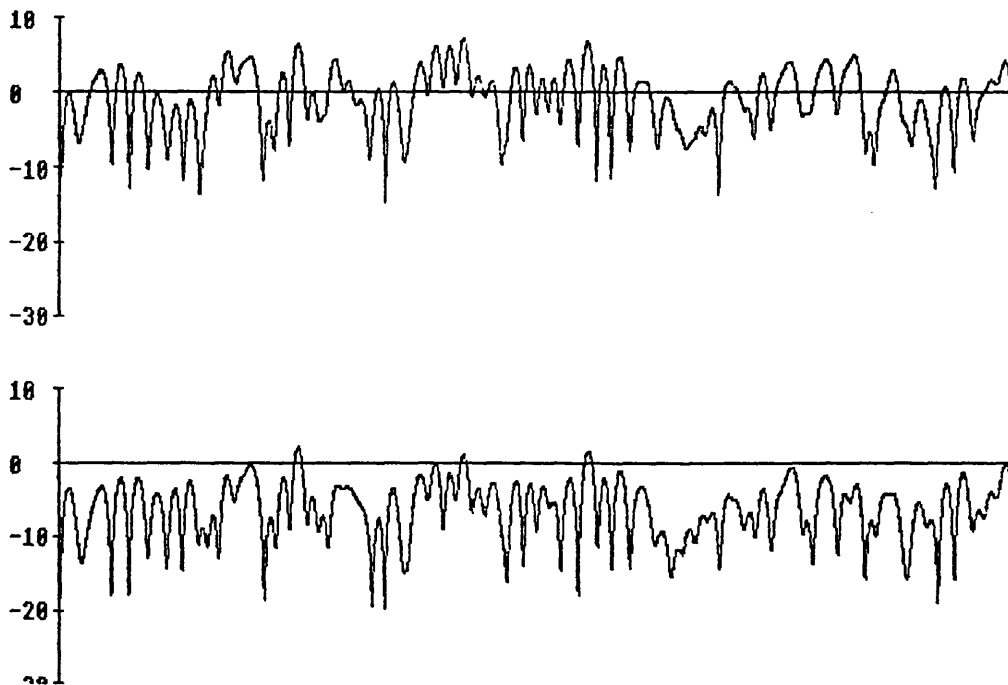
Antenna spacing =27λ

Cross correlation coefficient =0.9

δs =-5.6dB

Figure 4.18   Sample of signal strength data with slow

fading removed received via vertically spaced

antennas from the suburban route in High Street,

Twerton.

Antenna spacing =27λ

Cross correlation coefficient =0.58

δs =-2.58dB

Figure 4.19 Sample of signal strength data with slow
fading removed received via vertically spaced
antennas from the rural route on Dunkerton Hill.

Antenna spacing =6λ

Cross correlation coefficient =0

α_H =61°

Figure 4.20 Sample of signal strength data with slow
fading removed received via horizontally spaced
antennas from the urban route in Bathwick Street.

Antenna spacing =6λ

Cross correlation coefficient =0.012

α_H =29°

Figure 4.21   Sample of signal strength data with slow
fading removed received via horizontally spaced
antennas from the urban route in Bathwick Street.

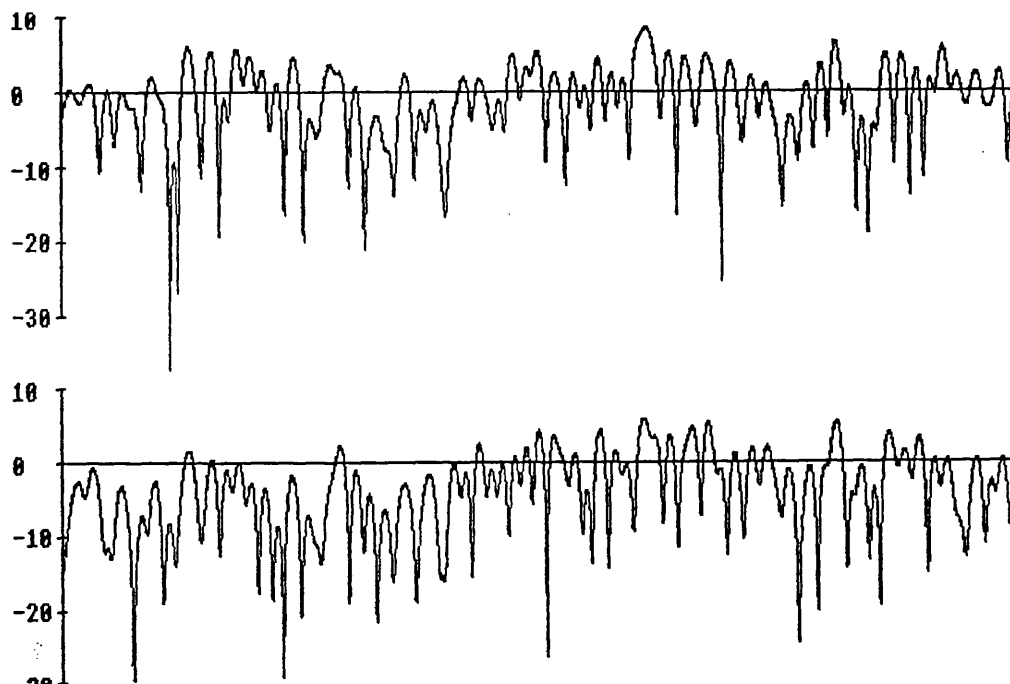Antenna spacing =6λ

Cross correlation coefficient =0.004

α_H =88°

Figure 4.22   Sample of signal strength data with slow
fading removed received via horizontally spaced
antennas from the suburban route in High Street,
Twerton.

Antenna spacing =6λ

Cross correlation coefficient =0.99

α_H =2°

Figure 4.23   Sample of signal strength data with slow fading removed received via horizontally spaced antennas from the suburban route in High Street, Twerton.
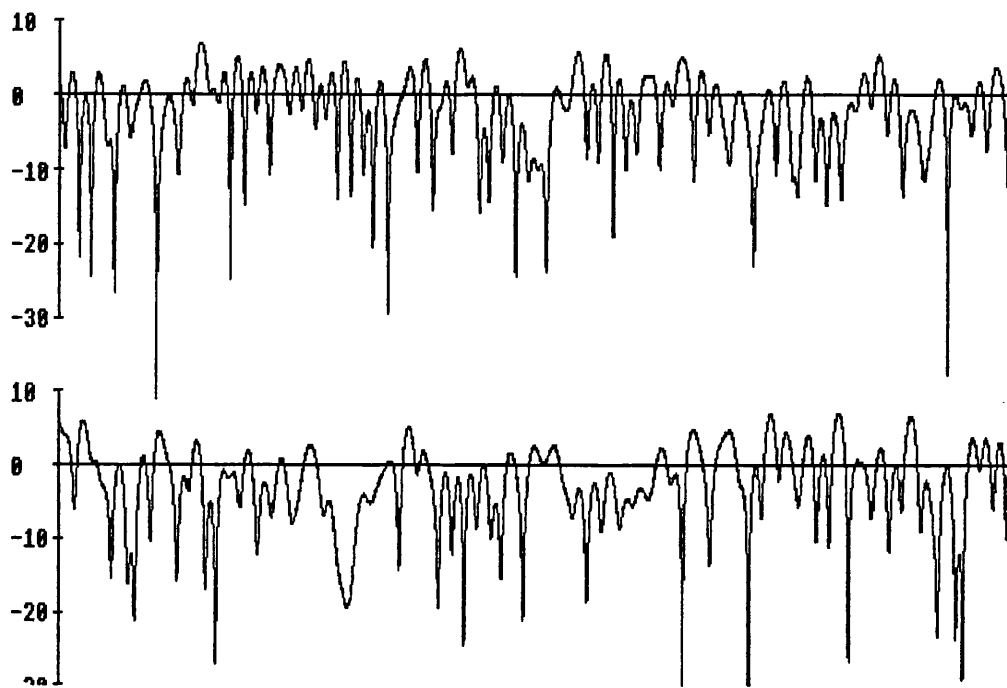
Antenna spacing =6λ

Cross correlation coefficient =0.003

α_H =55°

Figure 4.24 Sample of signal strength data with slow fading removed received via horizontally spaced antennas from the rural route on Dunkerton Hill.
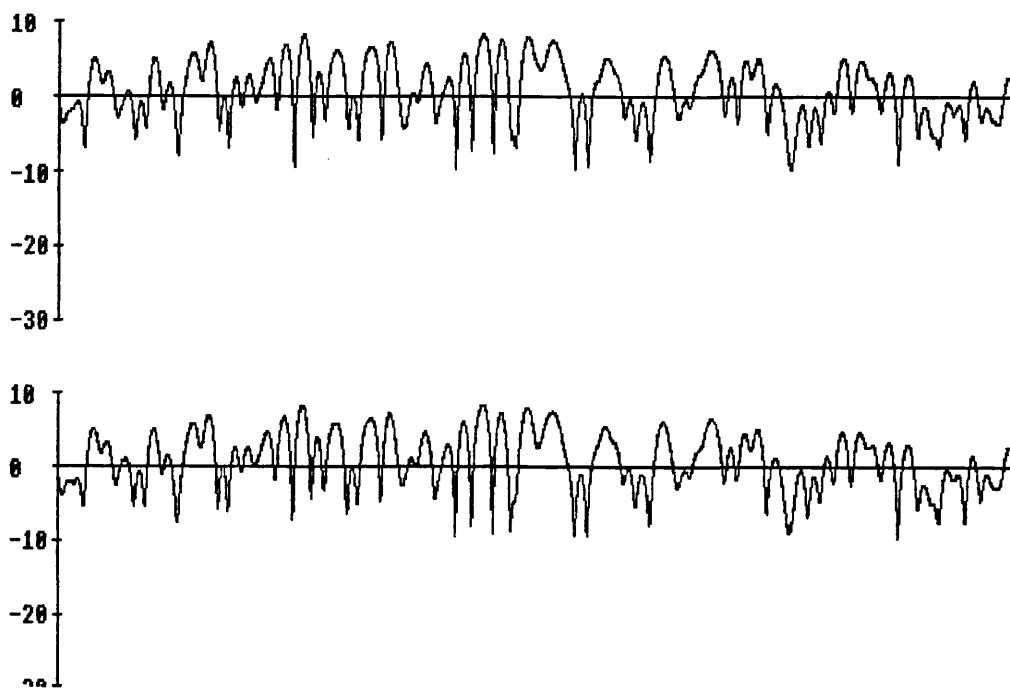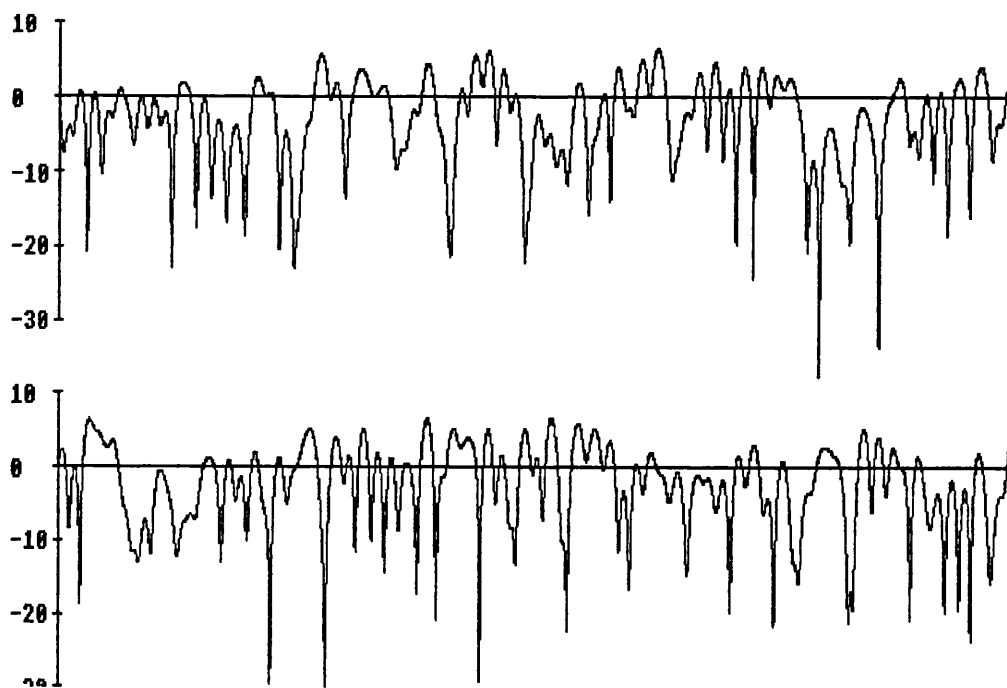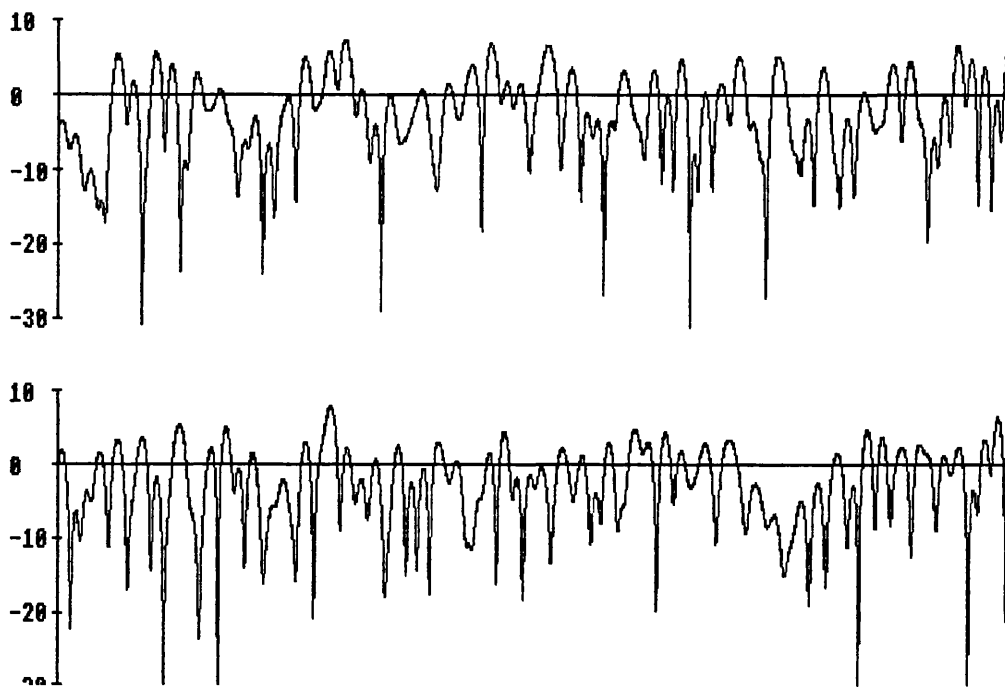
Antenna spacing $=6\lambda$

Cross correlation coefficient $=0.003$

α_H $=35°$

Figure 4.25   Sample of signal strength data with slow
fading removed received via horizontally spaced
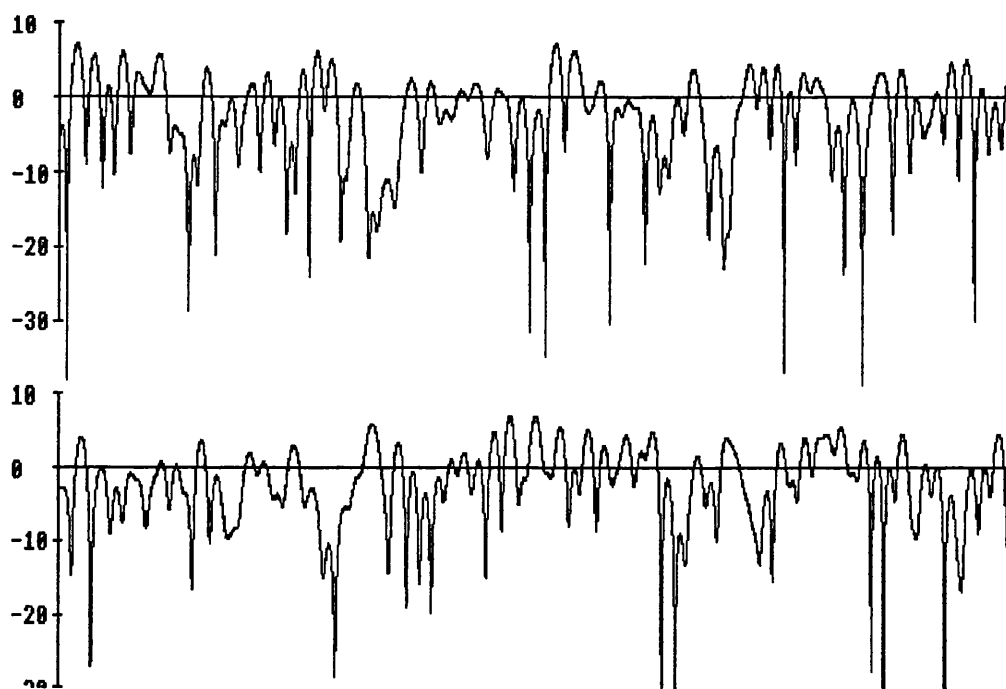antennas from the rural route on Dunkerton Hill.
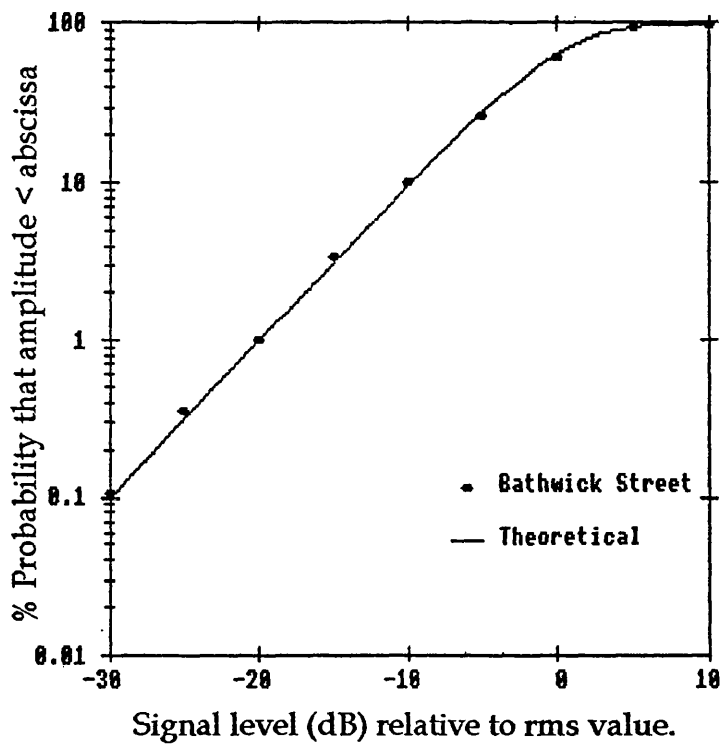
Figure 4.26 Cumulative distribution of fast fading component of signal received from urban test route along Bathwick Street.
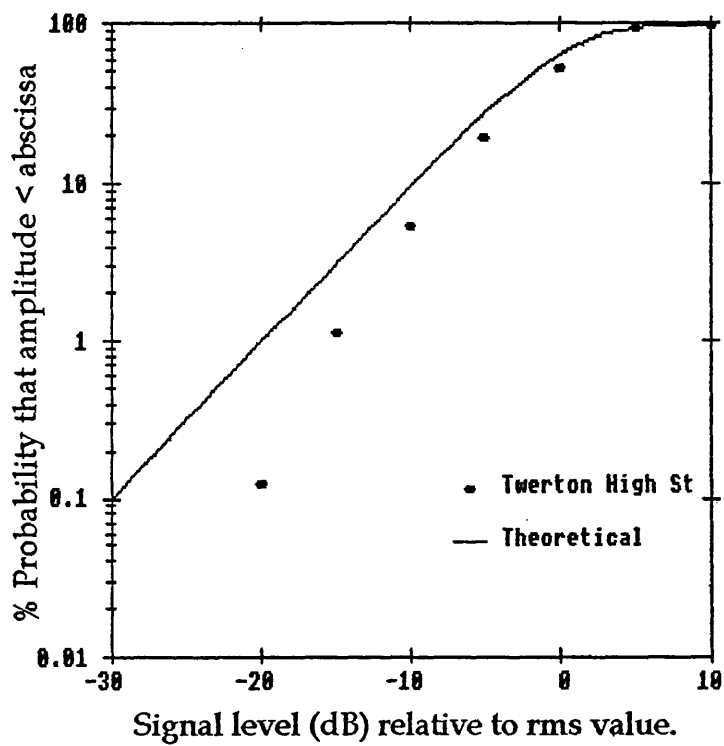
Figure 4.27 Cumulative distribution of fast fading component of signal received from suburban test route along High Street, Twerton.
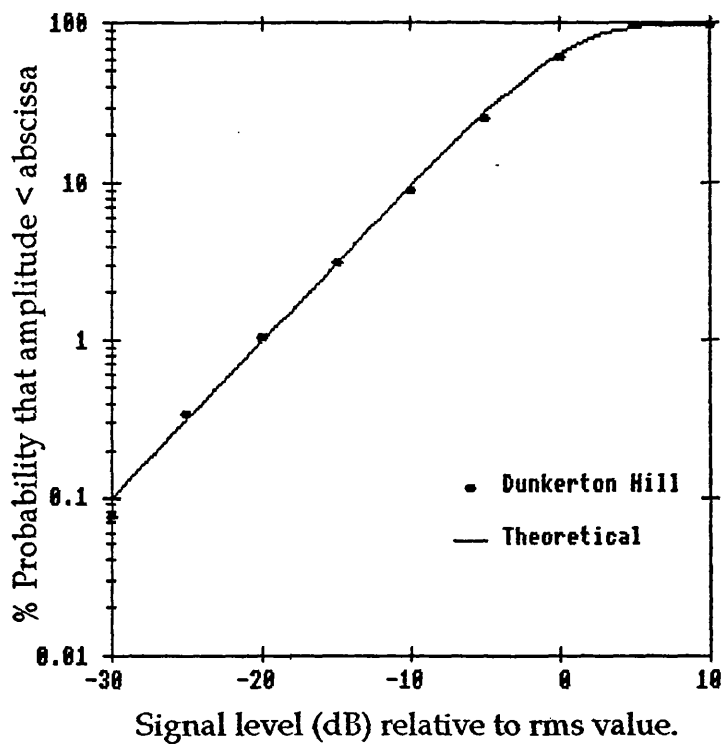
Figure 4.28 Cumulative distribution of fast fading component of signal received from rural test route at Dunkerton Hill
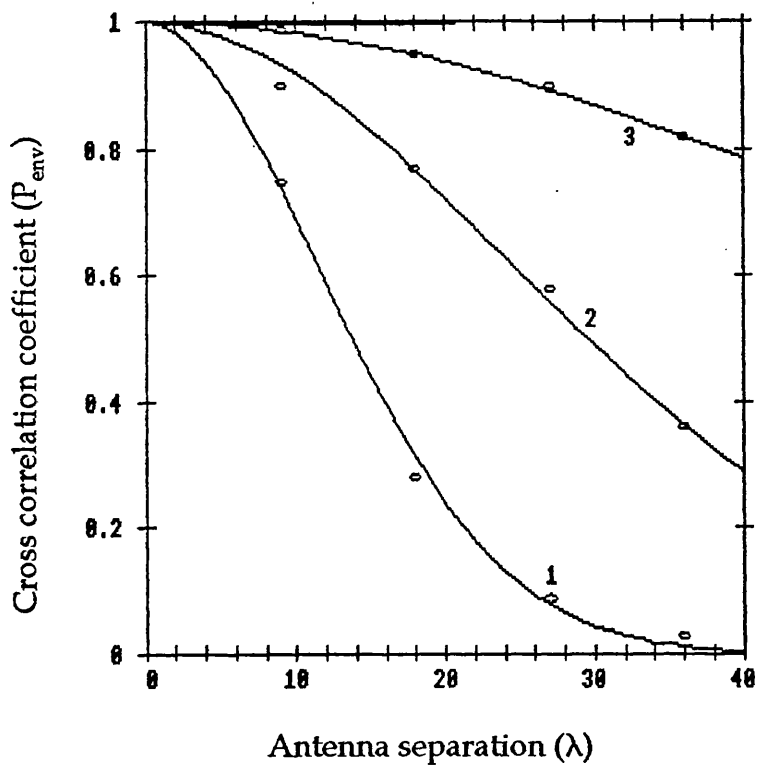
Figure 4.29 Measured cross correlation versus antenna spacing for vertically spaced antennas. (1) Urban route, (2) Rural route and (3) Suburban route.
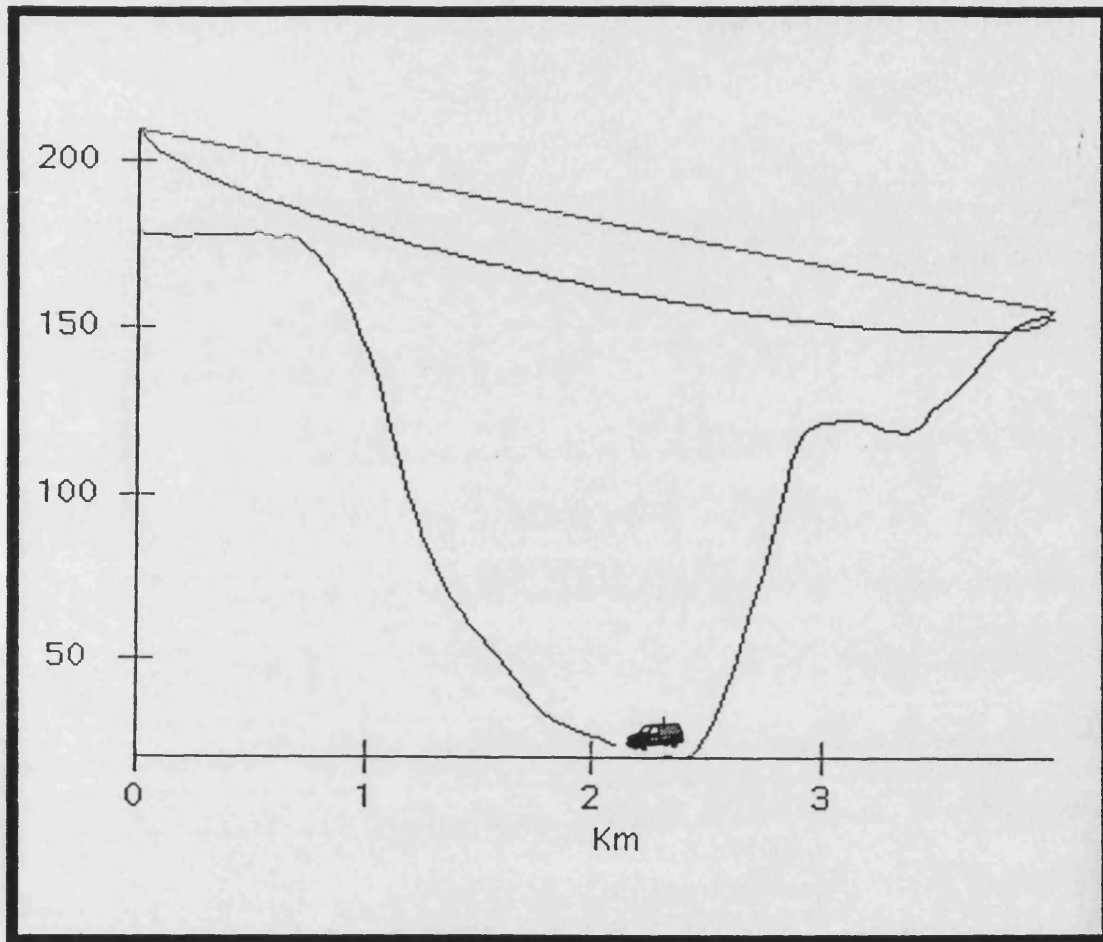
Figure 4.30 Path profile University - Bathwick St and beyond.
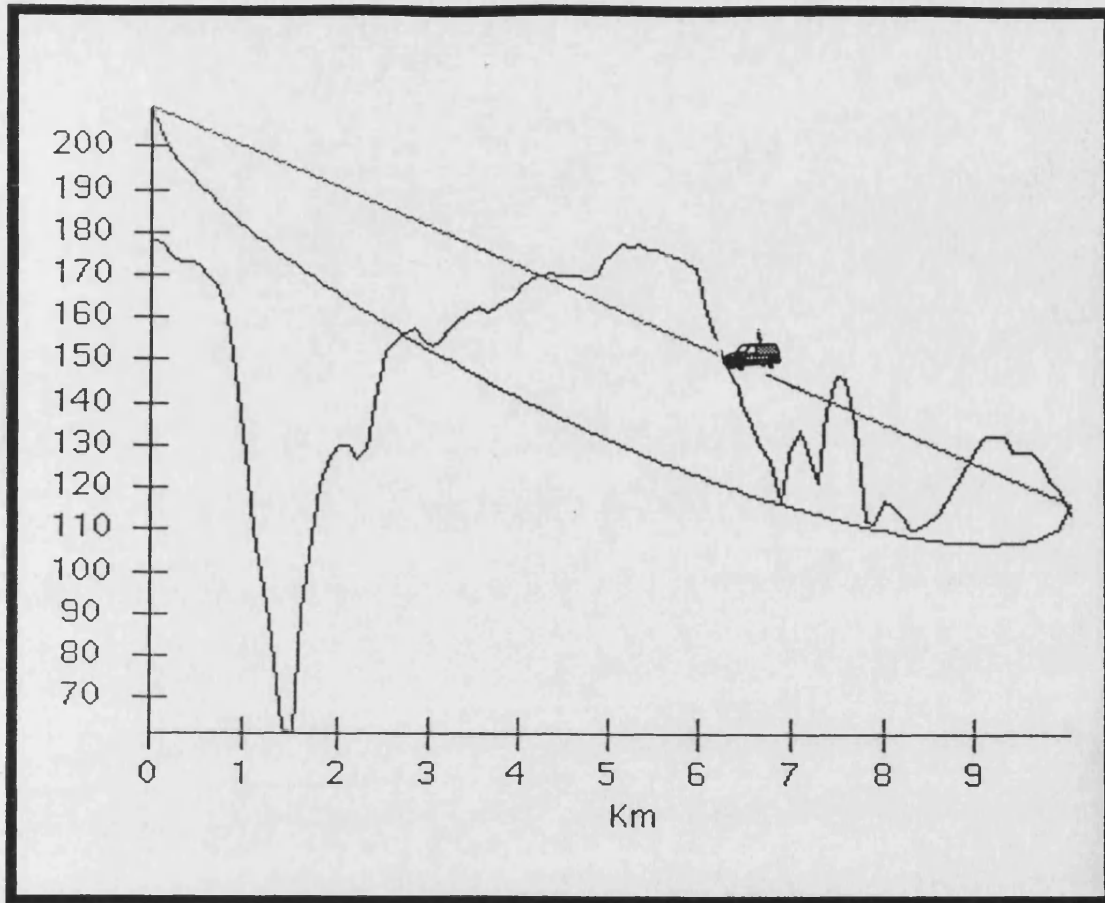
Figure 4.31 Path profile University - Dunkerton Hill
and beyond.

112
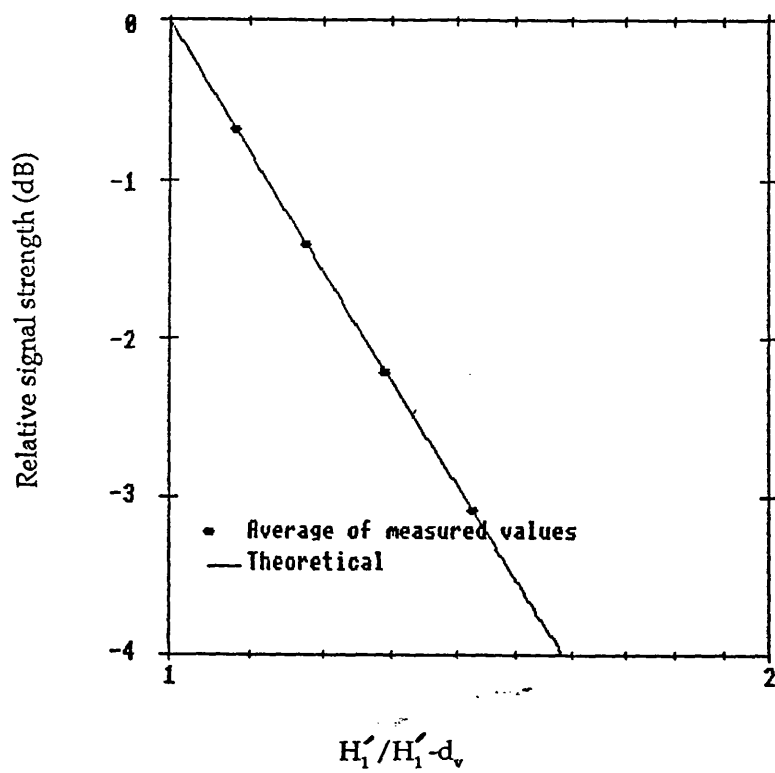
Figure 4.32 Measured and theoretical relative signal
strengths received from the urban test route via the
lower antenna (with respect to that received via the
upper antenna) for different effective antenna
ratios.
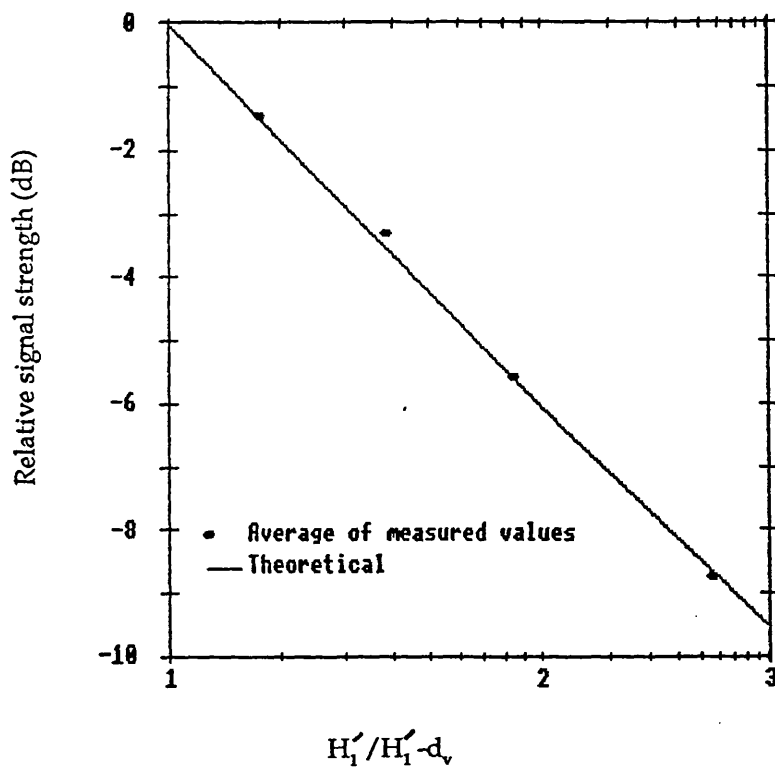
Figure 4.33 Measured and theoretical relative signal
strengths received from the suburban test route via
the lower antenna (with respect to that received via
the upper antenna) for different effective antenna
ratios.
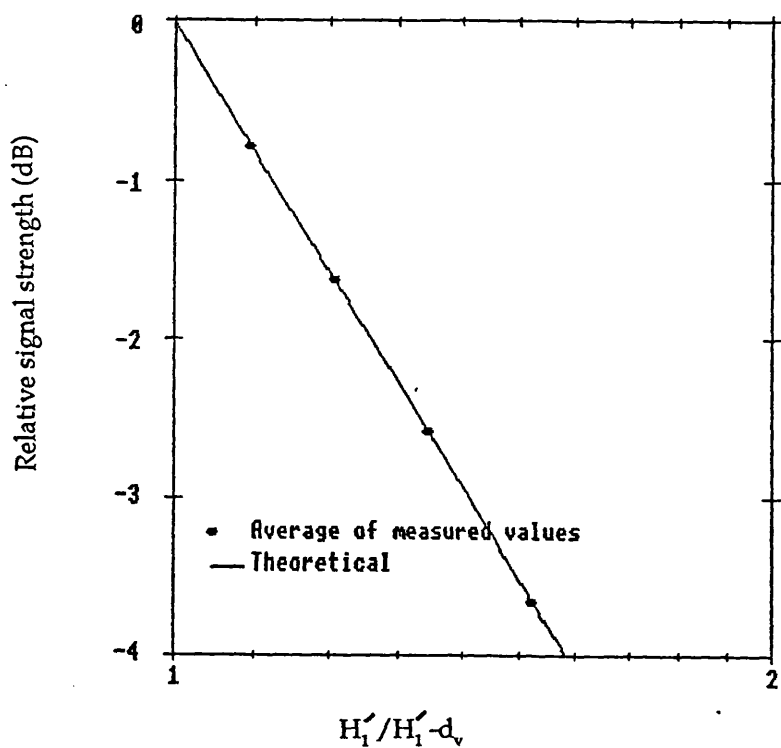
Figure 4.34 Measured and theoretical relative signal strengths received from the rural test route via the lower antenna (with respect to that received via the upper antenna) for different effective antenna ratios.
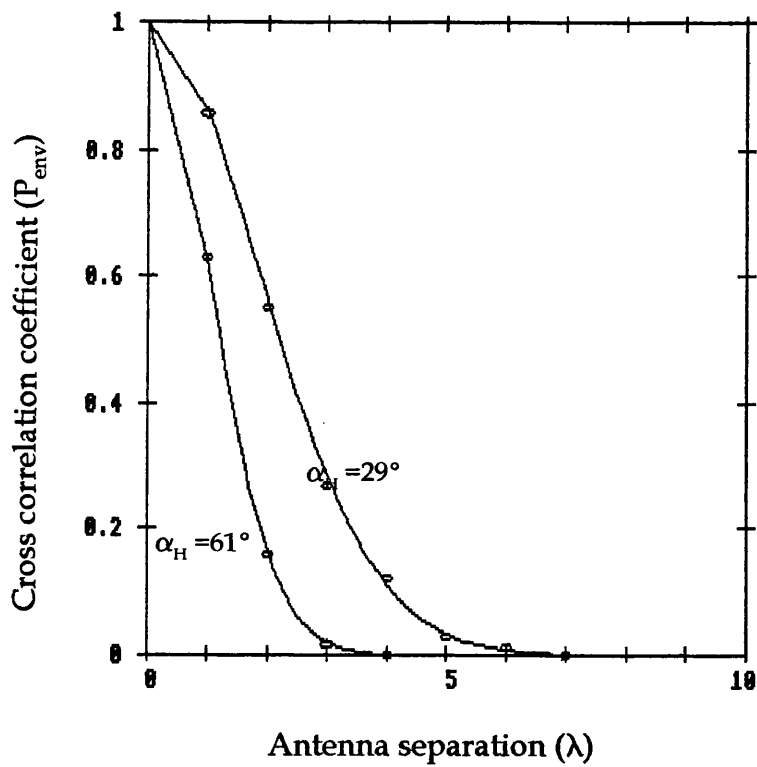
Figure 4.35 Measured cross correlation versus antenna spacing for horizontally spaced antennas using the urban test route.
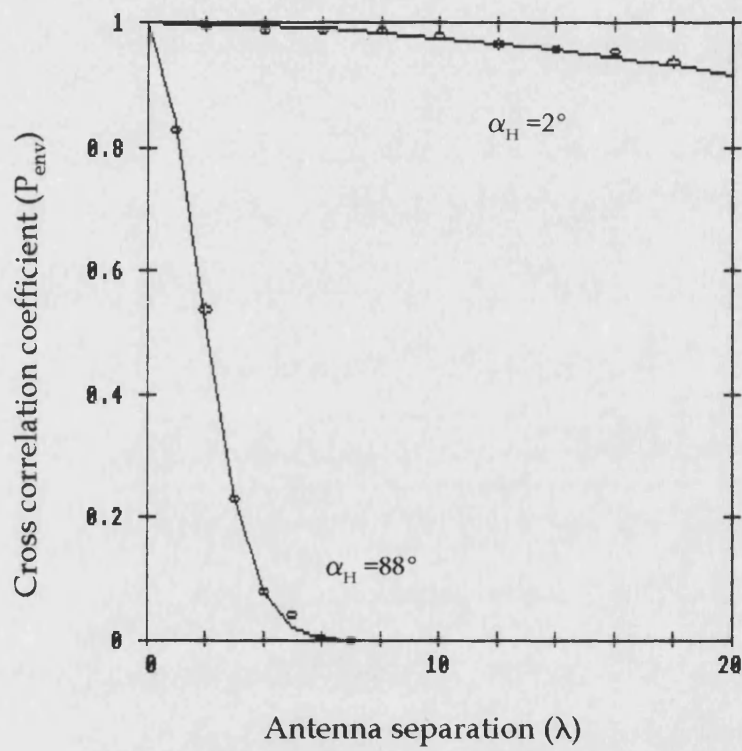
Figure 4.36 Measured cross correlation versus antenna spacing for horizontally spaced antennas using the suburban test route.
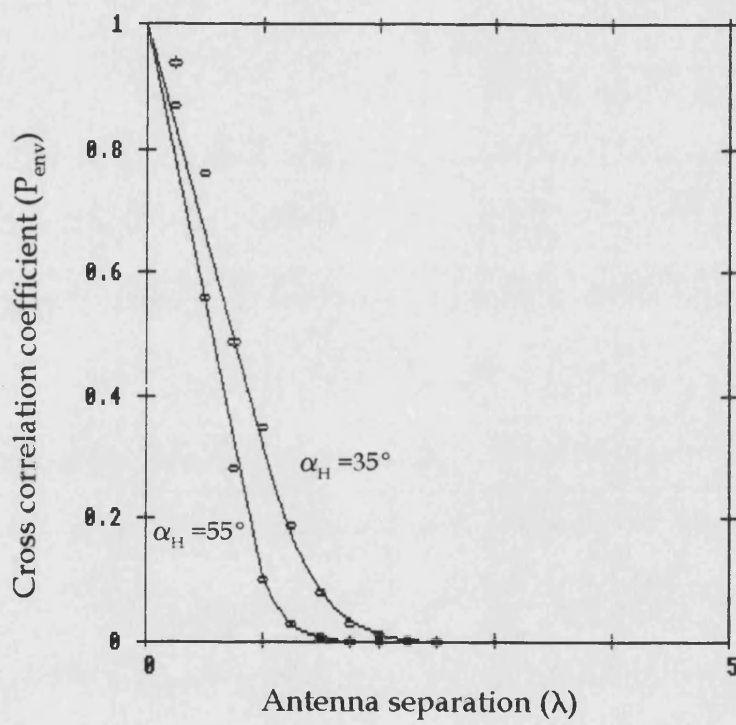
Figure 4.37 Measured cross correlation versus antenna spacing for horizontally spaced antennas using the rural test route.

CHAPTER 5

COMPUTER SIMULATION OF THE NARROW BAND DIVERSITY MOBILE

RADIO CHANNEL.

5.1 Introduction

Having completed and analysed the field measurements

the aim was to produce a computer model of a diversity

mobile radio channel that could simulate the signals

received via two spatially separated base station

antennas. The model must then have the capability to

combine or select the signals and the resultant signal

used to simulate the bit errors that would occur when

the signal was modulated with digital data. The model

would help ascertain what improvements in digital

transmission performance could be obtained from

different configurations of spatially separated base

station antennas. It was clear from the measurements

presented in Chapter 4 that the model should be capable

of simulating the fast and slow fading components. The

two branches must have selectable cross correlation,

mean strength and line-of-sight component.

Various laboratory simulators have been developed which

are capable of simulating the assumed statistical

properties of signals that are subject to propagation

in a mobile radio environment. Hardware simulators are usually based on either the Arredondo or Jakes model.

The Arredondo model shown in Figure 5.1 involves adding in quadrature, the outputs of two balanced modulators fed with uncorrelated low pass filtered Gaussian spectra noise sources. By suitably filtering the Gaussian noise, such that the roll-off frequency is equal to the required Doppler frequency, the required power spectral density of the Rayleigh fading signal is obtained[79-80]. The spectral density is approximated to the theoretical formulation by Clarke[25] and assumes that no significant line-of-sight component exists, the mobile antenna is omnidirectional in the azimuth plane and that the received partial waves are equally likely to originate from all azimuthal directions.

Various simulators based on the Arredondo model but utilising digital signal processors have subsequently been reported. Caples et al extended the model by generating several independent Rayleigh fading signals, subjecting them to time delays and adding them together to produce a Rayleigh distributed signal with excess multipath time delay (frequency selective fading)[81]. Arnold and Bodtmann described a frequency selective fading simulator which provided eight independent channels each with identical delay spreads[82]. Each of these channels is generated by adding eight Rayleigh

distributed signals with exponentially distributed path lengths. Goubran et al[83] developed the Arredondo simulator to include both shadowing and the addition of a line-of-sight component.

The Jakes model[84-85] shown in Figure 5.2 uses No low frequency oscillators with frequencies equal to the Doppler shifts Fm cos(2πn/$\tilde{N}$) n=1,2,...No plus one with frequency Fm are used to generate signals of equal amplitude apart from the last one which is reduced by 1/$\sqrt{2}$. The signals are added together and modulated onto quadrature carriers. The phases β_n of the individual components are chosen appropriately so that the probability distribution of the resultant phase is approximately uniform. The required amplitude and phase relationships are obtained by amplifiers with gains of 2cos β_n or 2sin β_n. From Figure 5.2 it is readily shown that:-

$$x_c(t) = 2 \sum_{n=1}^{No} \cos\beta_n \cos\omega_n t + \sqrt{2}\cos\alpha \cos\omega_m t \qquad 5.1$$

$$x_s(t) = 2 \sum_{n=1}^{No} \sin\beta_n \cos\omega_n t + \sqrt{2}\sin\alpha \sin\omega_m t \qquad 5.2$$

where

$$\beta_n = \frac{\pi n}{\tilde{N}} \qquad \omega_n = \omega \cos(2\pi n/\tilde{N}) \qquad \omega_m = 2\pi \frac{V}{\lambda} \qquad \tilde{N} = 2(2No+1)$$

The phase of the output y(t) must be random and uniformly distributed from 0 to 2π; this can be achieved by making $\alpha=0$.

The widespread availability of personal computers with both increasing memory size and processing speeds provides a means of simulating mobile radio transmission without recourse to special hardware that is not widely available. Fading is inherently a random process and is thus well suited to numerical techniques and thus to computer simulation. Smith described a computer simulation in FORTRAN based on the Arredondo model[86]. Comroe subsequently wrote a BASIC version of the program[87]. In their programs the Gaussian distributed Fourier coefficients of the noise are obtained from a random number generator and weighted by a spectral shaping factor. Two such independent signals are then Fast Fourier Transformed into the time domain and added in quadrature to provide a waveform of the appropriate spectral shape and with a Rayleigh distribution.

The main disadvantages of this Arredondo software model arises from the use of a FFT. Firstly for long time sequences the computation is lengthy and secondly the

sequence lengths are constrained to a radix 2 number and this requires interpolation to provide sequences of other lengths. Software simulation of both the Jakes and Arredondo models have been written. The simulation based on the Jakes model was found to be faster and slightly more accurate and is reported here. The simulation based on the Arredondo model is reported in Annex 2. The accuracy of the Jakes simulation is compared with theoretical formulations of probability distribution, normalised level crossing rates and autocorrelation.

The software is then expanded to provide a computer simulation programme with the following features:-

(i)   Generation of signals composed as required of a Rayleigh distributed signal with the power spectrum associated with vehicle motion, a log-normally distributed shadowing component and a line of site component.

(ii) Generation of diversity channels with both selectable cross-correlation and strength of the multipath component and selectable cross-correlation and standard deviation of the log-normally distributed mean.

The computer model to be described has been written in

a modular fashion using BASIC procedures. It is capable of being extended to provide frequency selective fading, this has not been implemented because the data transmission to be analysed is medium speed (up to 8000 baud) over narrow bandwidth channels.

5.2 Computer simulation of Rayleigh Fading based on the Jakes model.

Equations 5.1 and 5.2 are readily implemented in a discrete form by the procedure PROCjakes_simulation shown in Annex 3. A value of No=8 was used since it was found that there was no improvement in the statistical properties of the simulated signal when this value was increased.The quadrature signal y(t) being obtained by adding equations 5.1 and 5.2 in quadrature and normalising to 0dB. The random phase B_n being generated using the BASIC RND function. The number of samples per second is determined by the value M%. A default value of 10 samples per Doppler Hz is used and the results presented in this chapter are based on this value. Examples of signals generated at Doppler frequencies of 50 and 90Hz are shown in Figure 5.3

5.3 Validity of the simulated Rayleigh signals

The cumulative probability distribution (CPD) of the

124

amplitude of the simulated signals are shown in Figure 5.4 along with theoretical formula based on equation 2.2. The measured CPD is very similar to the theoretical.

Normalised level crossing rates (lcr) of the simulated signals are shown alongside the theoretical values based on equation 2.4 in Figure 5.5. The lcr of the simulated signal follows the theoretical formulation apart from at low signal levels where it deviates slightly.

The autocorrelation function of a function x(nT) provides a useful measure of how dependent a particular value of sample function is on another that is removed in time[88]. For a discrete signal x(nT) of length N samples the autocorrelation can be defined as:-

$$r_j = \frac{1}{N} \sum_{k=1}^{N-j} X(k) \ X(k+j) \qquad 5.3$$

Normalising 5.3 the normalised autocorrelation function becomes:-

$$p(j) = \frac{r(j) - m^2}{r(0) - m^2} \qquad 5.4$$

where m is the mean value of X(nT) given by:-

$$m = \frac{1}{N} \sum_{k=1}^{N} X(k) \qquad 5.5$$

By implementing equations 5.4 and 5.5 in a BASIC procedure PROCautocorrelate, the measured normalised autocorrelation of the simulated Rayleigh signals has been computed using sequence lengths of 10^3 samples and is shown in Figure 5.6. The computed autocorrelation deviates from the theoretical formulation after the first zero crossing*.

5.4 Simulation of correlated Rayleigh signals.

The correlation coefficient of two sequences with signal envelopes x(i) and y(i) is defined by the following relationship:-

$$\rho_{env} = \frac{\sum_{i=1}^{N} (x(i) - \bar{x})(y(i) - \bar{y})}{\sqrt{\sum_{i=1}^{N} (x(i) - \bar{x})^2 \sum_{i=1}^{N} (y(i) - \bar{y})^2}} \qquad 5.6$$

Where x and y are the respective mean values of x(i) and y(i).

The Jakes model is extended to provide correlated signals by correlating the random phases β_n of the two sets of signals. From 5.1 and 5.2 it is readily shown that:-

$$x_{c1}(t) = 2 \sum_{n=1}^{No} \cos \beta_n \cos \omega_n t + \sqrt{2}\cos\alpha \cos\omega_m t \qquad 5.7$$

---

* When the model is subsequently used to simulate received data bit error sequences the effect of this slight departure will not alter the mean bit error rates but it may have a very small effect on the resultant bit error distribution.

$$X_{s1}(t) = 2 \sum_{n=1}^{No} \sin\beta_n \cos\omega_n t + \sqrt{2}\sin\alpha \sin\omega_m t \quad 5.8$$

$$X_{c2}(t) = 2 \sum_{n=1}^{No} \cos\gamma_n \cos\omega_n t + \sqrt{2}\cos\alpha \cos\omega_m t \quad 5.9$$

$$X_{s2}(t) = 2 \sum_{n=1}^{No} \sin\gamma_n \cos\omega_n t + \sqrt{2}\sin\alpha \sin\omega_m t \quad 5.10$$

By generating random phases:-

$$\beta_n = \pi(2RND(1)-1) \quad \epsilon_n = \pi(2RND(1)-1) \quad 5.11$$

Then generating a third phase being a partially correlated version of these two random phases:-

$$\gamma_n = (c_f \beta_n) + (1-c_f)\epsilon_n \quad 5.12$$

for $0 \leq c_f \leq 1$

The relationship between this correlation factor c_f and correlation coefficient p_{env} is shown in Figure 5.7

BASIC procedures were written for maximal ratio, equal gain and selection combining. In the first two procedures the signals were converted to linear form. Using the assumption that the noise associated with

127

each signal was constant, the signals were added as defined in equations 2.32 and 2.33, and converted back to logarithmic form. Selection combining was achieved by selecting the larger of the two signals at each sampling interval. The BASIC procedures are shown in Annex 4. The cumulative probability distribution of the three simulated combiners are shown alongside their theoretical values in Figures 5.8 to 5.10. The distributions of the simulated combiners show reasonable similarity to the theoretical distributions. Figures 5.11 to 5.13 show examples of simulated Rayleigh signals with different degrees of cross correlation and their selectively combined form.

5.5 Simulation of log-normal fading.

In section 2.3 it was stated that the shadowing component of a received mobile radio signal, if measured every few tens of wavelength, is found to be log-normally distributed. One method of generating log-normally distributed random variables with the cumulative distribution function given in equation 2.4 is to carry out a statistical transformation from a random variable with a uniform distribution. Since the required CDF is not explicit, numerical integration is required. A simpler solution to generating the required random variables is to make use of the central limit theorem. A random variable may be obtained by

determining the mean of n independent uniformly distributed samples, which are in the range 0 to 1, when N tends to infinity. The mean value of the resultant distribution is N/2 and the standard deviation is $\sqrt{(N/12)}$. The random variables can be generated with the use of the following:-

$$x_{db}(j) = \sqrt{\frac{12}{N} \sum_{i=1}^{N} rnd_i - \frac{N}{2}} \qquad 5.13$$

rnd_i is the ith of N uniformly distributed random variables in the range zero to unity. The resultant distribution has a mean value of zero and a standard deviation of unity. The expression can be modified to enable random variables to be generated with a standard deviation σ such that:-

$$x_{dB} = \sigma \sqrt{\frac{12}{N} \sum_{i=1}^{N} rnd_i - \frac{N}{2}} \qquad 5.14$$

It is found that a good approximation can be made with a value of N=12. Taking this latter value equation 5.14 simplifies to:-

$$x_{dB} = \sigma \sum_{i=1}^{12} rnd_i - 6 \qquad 5.15$$

Because the shadowing component frequency is directly related to the mobile speed it is useful to be able to

set this frequency as a ratio of the Doppler frequency. For a sequence of log-normal samples a negative zero crossing will occur if $x_{dB}(i) > 1$ and $x_{dB}(i+1) < 1$. The individual probabilities of these events are clearly 0.5, it follows that the probability of a zero crossing occurring between two samples=0.25.

If we generate a log-normal sample every a wavelengths at a Doppler frequency of F_n the time between log-normal samples τ_s is given by:-

$$\tau_s = \frac{a}{F_n} \qquad 5.16$$

If on average we get one zero crossing per four log-normal samples then the shadowing frequency (F_s) is given by:

$$F_s = \frac{1}{4a/F_n} = \frac{F_n}{4a} \qquad 5.17$$

The ratio of shadowing to Doppler frequencies is therefore given by:-

$$\frac{F_s}{F_n} = \frac{1}{4a} \qquad 5.18$$

Whilst the Rayleigh distributed samples are necessarily generated at short intervals (at least 10 samples per Doppler Hz and when simulating data transmission at

1/bit rate) the log-normal samples are generated over several tens of wavelength (typically 30). This necessitates interpolating the log-normal samples to intervals equal to the reciprocal of the Rayleigh sampling rate as shown in Figure 5.14, so that the two components can be combined. If the mobile is experiencing a Doppler frequency shift F_n as defined in equation 2.9, then a log-normal sample is required every a/F_n seconds. Consequently the number of shadowing components (N_{sh}) to be interpolated between each log-normal sample is given by:-

$$N_{sh} = \frac{Ms}{F_n} \qquad 5.19$$

Where s is the sample rate of the Rayleigh signal sequence onto which the shadowing component is to be added. The procedure used to generate these shadowing components is PROCshaddowing and is outlined in Figure 5.15. Examples of Rayleigh fading signals superimposed on a log-normally distributed mean are given in Figure 5.16.

Figure 5.17 shows the close correlation between the theoretical and measured cumulative distributions. Because the log-normal fading is not dependent on the Doppler frequency its validity is only required for its amplitude distribution.

Using simulated sequences of N=10⁴ (corresponding to
100 seconds) the autocorrelation of a number of
simulated signals have been calculated and are shown in
Figures 5.18 to 20. These indicate that the length of
memory is inversely proportional to the Doppler
frequency and secondly that the existence of shadowing
significantly increases the length of memory.

5.6 Simulation of correlated log-normally distributed signals.

By generating two independent log-normal signal
sequences Xi_n and Xj_n a third sequence Xk_n can be
formed by correlating the first two with a correlation
factor c_f where $0 \leq c_f \leq 1$:-

$$Xk_n = c_f Xi_n + (1 - c_f) Xj_n \qquad 5.20$$

The correlation coefficient of the two sequences Xi_n and
Xk_n has been computed (using equation 5.3) and is
related to the correlation factor as shown in Figure
5.21.
Examples of log-normal signals with varying degrees of
correlation are shown in Figures 5.22 and 5.23.

5.7 Simulation of line of sight component.

A line of sight component is generated in PROCricean by
adding, in linear form, a constant signal to the

132

Rayleigh signal. Figure 5.24 shows how the effect of a line-of-sight component, at different levels with respect to the Rayleigh signal, reduces the fading.

5.8   Generation of bit errors.

Having produced a software model of the mobile radio channel the next stage was to extend the model to allow it to simulate the bit errors that would be generated when data was transmitted on the channel. In Chapter 2 the inevitable fading experienced on a land mobile radio channel as a result of multipath propagation and time-variant shadowing has been analysed. This fading causes the signal level to become comparable with the noise resulting in bit errors in the received data by three independent processes.

i. Time variation of the received signal to noise ratio.

If the probability of bit error at a given signal/noise ratio (SNR) is distributed according to a density function $P(\gamma)$, but remains approximately constant during a bit, then the overall probability of bit error, $Pe(\gamma)$, is given by

$$\overline{Pe}(\gamma) = \int_0^\infty Pe(\gamma) P(\gamma) \, d\gamma \qquad 5.21$$

ii. Random FM noise arising from the statistical phase fluctuations of the received signal.

The phase fluctuations of the received RF signal are characterised by a random frequency modulation. The characteristics of this random FM noise are well understood in terms of its probability distribution and power spectrum[89]. The effect on data transmission is to generate random errors irrespective of the received signal level. The bit error rate is termed irreducible and has been reported for many FSK and PSK based systems[90-92].

The irreducible bit error probability due to random FM for FM systems utilising limiter/discriminator detection can be shown to be given by[93]:

$$Pe_{IBER} = \frac{1}{2}(1 - \sqrt{2}\frac{F_D}{F_d}(1 + 2\frac{F_D^2}{F_d^2})^{-\frac{1}{2}})$$ 5.22

where F_d=Doppler fading frequency.

and F_D=Peak deviation of the FM systems.

iii. Time delay associated with multi-path propagation. This thesis is concerned with narrow-band systems supporting data rates of up to 9600 bits/sec and consequently this error process can be ignored.

Another cause of bit errors is man-made impulsive noise arising primarily from automobile ignition systems,

power lines and industrial machinery (see Annex 5).
Base station antennas are usually sited clear of
sources of man made noise sources and this contribution
can usually be ignored at the base station particularly
at UHF. Other sources of bit error exist due to
cochannel interference and intermodulation. These
contributions can be minimised by careful system design
and are not given further consideration.

5.9 Relationship between signal to noise levels and probability of bit error.

In order to simulate the generation of bit errors it is
clearly necessary to know the relationship between
signal/noise ratio and the probability of bit error and
the relationship between Doppler frequency and
probability of irreducible bit error. Measurements of
the relationship between signal/noise level and
probability of bit error have been made for a number of
data modulation schemes and bit rates. These
measurements are reported in Annex 6. Empirical
relationships were produced from the measured results
and these relationships used in the DMRCS to predict
the performance of different modulation schemes. The
measurements reported here are with 8000bits/sec GMSK
using a BT value of 0.3 (BT is the 3dB signal bandwidth
in KHz multiplied by the bit duration in ms). For the
modem used, which was typical of those used in public

mobile data networks, the following relationship was found.

$$Pe(\gamma) = \frac{1}{2} e^{-(.503\gamma^{.724})} \qquad 5.23$$

The empirical relationship between the fading frequency and irreducible error rate for the GMSK modem is given by:-

$$Pe_{IBER} \approx 7.9 \ x \ 10^{-6} \ 10^{.0325F_d} \qquad 5.24$$

for 5Hz $\leq F_d \leq$ 50 Hz

5.10 Simulation of bit errors.

The procedures used to simulate bit errors are summarised in Figure 5.25. The simulations were undertaken at a sample rate equal to the data bit rate so that a signal strength sample corresponded to each bit. This provided a probability of bit error to be available for each data bit. These values were combined with the irreducible bit error probabilities. The mechanisms described in sections 5.8 for generating bit errors are independent and the analysis required to ascertain their cumulative effect can therefore be

undertaken independently. The combined probability of bit error is given by:-

$$\dot{P}e(\gamma) = Pe(\gamma) + Pe_{IBER} - Pe(\gamma) Pe_{IBER} \qquad 5.25$$

for $Pe(\gamma) > Pe_{IBER}$

and:-

$$\dot{P}e(\gamma) = Pe_{IBER} \qquad 5.26$$

for $Pe(\gamma) < P$.

These equations are implemented in PROCiber. For very small values of bit error probability such that $Pe(\gamma)Pe_{IBER} \ll Pe(\gamma) + Pe_{IBER}$ then the combined probability is effectively the sum of the two error probabilities.

In order to generate an error sequence use was made of the BASIC random number generator RND which provides random numbers between zero and unity. For each data bit with probability of error Pe an error was generated if Pe< RND. This error sequence, ei, is defined as:

$$ei = ti \oplus ri \qquad 5.27$$

where ti and ri are the transmitted and received data sequences.

5.11 Application of the DMRCS in predicting data transmission performance.

In order to interpret the simulated bit error sequences various BASIC procedures were written to provide statistics on the error distributions. One such procedure was PROCbler which divided the simulated bit error sequence into blocks and determined the cumulative distribution of errors in each block.

Using the parameters in Table 5.1 simulations were made to examine the benefit of diversity on reducing the block error rates on the fringe of radio coverage.

DMRCS Simulation Parameters	
Signal Branch 1	0 dBμV
Signal Branch 2	0 dBμV
Doppler Frequency	20 Hz
Standard deviation of local mean	0 dB
Data Modulation	8 kbps GMSK
Data Sequence Duration	1000 seconds
Correlation coefficient i	1 (single branch)
ii	0.7
iii	0

Table 5.1 Parameters used to determine the cumulative distribution of errors in a 512 bit block.

Figure 5.26 illustrates the cumulative distribution of errors in blocks of 512 bits for different values of envelope cross correlation.
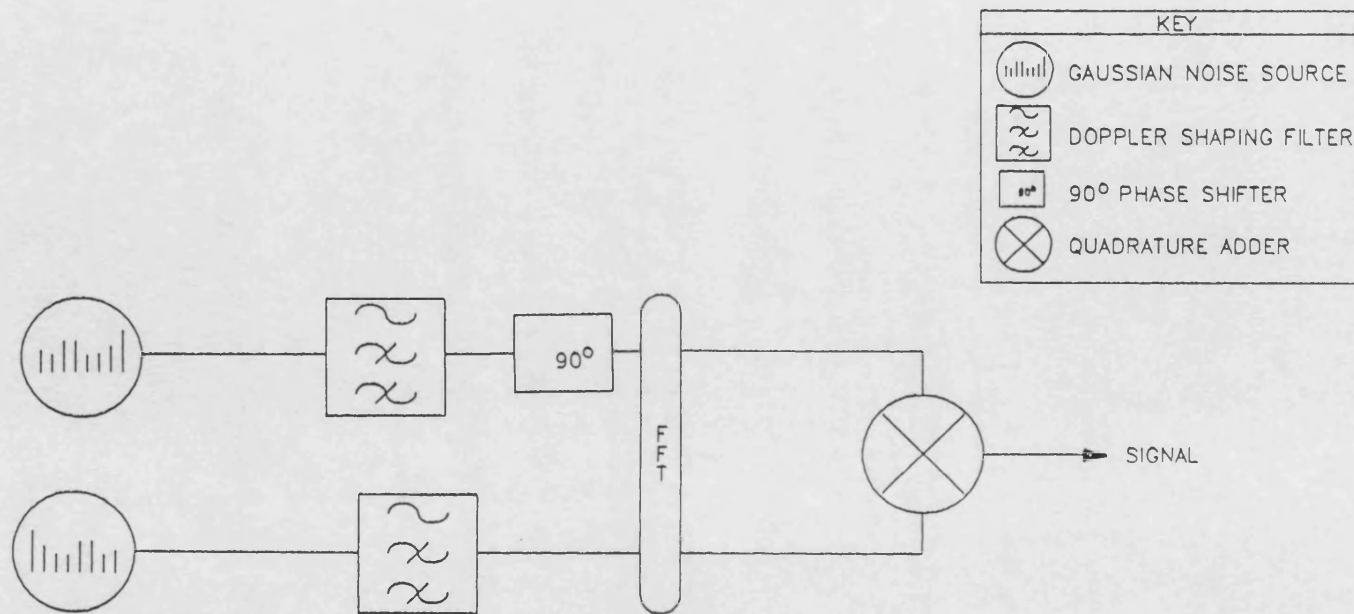
Figure 5.1 Schematic of the Arredondo Rayleigh fading simulator.
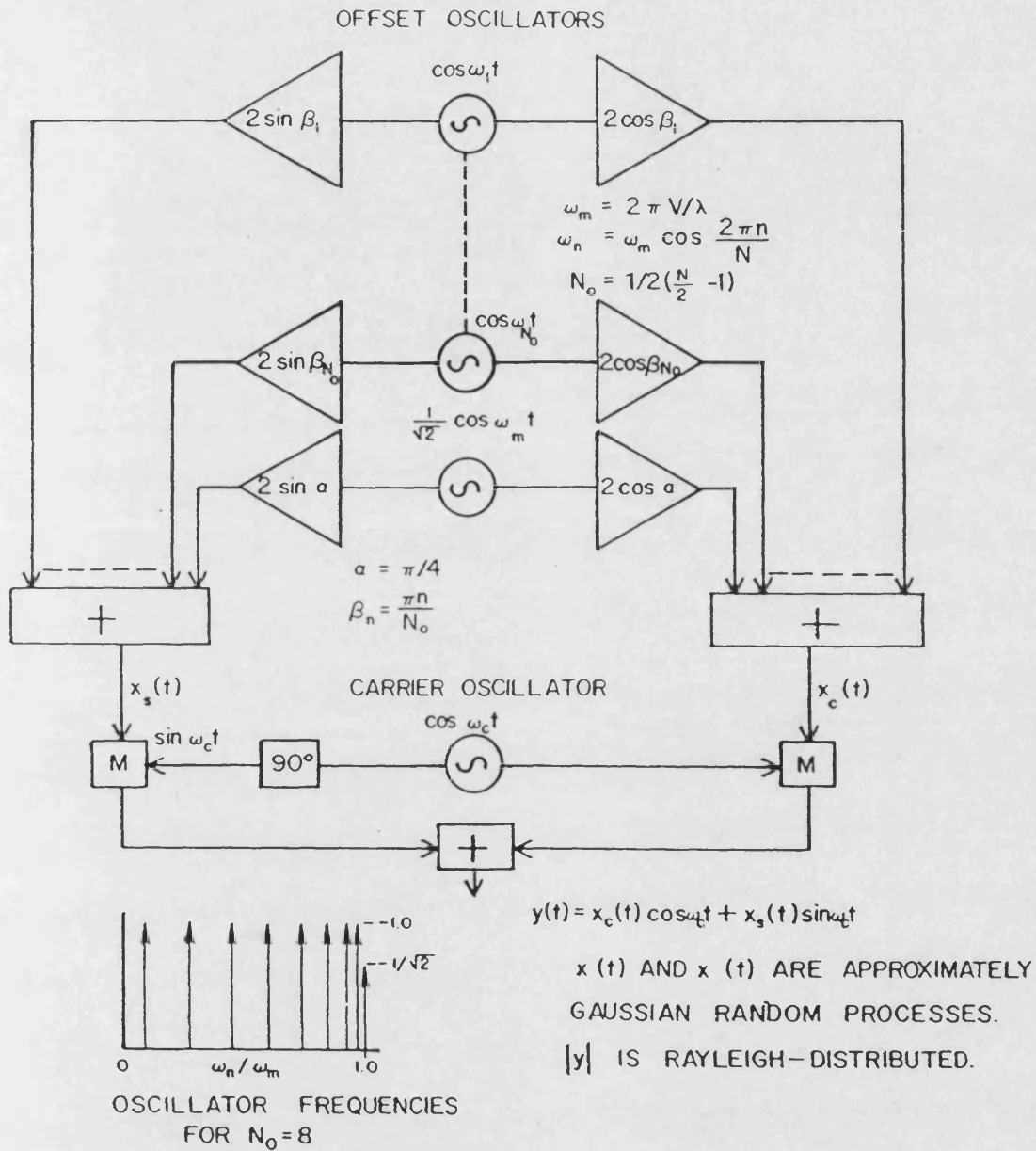
Figure 5.2 Schematic of the Jakes Rayleigh fading simulator.
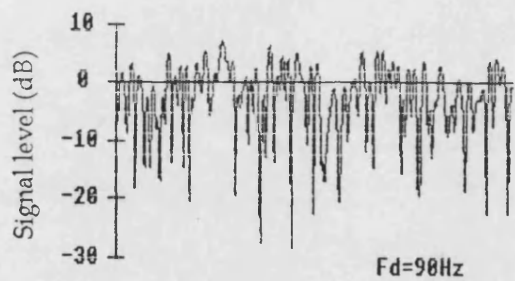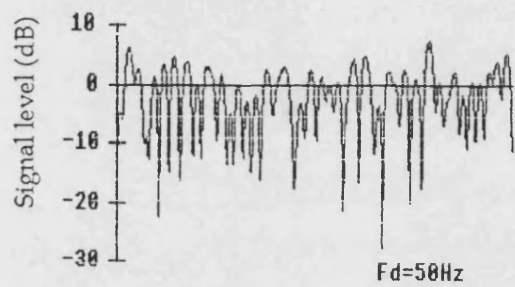
Figure 5.3   Simulated Rayleigh signals with Doppler
frequencies of 50 Hz and 90 Hz using Jakes type
simulator. The horizontal scale corresponds to one
second in time.
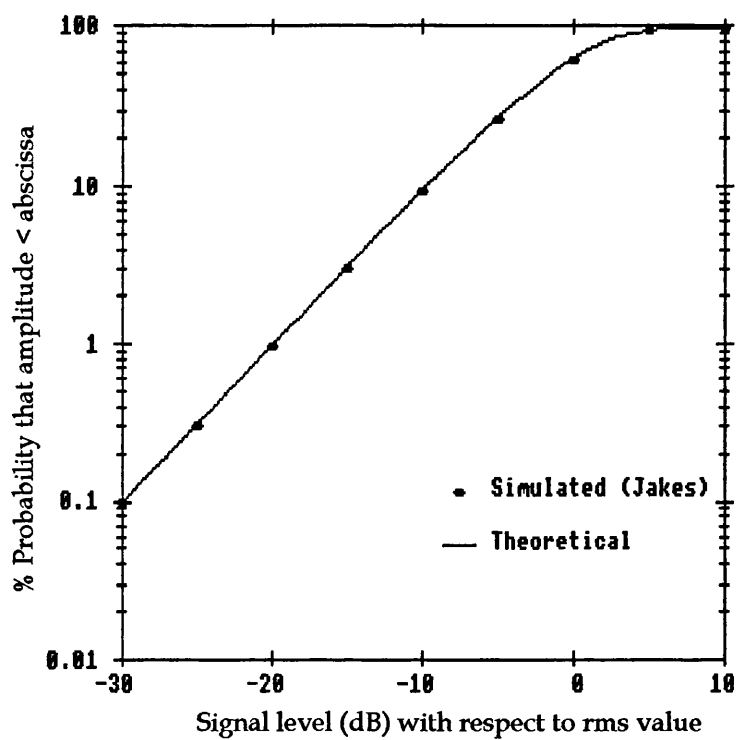
Figure 5.4 Cumulative distribution of theoretical and simulated Rayleigh signals.
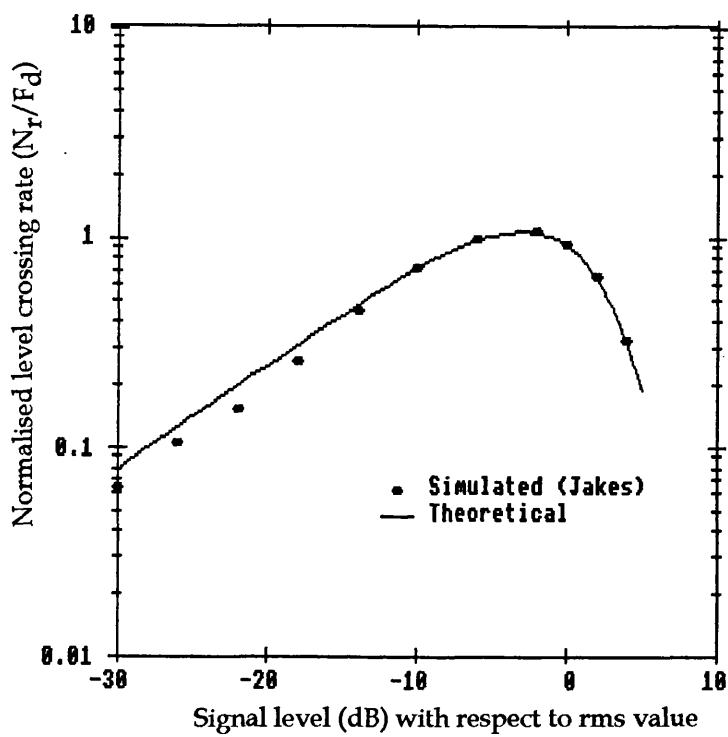
Figure 5.5   Normalised level crossing rates using Jakes
simulator.
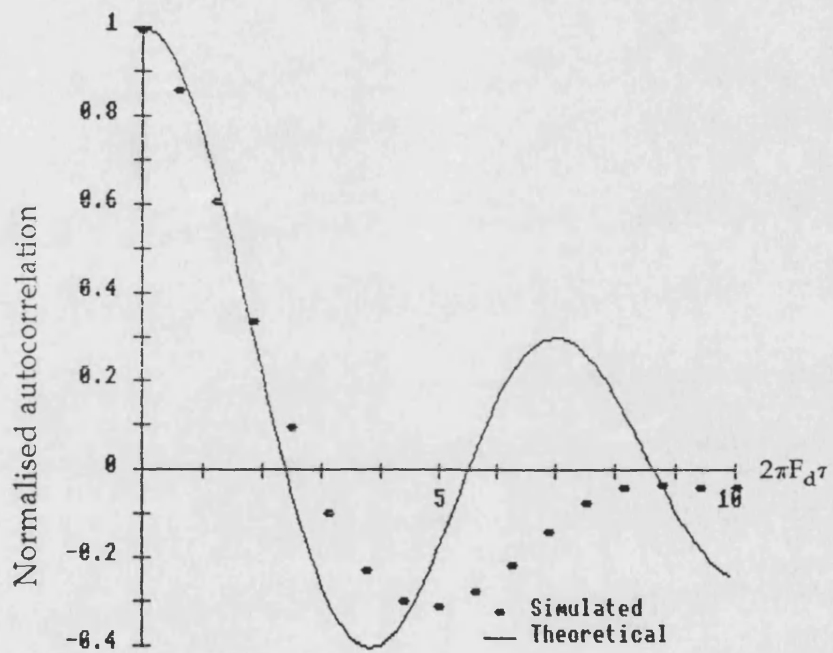
Figure 5.6 Computed auto-correlation of simulated Jakes simulator.
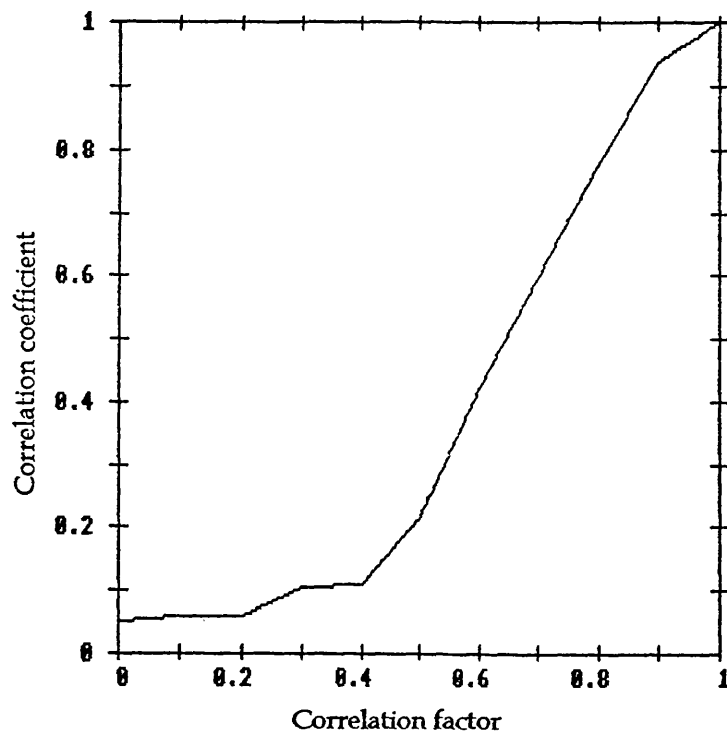
Figure 5.7 Relationship between Correlation factor and
correlation coefficient (Jakes model).
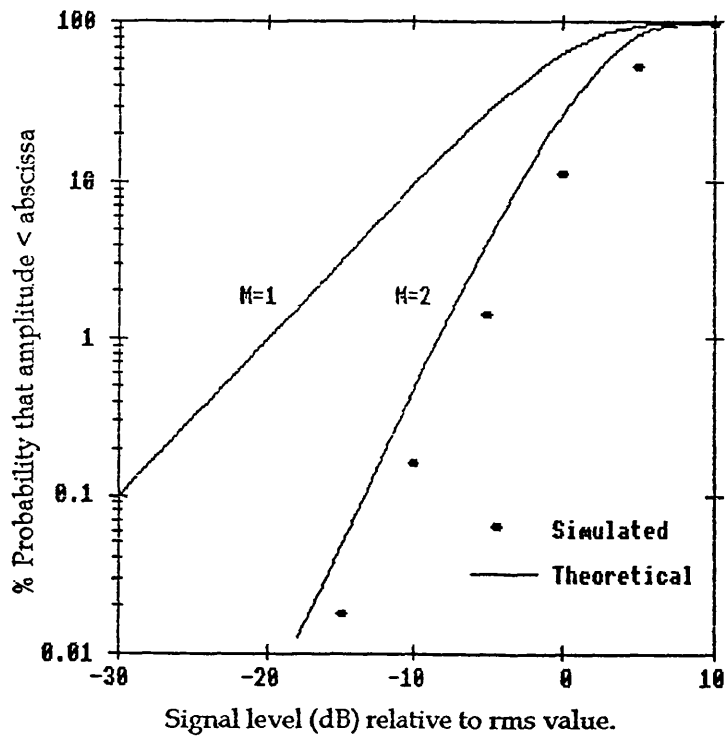
Figure 5.8 Cumulative probability distribution for simulated maximal ratio combiner.
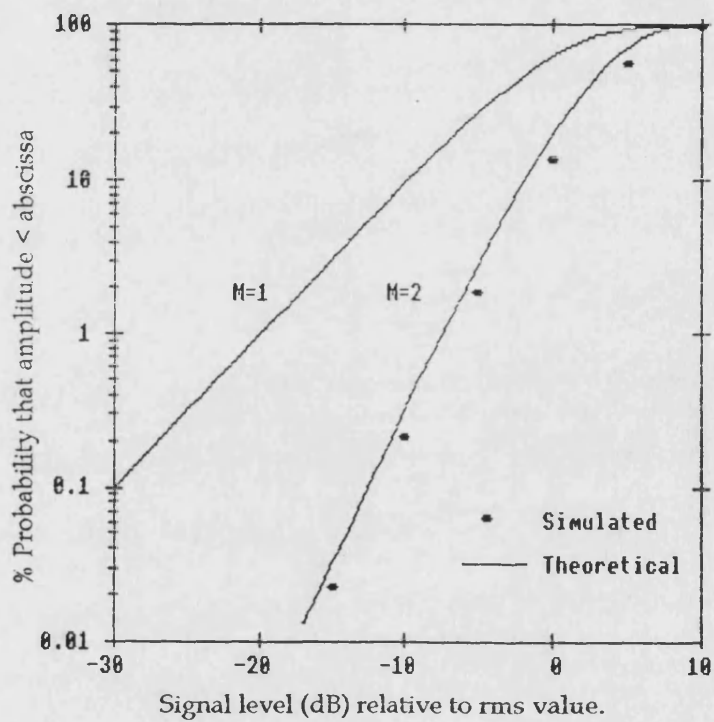
Figure 5.9 Cumulative probability distribution for simulated equal gain combiner.

147
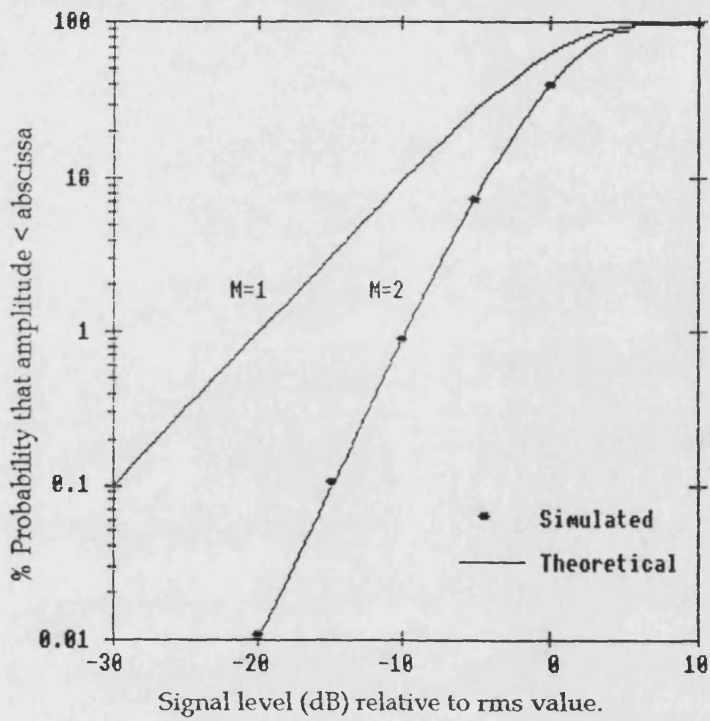
Figure 5.10   Cumulative probability distribution for
simulated selection combiner.
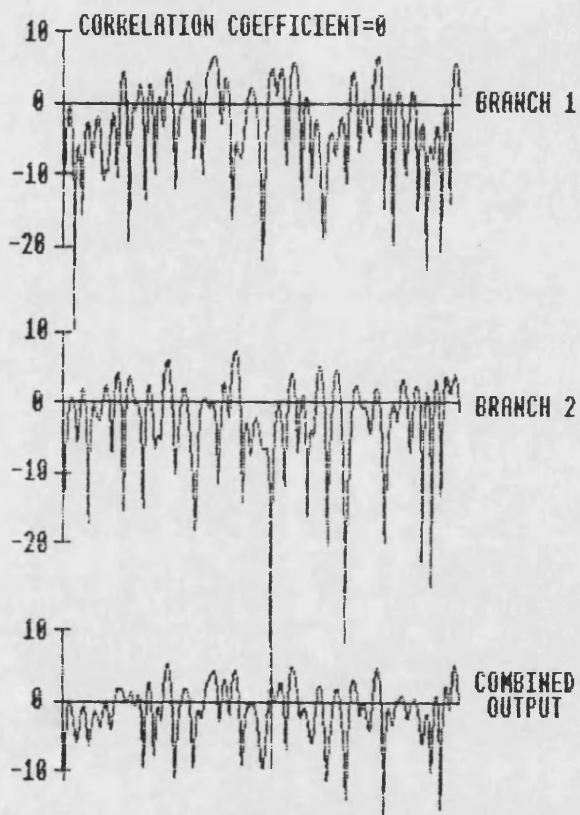
Figure 5.11 Simulated uncorrelated diversity Rayleigh
signals with the selective combined output.

149
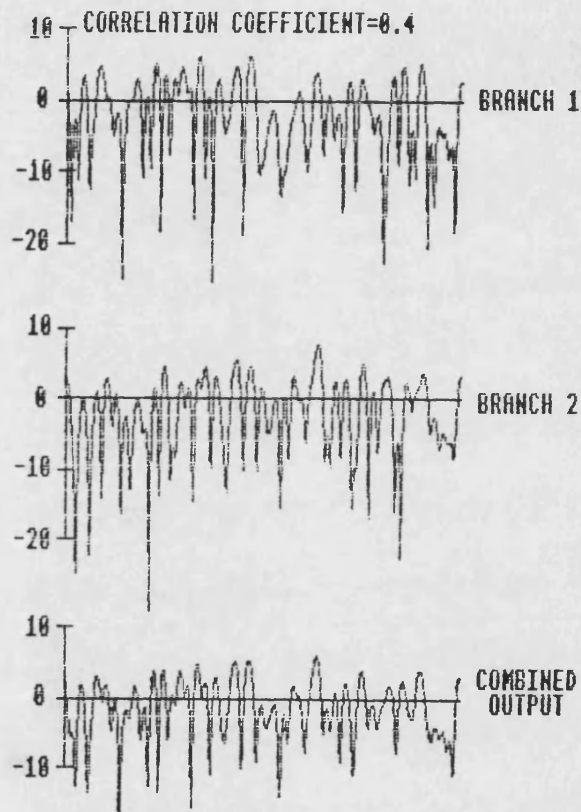
Figure 5.12 Simulated diversity Rayleigh signals (with cross correlation of 0.4) and the selectively combined output.
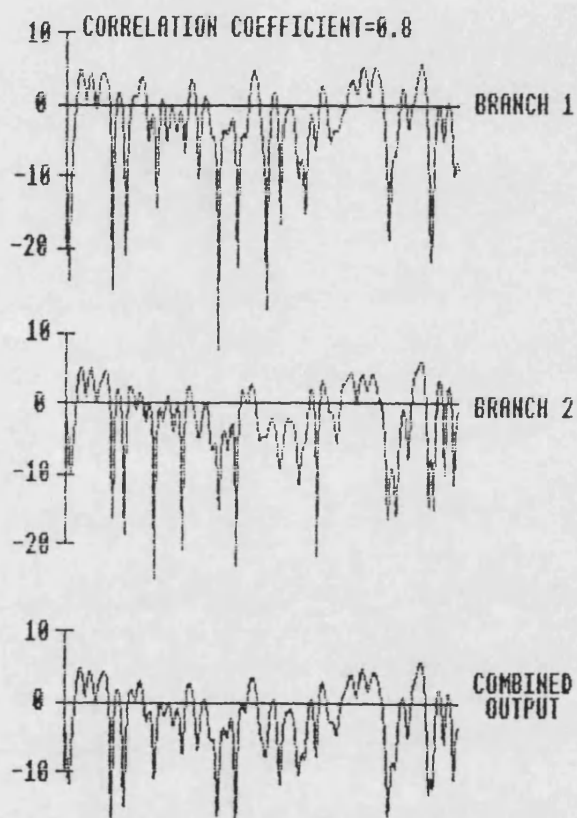
Figure 5.13 Simulated diversity Rayleigh signals (with a cross correlation of 0.8) and the selectively combined output.
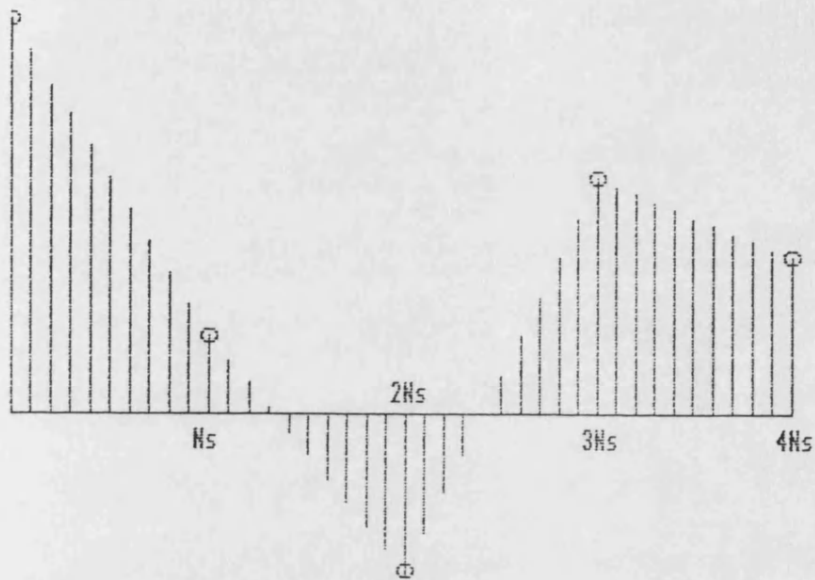
Figure 5.14   Interpolation of log-normally distributed samples (generated every 30 wavelengths) to provide samples at the sampling rate.
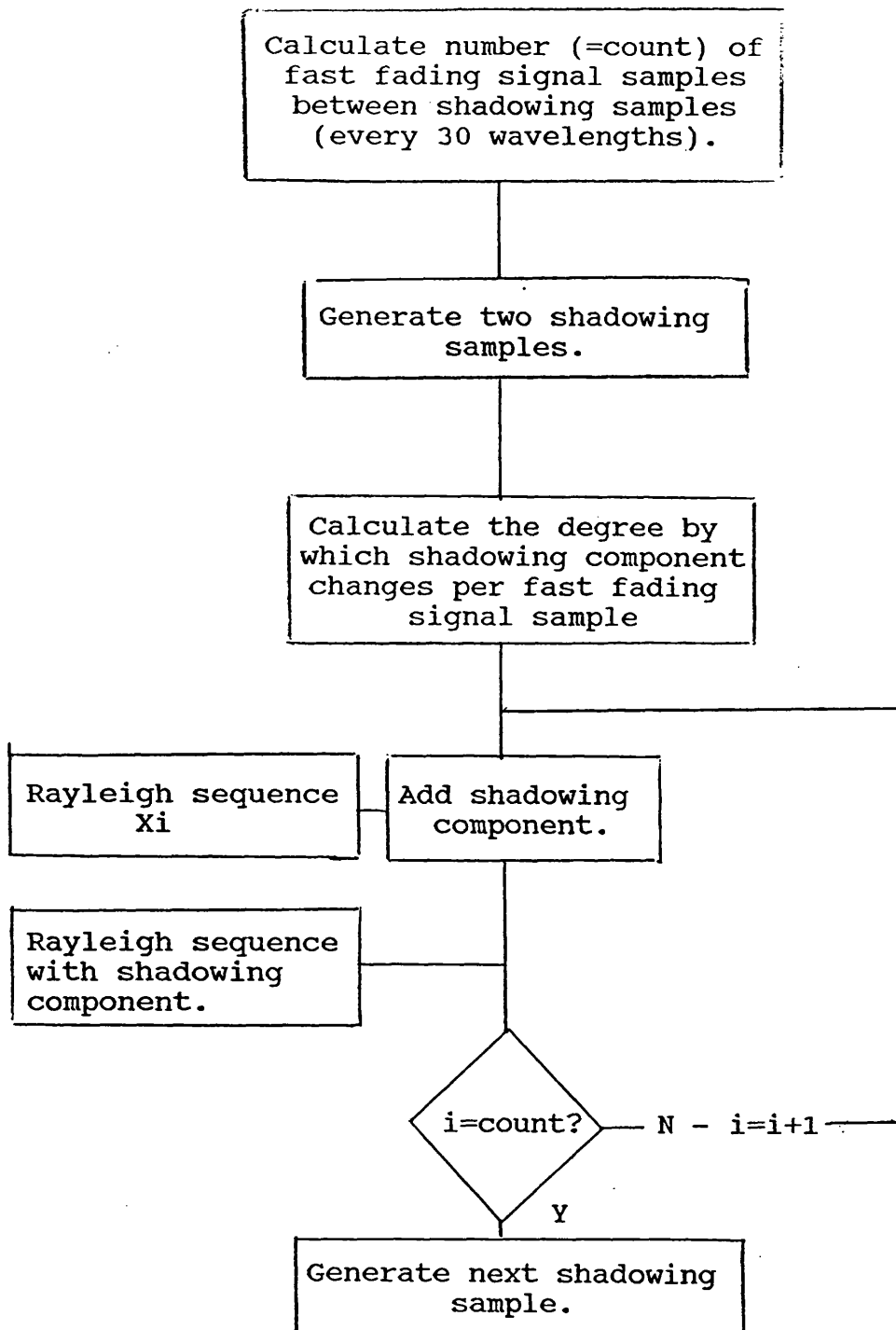
Figure 5.15 Procedure for generating log-normal (shadowing) component.
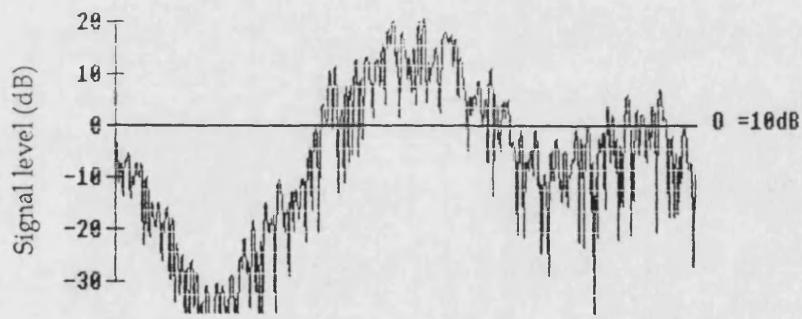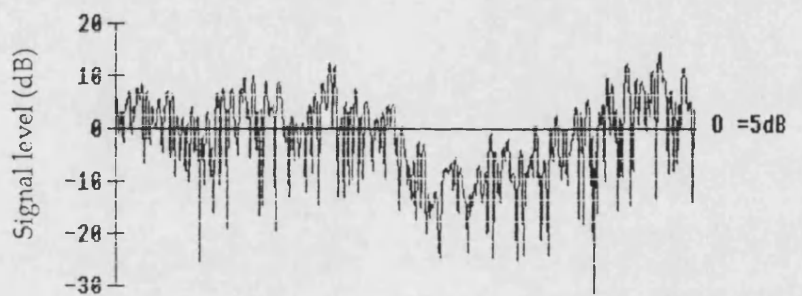
Figure 5.16 Rayleigh signal (Doppler frequency = 10
Hz) superimposed on a log-normally distributed mean
having a standard deviation of 5dB and 10dB. The
horizontal axis corresponds to 16 seconds.
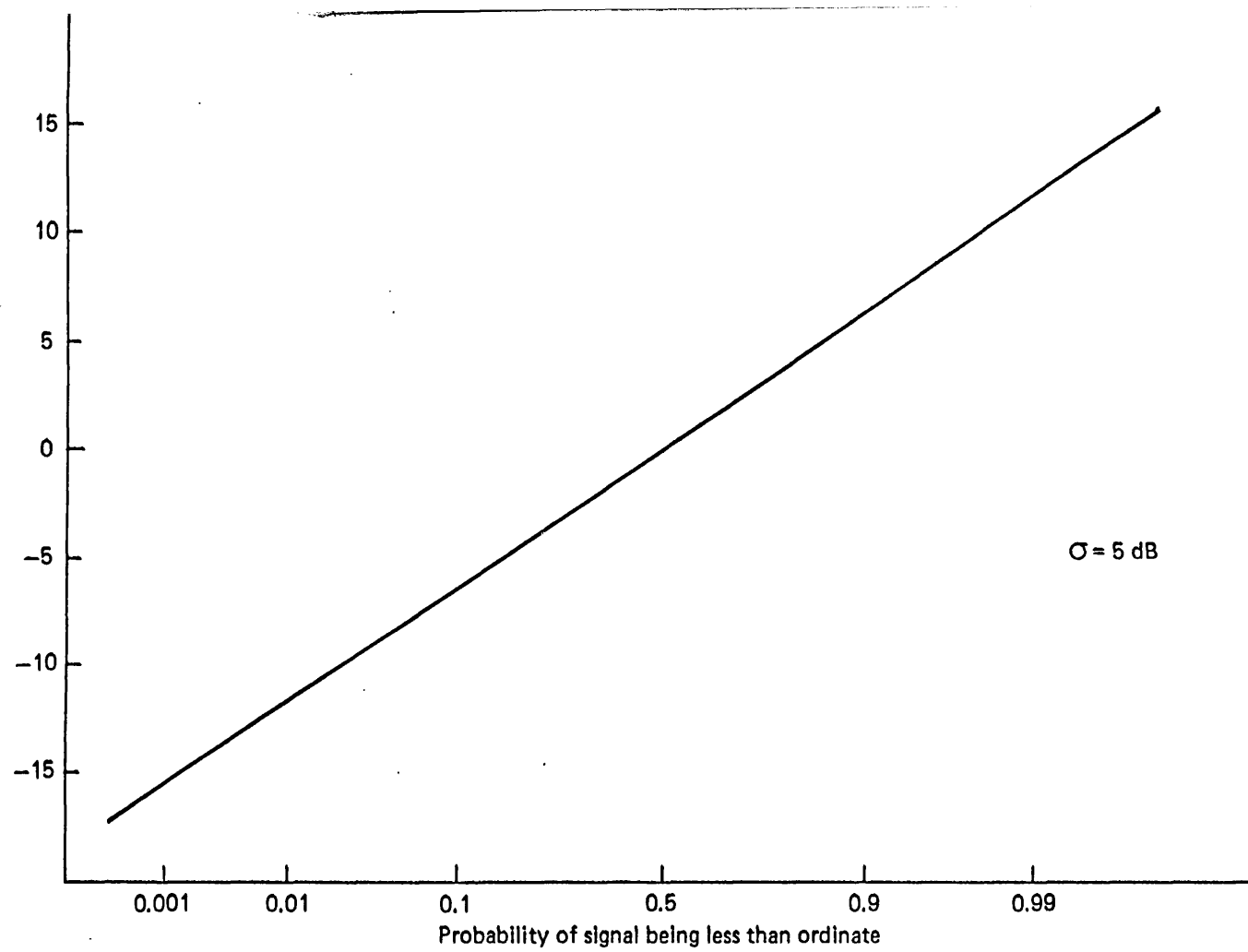
Figure 5.17   Cumulative distribution of log-normal signal.
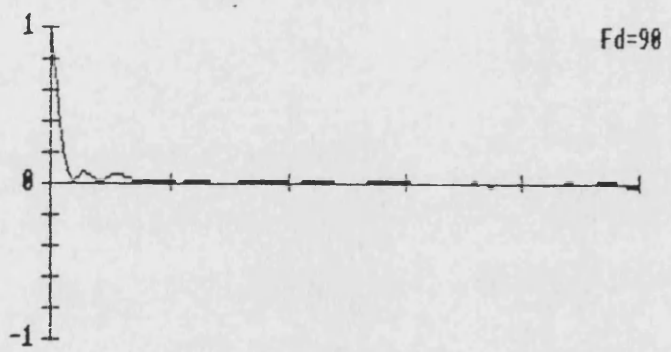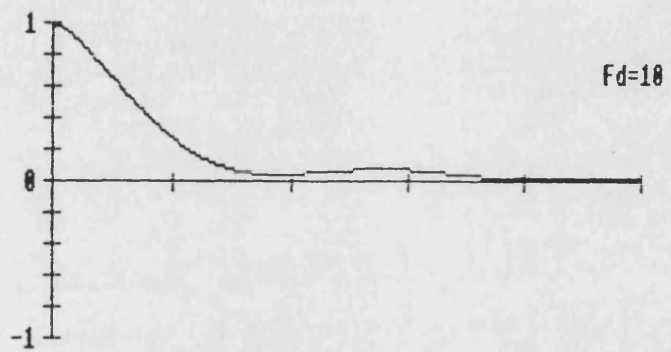
Figure 5.18   Autocorrelation function of simulated Rayleigh fading signal (with no shadowing component). Horizontal axis corresponds to 250 ms.
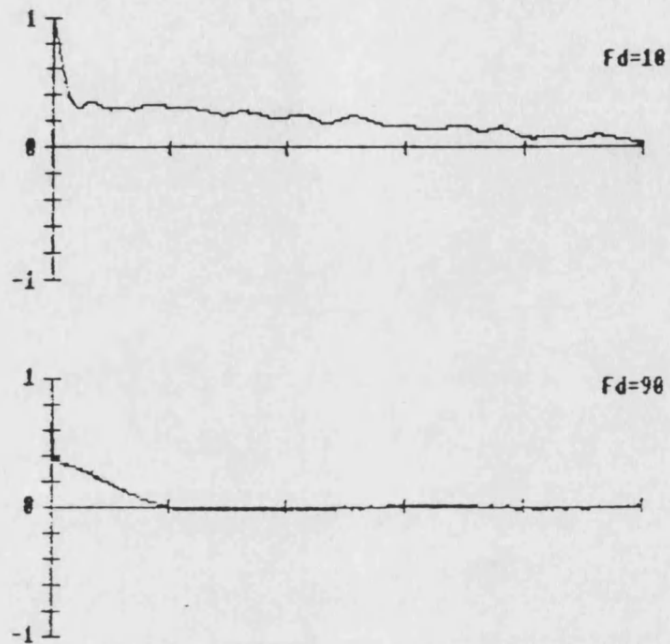
Figure 5.19 Autocorrelation function of simulated Rayleigh fading signal (with shadowing component having a standard deviation of 5dB). Horizontal axis corresponds to 2s.
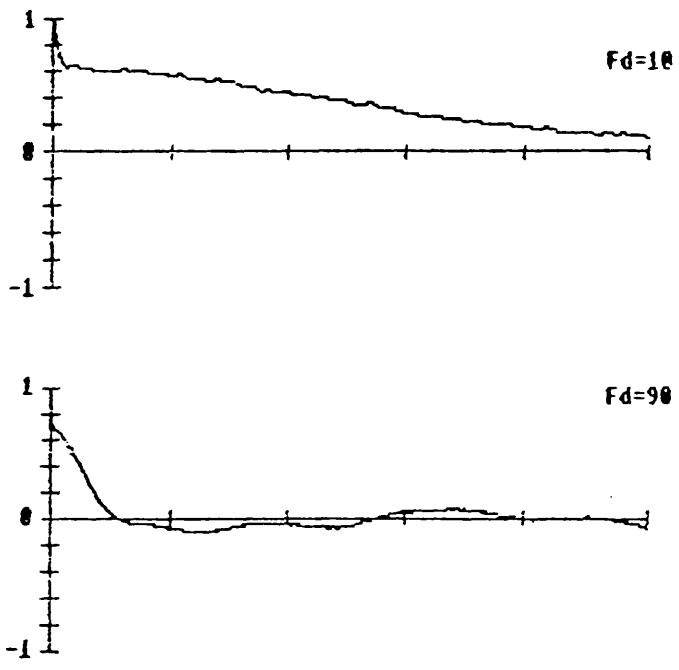
Figure 5.20 Autocorrelation function of simulated rayleigh fading signal (with shadowing component having a standard deviation of 10 dB). Horizontal axis corresponds to 4s.
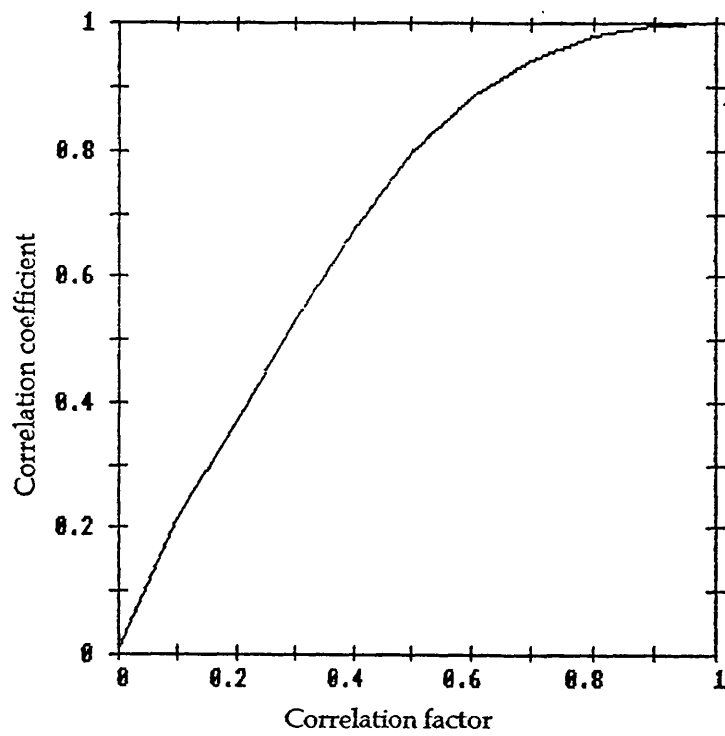
Figure 5.21 Relationship between correlation factor and correlation coefficient of log-normal signals.
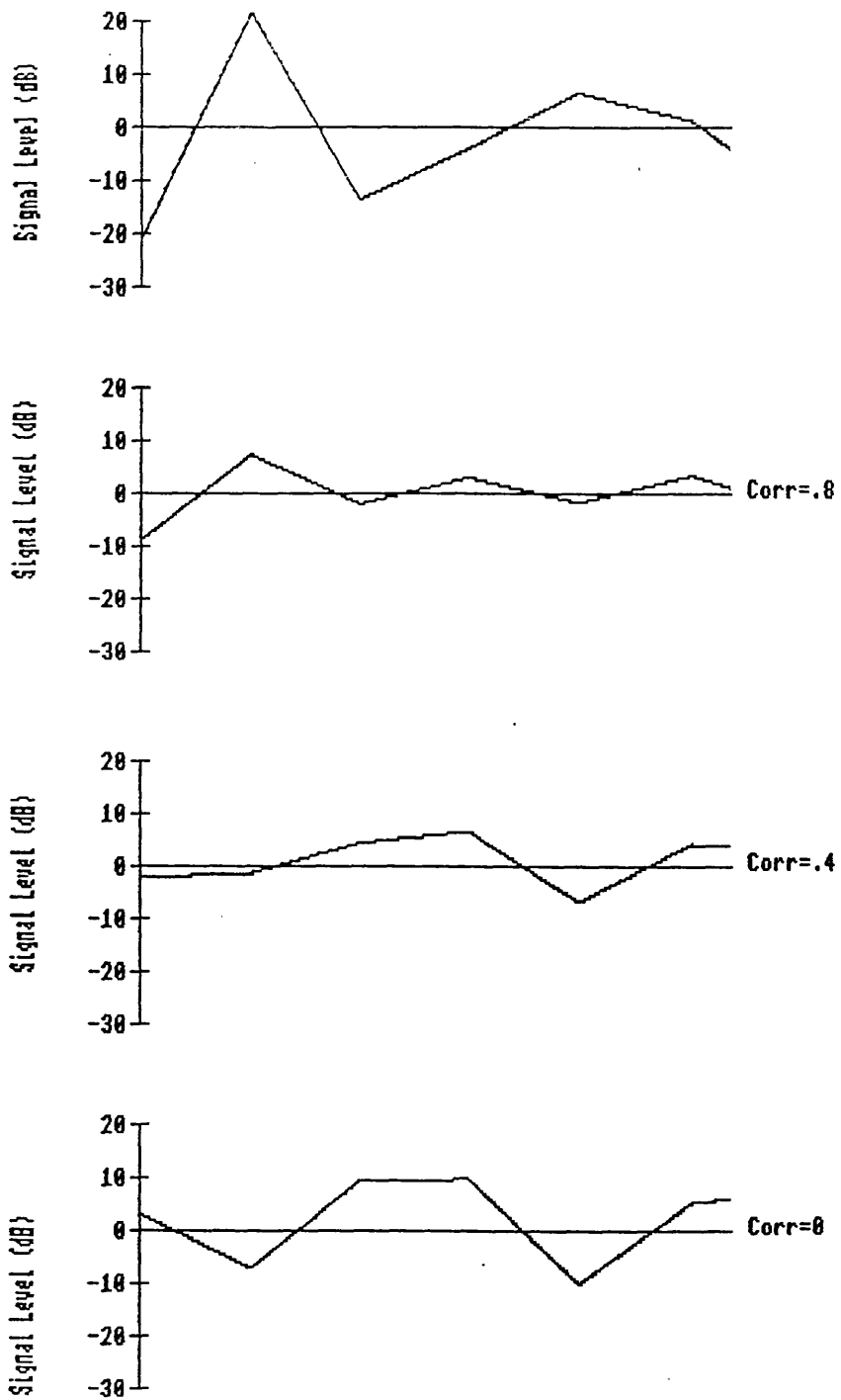
Figure 5.22   Simulated log-normal signals with selectable cross correlation.
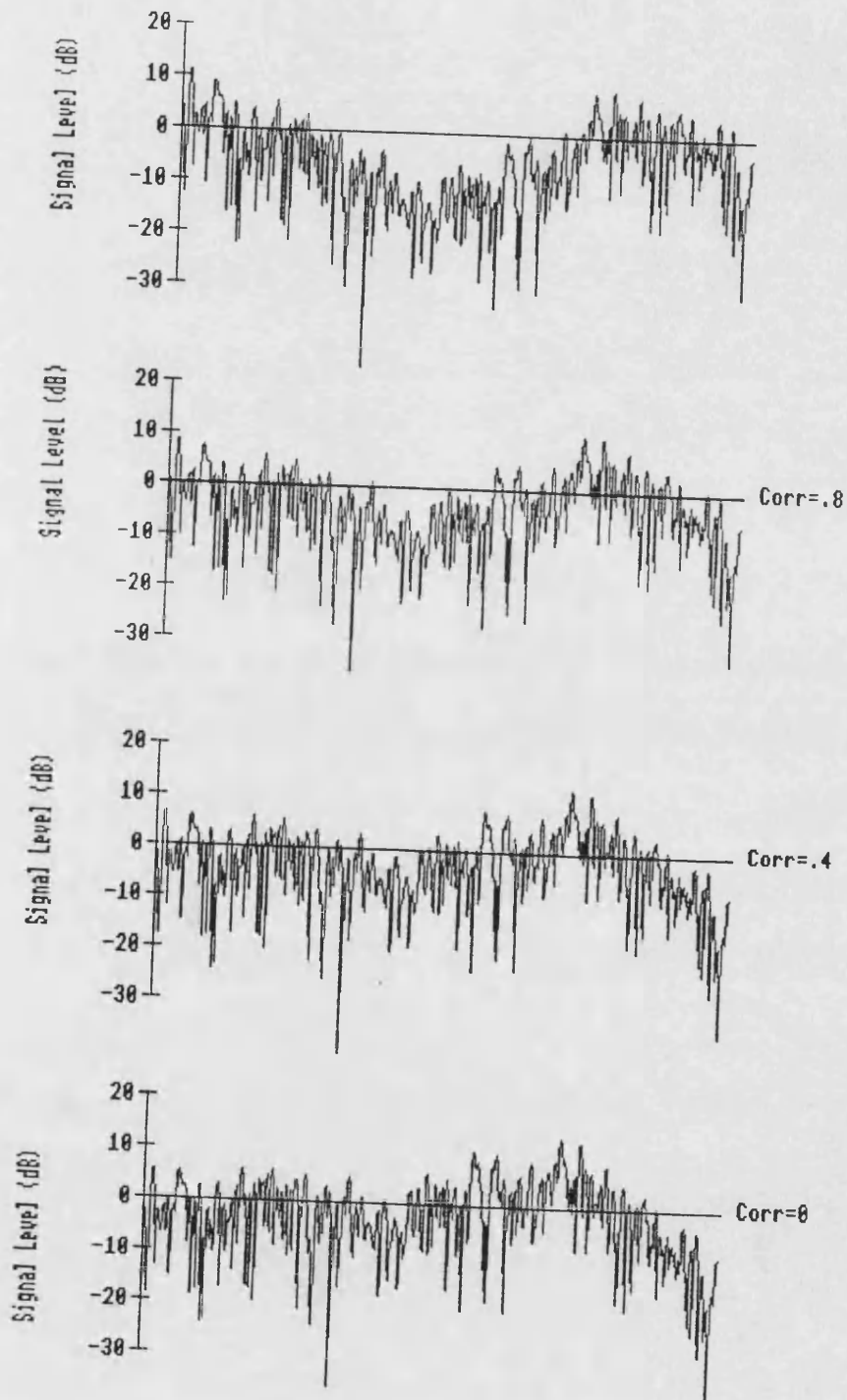
Figure 5.23 Simulated log-normal signals with selectable cross correlation superimposed on a Rayleigh signal.
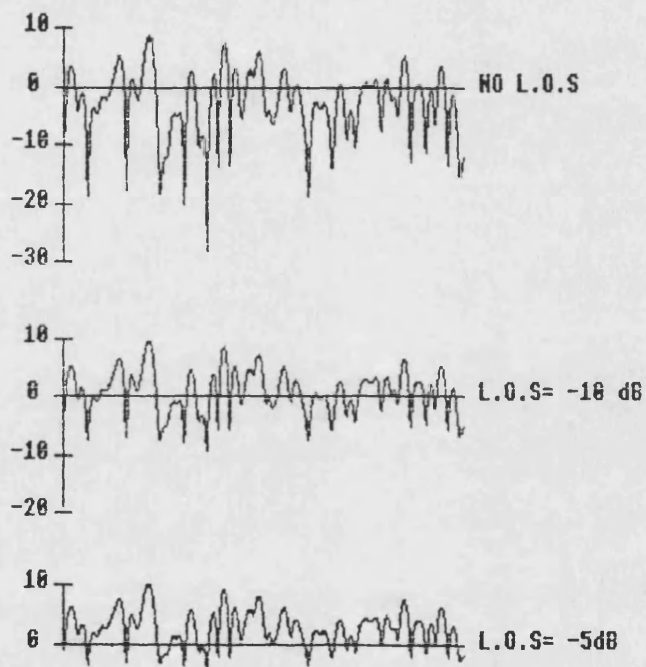
Figure 5.24   Simulation of Rayleigh signals with the
addition of line of sight components at different
levels.

```
┌─────────────────────────────────────────────────────┐
│                                                     │
│  Convert signal level to probability of bit error   │
│                                                     │
│      PROCber_ffsk or PROCber_gmsk etc               │
│                                                     │
└─────────────────────────────────────────────────────┘
                          │
                          │
           ┌──────────────────────────────────────┐
           │                                      │
           │  Add effect of irreducible bit error rate │
           │                                      │
           │            PROCiber                  │
           │                                      │
           └──────────────────────────────────────┘
                          │
                          │
              ┌──────────────────────────────┐
              │                              │
              │  Generate array of bit errors │
              │                              │
              └──────────────────────────────┘
```
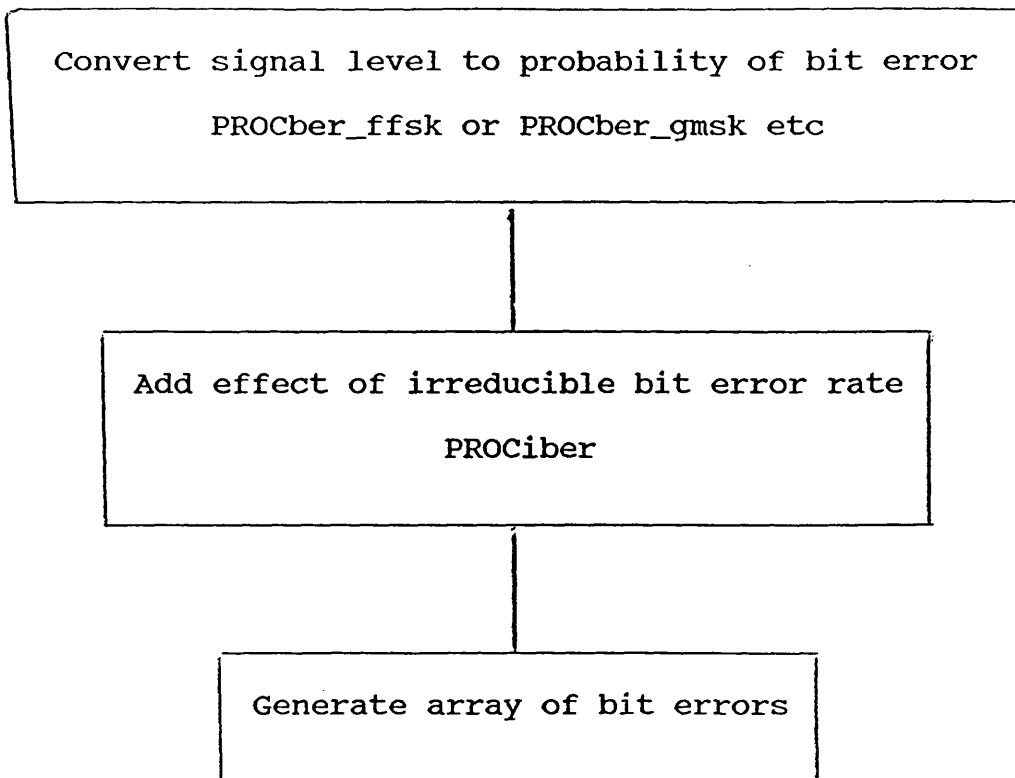
Figure 5.25   Procedures for simulating bit errors.
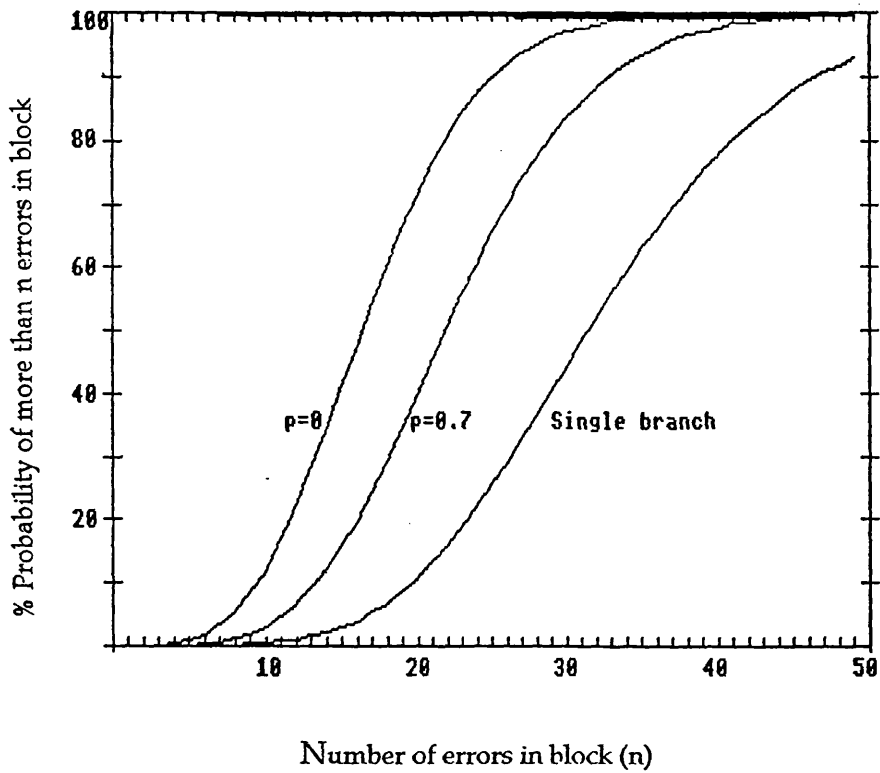
Figure 5.26 Cumulative distribution of errors in blocks of 512 bits using 8 kbits/sec GMSK.

CHAPTER 6

FIELD MEASUREMENTS OF MOBILE DATA TRANSMISSION WITH BASE STATION ANTENNA DIVERSITY.

6.1 Introduction

Field measurements were made to demonstrate the possible benefits of base station antenna diversity in improving the performance of mobile - base data transmission from areas of marginal radio coverage. The urban test route along Bathwick Street was used because of the three routes described in Chapter 4 this was the one yielding sufficiently uncorrelated signals with vertically spaced base station antennas. Measurements of received bit error distributions were made at around 450MHz (the same frequency used to determine cross correlation in Chapter 4), with both vertically and horizontally spaced antennas.

Computer simulations of the received bit error distributions were undertaken with the DMRCS. The simulated bit error distributions are compared with the measured results.

6.2 Antenna positions

The geographic location of the base station antennas

were as those described in Chapter 4. For the vertically spaced antennas, mounted on the transportable mast in the University Car Park, the top antenna was at a height of 36 metres. The first consideration was to determine the optimum vertical antenna separation required to yield the largest possible combined or selected signal. In Chapter 4 it was deduced from the urban test route that the spread in arrival angle in the vertical plane, ϕ_v, was 0.0184 radians (see Table 4.6). The effective base station antenna height H_1' for the urban route was found to be 80m (equal to 120λ at 450 MHz). Using these two figures the curves illustrating optimum vertical antenna spacing in Figure 2.21 indicate that the optimum spacing is approximately 27λ (18 metres). At this separation the expected signal strength in the lower branch was -2.214dB relative to the strength in the upper branch and the cross correlation of the signal envelopes equal to 0.09.

For the horizontally spaced antennas, mounted on the main University building, the antennas were spaced by 6λ (4 metres) and oriented such that α_H was equal to 61 degrees yielding an expected zero cross correlation of received signal envelopes.

6.3 Hardware Configuration

The mobile installation comprised a data message

166

generator, GMSK modem and mobile radio. The data
generator provided continuous repeated sequences made
up of a 16 bit frame synchronisation word followed by
50 concatenated 512 bit blocks. This data sourced a
GMSK transmit modem in turn connected to the UHF mobile
radio. The mobile radio was connected via a variable
attenuator to a quarter wave antenna mounted on the
centre of the roof of a small saloon car. The
attenuator was used to adjust the radiated power so
that a mean signal level of OdBuV was received at the
base station. This level was chosen because it is below
the minimum useable signal level usually necessary in
mobile data schemes allowing the use of diversity to
yield improvements in performance. This signal level
was not so low that the receive modems regularly lost
synchronisation.

In each test run the message generator in the mobile
was keyed just prior to the start of the geographical
start marker and de-keyed just after the end of the
route. A mobile speed as close as possible to 40 Km/hr
was maintained along the test route.

The antennas were each connected via low loss co-axial
cable to the base station receivers used in the earlier
work. The receivers were connected to GMSK modems the
serial outputs of the modems were gated by a signal
selector connected to the signal strength outputs from
these receivers. The selected data output was compared
with the transmitted sequence and calculations of error

rates computed.

A schematic diagram of the hardware is shown in Figure 6.1.

6.4 Results

The cumulative distribution of measured errors received in blocks of 256 and 512 bits is shown in Figures 6.2 to 6.5 for vertically spaced and horizontally spaced antennas.

The improvements in received bit error rate indicated that with horizontal separation a 3dB improvement in performance was obtained with the use of diversity. With the vertical separation used the improvement was 2.2dB.

6.5 Simulations with the DMRCS

Prior to undertaking field measurements the DMRCS was used to simulate the transmission of 8Kbits/sec GMSK data from the urban test route to spatially separated antennas at the university. A summary of the parameters used to undertake simulation with vertically and horizontally spaced antennas are shown in Tables 6.1-2.

DMRCS Simulation Parameters	
Signal Branch 1	0 dBμV
Signal Branch 2	-2.214 dBμV
Doppler Frequency	17 Hz
Standard Deviation of Local Mean	6.8 dB
Data Modulation	8 kbps GMSK
Data Sequence Duration	1000 seconds
Correlation Coefficient	0.09

Table 6.1   Parameters used for simulating propagation of signals received via vertically spaced antennas.

DMRCS Simulation Parameters	
Signal Branch 1	0 dBμV
Signal Branch 2	0 dBμV
Doppler Frequency	17 Hz
Standard deviation of local mean	6.8 dB
Data Modulation	8 kbps GMSK
Data Sequence Duration	1000 seconds
Correlation coefficient	0

Table 6.2   Parameters used for simulating propagation of signals received via horizontally spaced antennas.

The cumulative distributions of simulated errors received in blocks of 256 and 512 bits are shown in

Figures 6.2 to 6.5 alongside the measured results.
The simulated distributions show close correlation with
the field measurements. Very slight differences are
noticeable for high numbers of errors in a block
because of the low probability of these events in the
40 seconds of each test route.

6.6   Sensitivity of vertical antenna spacing on diversity gain

The DMRCS has been used to illustrate how the received
bit error rate of the combined signal is sensitive to
antenna spacing. For the urban test route used in the
field measurements the parameters given in Table 6.3
can be calculated.

The DMRCS has been used with the doppler frequency,
standard deviation of local mean, data modulation and
sequence duration shown in Table 6.1. The results are
shown in Figure 6.6 and indicate that for the urban
test run the performance should be largely unaffected
for spacing variations of between 12 and 32
wavelengths.

Antenna Separation		Signal 2/ Signal 1 (dB)	p_{env}
Metres	λ		
0	0	0	1
2	3	-0.22	0.966
4	6	-0.45	0.873
6	9	-0.68	0.741
8	12	-0.92	0.592
10	15	-1.16	0.446
12	18	-1.41	0.316
14	21	-1.67	0.213
16	24	-1.94	0.134
18	27	-2.21	0.081
20	30	-2.50	0.045
22	33	-2.79	0.024
24	36	-3.10	0.012
26	39	-3.41	0.006
28	42	-3.74	0.002
30	45	-4.08	0.001
32	48	-4.44	0

Table 6.3 Calculated cross correlation and relative signal strength at different antenna spacings.

C=1 Channel 1 is stronger
C=0 Channel 2 is stronger

Output =Channel1 C + Channel2 $\overline{C}$
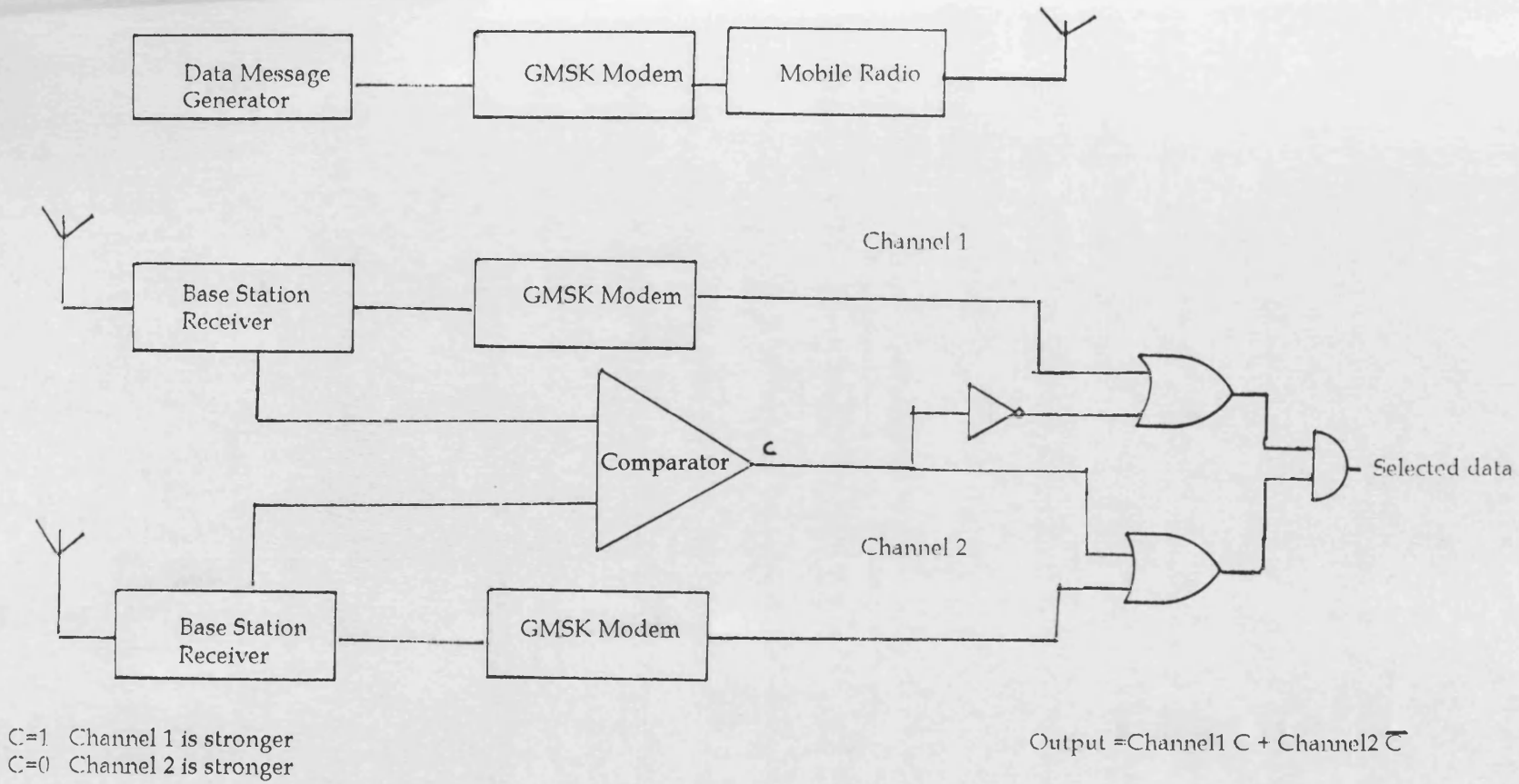
Figure 6.1   Schematic diagram of the hardware used in the field measurements.
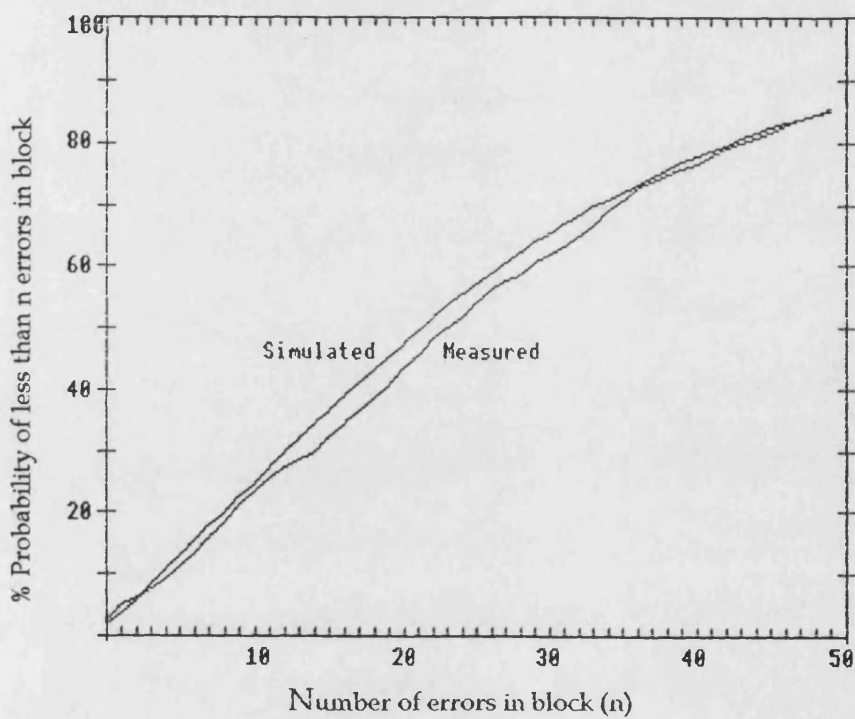
Figure 6.2 Distribution of the number of errors in 512-bit blocks for 8000 bits/sec GMSK transmission for measured and simulated signals received via vertically spaced antennas.
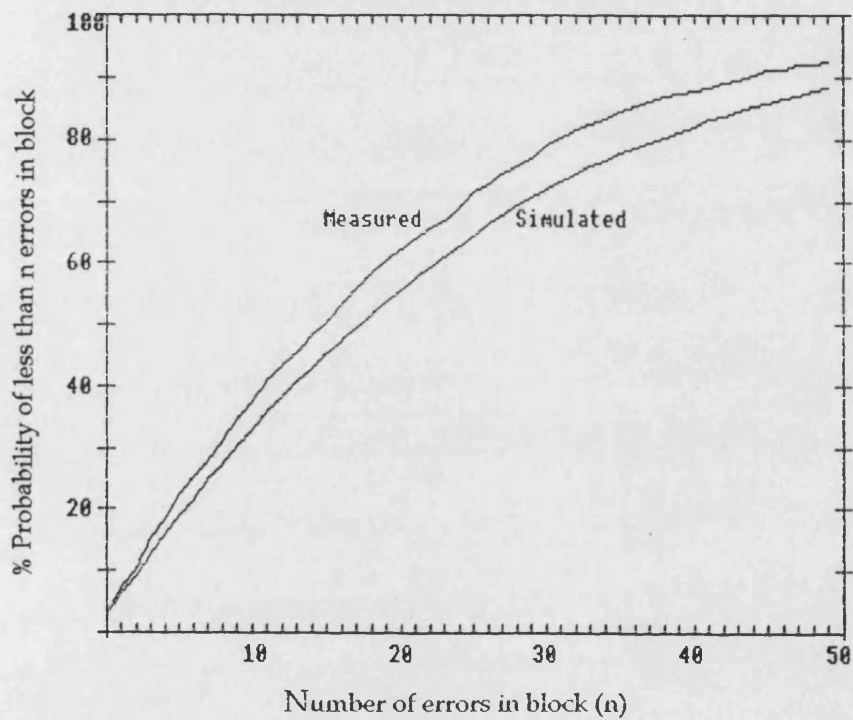
Figure 6.3   Distribution of the number of errors in
512-bit blocks for 8000 bits/sec GMSK transmission for
measured   and   simulated   signals   received   via
horizontally spaced antennas.
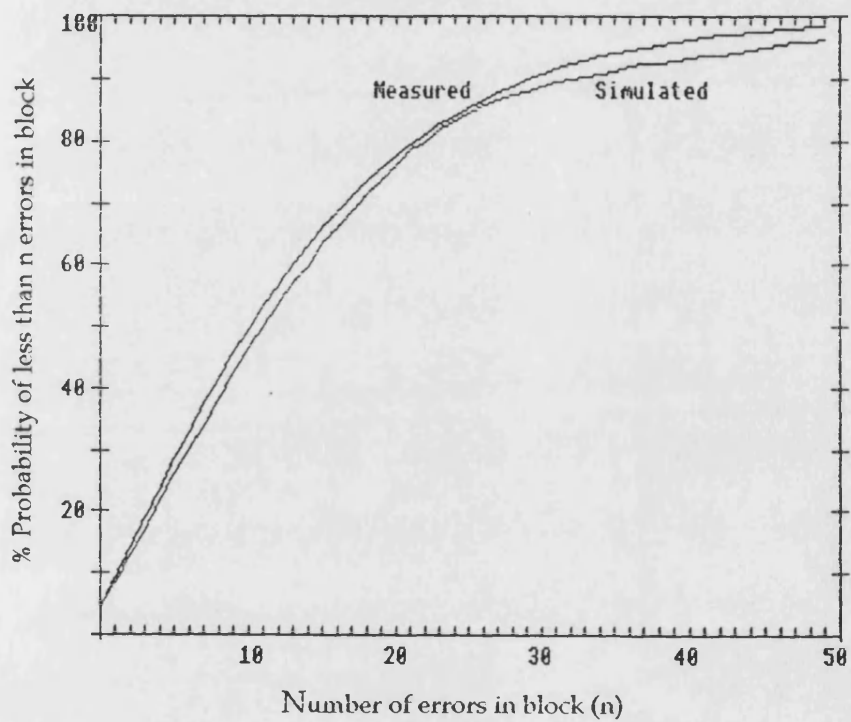
Figure 6.4   Distribution of the number of errors in 256-bit blocks for 8000 bits/sec GMSK transmission for measured and simulated signals received via vertically spaced antennas.
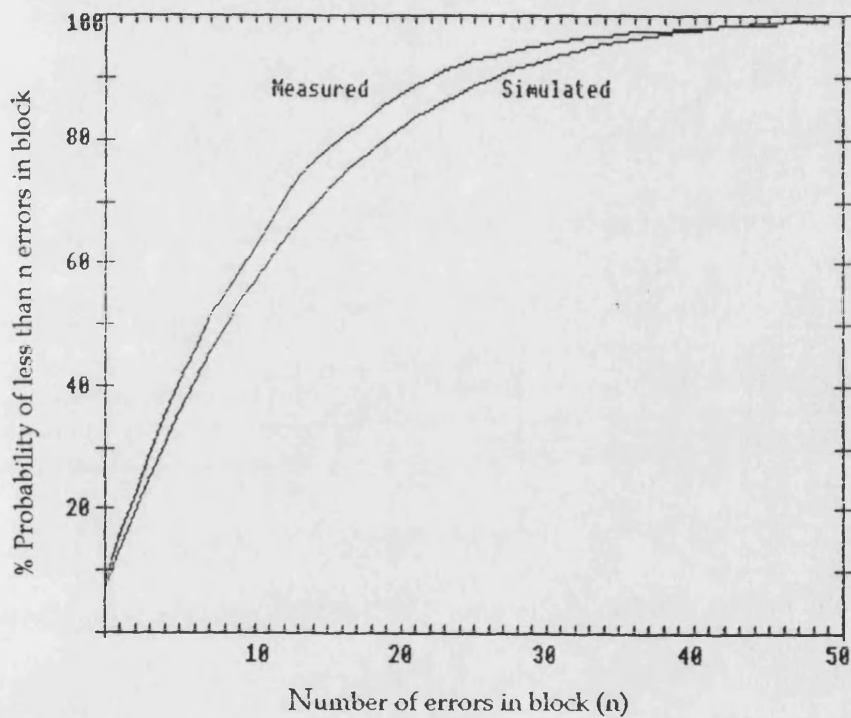
Figure 6.5   Distribution of the number of errors in 256-bit blocks for 8000 bits/sec GMSK transmission for measured and simulated signals received via horizontally spaced antennas.
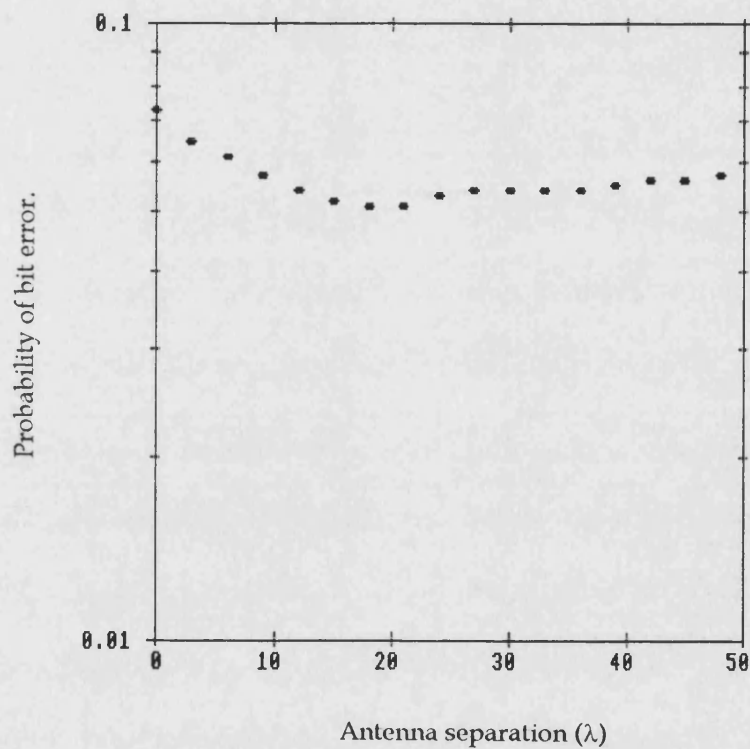
Signal in top antenna   0dBuV

ϕ_v .0184 radian

H_1 80m

σ 6.8dB

Figure 6.6 Estimation of probability of bit errors for different antenna separation based on simulation made with the DMRCS.

177

CHAPTER 7

CONCLUSIONS

The research set out to examine the viability of implementing base station antenna diversity in UHF digital mobile radio networks and to produce a means of predicting the benefits of its use. The cross correlation between signal envelopes received via base station antennas separated both vertically and horizontally have been both theoretically predicted and measured in the field. All of the reviewed published literature has been concerned with measurements made at 800/900 MHz and the emphasis has been with antennas separated horizontally. The published literature indicates that provided the received waves are at least 10 degrees from the inline then received signals can be sufficiently uncorrelated with separations of five to twenty wavelengths depending on the sector of signal arrival angle from the mobile. The work reported in this thesis indicates similar results with horizontal separation at 450 MHz. The implementation of base station antenna diversity at low-UHF with horizontally spaced antennas is not always feasible, particularly when the antennas are mounted on a mast. The attraction of mounting vertically spaced antennas is apparent.

It has been shown that with antennas spaced vertically rather than horizontally the signals become correlated more quickly as the mobile moves away from the base station. This has been verified by the field measurements and in certain situations it places a limitation on the usefulness of this form of diversity. Another constraint in the performance with antennas spaced vertically is that the signal level in the lower antenna will be less than that in the upper antenna. It has been shown that there is a trade-off in performance in that whilst increasing the vertical separation reduces the signal envelope cross-correlation, the signal strength in the lower branch is also reduced. It has been shown that optimum antenna separations exist which are dependent on the effective base station antenna height "seen" by the mobile and the spread in arrival angle of the multi-path waves at the base station. This inevitably necessitates some compromise in the implementation of vertically spaced antenna diversity because the optimum spacing will change for signals received from different geographic areas. The DMRCS has been demonstrated to be a useful tool in examining the effects of different spacing on the received bit error rates.

This compromise in spacing does not exist with horizontally separation of antennas since the spacing would be chosen to provide the necessary uncorrelated signals with the upper limit of spread in arrival angle

of the multi-path waves.

It is concluded that in the low UHF band vertically spaced base station antennas will generally only yield diversity gains in small radio cells where the radio coverage becomes marginal within two or three kilometres from the base. In practice base stations operating in such cells will usually be low elevation sites and the receive antennas will be more likely to receive signals via local scatterers; this will yield less correlated signals for a given antenna separation than indicated in the presented theoretical formulations that are based on the assumption that the principal scatterers are close to the mobile.

Horizontally spaced base station antennas will yield diversity gains in larger cells apart from a small range of horizontal arrival angle of the multi-path waves when they are approximately inline with the two antennas. This effect can be minimised by ensuring that the antennas are oriented so that they are placed broadside to the geographic areas where radio coverage requires enhancing.

Field measurements have been made at low UHF using 8 Kbits/sec GMSK data modulation. The measurements were from a mobile in an urban environment approximately two kilometres from a base station. Without diversity the

signal received at the base station was marginal. By implementing base station antenna diversity reductions in the received bit error rates corresponding to an improvement of 3dB have been demonstrated.

ANNEX 1

A Review of European Public Packet Switched Mobile

Data Networks.

Swedish Telecom and Ericsson developed the Mobitex

standard from 1980 and the first Mobitex mobile data

network operated by Swedish Telecom was launched in

October 1986. Because of the initial low take up of its

services it was allowed to support analogue voice

communications. There are presently about 10,000

subscribers and population coverage exceeds 99%. Unlike

more recent Mobitex networks this is a 1200 bits/sec

FFSK network.

The Helsinki telephone company launched a Mobitex

system in Finland in 1990. The network provides

coverage to over 70% of the population and plans exist

to increase this to 90% by the end of 1995. Telecom

Norway opened its Mobitex network in March 1991.

Coverage is presently provided for Oslo with plans to

extend coverage to other major population centres.

The UK government licensed five companies to provide

national mobile data networks. Two of the licenses were

returned but three national networks were developed.

Cognito launched its network in 1991 using a

proprietary protocol. They offered a two-way messaging service called Emissary utilising handheld Messager terminals. Cognito was closed after the acquisition of Dowty by the TI Group in 1992 but was subsequently relaunched when it was acquired by Sonnaire a Swiss based investment company. Cognito have 4,500 subscribers on their VHF network and provide coverage to 85% of the population. Cognito have recently announced monthly operating profits.

Huthchinson Mobile Data operated a 4.8 kbits/sec UHF network based on the MMP (mobile message protocol). This was subsequently replaced by RD-LAP (Radio Data Link Access Protocol) operating at 9.6 kbits/sec. Hutchison withdrew from the mobile data market in 1993. RAM Mobile Data operate a Mobitex UHF network and provide coverage to over 80% of the population using 217 base stations RAM have announced the deployment of an additional 50 new base stations over the next four years. RAM Broadcasting and BellSouth own 65% of the company, while France Telecom, Bouygues and Telia International (formerly Swedish Telecom) own the rest. They are believed to have about a 1000 subscribers. The third UK network is the one operated by Paknet a Vodafone subsidiary company. Originally holding a license for a fixed radio data service this licence was extended to cover mobile services. Paknet have 25,000 subscribers of which 23,000 are fixed site customers; their market specialisation areas are in the telemetry

and security. Their VHF network provides coverage to 88% of the population.

RAM Mobile Data have Mobitex networks in The Netherlands and Belgium. The Netherlands system provides national coverage with 98% of the population within mobile and 80% within 80% coverage. The licence for RAM Mobile data Belgium was awarded in April this year and commercial operation is about to start in Belgium in Brussels, Antwerp, Ghent and Bruges. Plans exist to extend coverage to 80% of the population.

Two licences were granted for mobile data networks in France in 1993; both are based on Mobitex. France Telecom presently provides coverage into Paris with coverage to be shortly extended into the Lyon region. By the end of 1996 coverage is planned for 60% of population including all towns with populations exceeding 100,000. The second licensee TDR, owned by COFIRA provides coverage into Paris, Lyon Grenoble and St Etienne with plans to extend coverage in the Nord-Pas-de-Calais and Provence Cote D'Azur by the end of 1994. Coverage to 60% of the population is planned by the end of 1995

In Germany Deutsche Telekom's mobile arm, DeTe Mobil, has an operational Motorola based RD-LAP network called Modacom. A second licence has been granted to the consortium Gesellschaft fur Datenfunk mbH. The plan is to offer services in mid 1995 and to cover 60% of the

population by April 1996. When the network is completed at the end of 1997 it will cover 80% of the geographical areas and 90% of the population.

In Switzerland, Modacom Suisse was recently awarded a licence to operate a network. Modacom are backed by DeTe Mobil and a the RD-LAP network.

Mobile data usage has not developed quickly in Europe largely because of the lack of development into applications and software. This situation has changed over the last couple of years helped by de facto standards for public packet switched mobile data networks.

ANNEX 2

Computer simulation of Rayleigh fading based on the Arredondo model.

Computer Simulation

Two arrays of Gaussian distributed Fourier Coefficients are generated, as illustrated in Figure A2.1, by weighting random numbers by an array containing the discrete spectrum of the z- directional electric field components (derived from equation 2.11).

$$E_i(i) = \sum_{i=1}^{F_d} rnd_i (1 - (\frac{i-1}{F_d})^2)^{0.5}$$

$$E_j(j) = \sum_{j=1}^{F_d} rnd_j (1 - (\frac{j-1}{F_d})^2)^{0.5} \quad A2.1$$

The BASIC function RND(1) provides a random variable uniformly distributed between zero and unity. The random numbers rnd_i and rnd_j are generated by summing 12 such random variables and subtracting the number 6 to provide normalised random numbers with zero mean and unity variance. The two arrays are transformed by a FFT routine to provide time domain sequences. The quadrature components of each signal are added in rms

186

fashion and normalised to 0dB to produce a waveform with a Rayleigh distribution and appropriate spectra. Figure A2.2 provides a summary of these procedures. Examples of waveforms generated by the program for Doppler frequencies of 50 and 90 Hz are shown in Figure A2.3.

Validity of model

The cumulative probability distribution of the amplitude of the simulated signal is shown in Figure A2.4 along with theoretical formula based on equation 2.2. The measured CPD is very similar to the theoretical.

Normalised level crossing rates (lcr) of the simulated signal are shown alongside the theoretical values based on equation 2.4 in Figures A2.5. The measured normalised lcr shows good fit with the theoretical and the Arredondo simulator provides more accurate lcr performance compared with the Jakes simulator (Figure 5.5).

Average fade duration is readily calculated from LCRs as described in Chapter 2. A theoretical expression for the fade duration distribution appears mathematically intractable however an empirical expression can be formulated. Figure A2.6 provides the occurrence probability of 10 dB fades with a given duration. The

probability scale is normal and the fade duration is normalised to the average fade duration and plotted on a logarithmic scale. Fade statistics taken from the simulated Rayleigh signal are described by a straight line indicating a log normal distribution which is of the form:-

$$P(fade > t) = 0.5 \ erfc(\frac{\log_e u - u_0}{\sqrt{2}\sigma}) \qquad A2.2$$

where t is the normalised fade duration. It can be shown that u=-0.27 and σ=0.84

It follows that the fade durations are distributed as follows:-

$$p(t) = \frac{1}{\sigma t \sqrt{2\pi}} \ e^{\frac{-\log_e \frac{t}{t_m}}{2\sigma^2}} \qquad A2.3$$

where tm is the median fade duration. This normal distribution of fade duration has been observed empirically at 4 and 6 GHz on line of site transmission paths[32].

The normalised autocorrelation of the simulated Rayleigh signals has been computed using sequence lengths of 65536 samples corresponding to 64 seconds. Results are shown in Figure A2.7. The autocorrelation of the Arredondo simulation is inferior to that of the

188

Jakes simulation (Figure 5.6).

Simulation of cross correlated Rayleigh signals

The Arredondo model is readily extended to provide two (or more) Rayleigh signals with a predetermined cross correlation. This is achieved by correlating the two complex arrays as shown schematically in Figure A2.8 before being Fast Fourier Transformed. The relationship between the correlation factor and the correlation coefficient of the signals is shown in Figure A2.9.

The following program generates two partially correlated Rayleigh signals using the Arredondo model.

```
10 REM   PROGRAM GENERATES TWO PARTIALLY
20 REM   CORRELATED RAYLEIGH SIGNALS USING
30 REM   ARREDONDO MODEL
40 :
50 INPUT "MEAN SIGNAL LEVEL 1 (dBuV) ";mean_signal_1
60 INPUT "DOPPLER FREQUENCY ";DOPPLER%
70 INPUT "MEAN SIGNAL LEVEL 2 (dBuV) ";mean_signal_2
80 :
90 DIM X(19200,3),X1(2500)
100 Z=RND(-TIME)
110 :
120 M%=14: sample_sequence_length%=16384
130 REM GENERATE DOPPLER ARRAY
140 PROCdoppler_array
150 :
160 FOR I%=0 TO sample_sequence_length%
170 FOR J%=0 TO 3: X(I%,J%)=0: NEXT: NEXT
180 :
190 REM GENERATE COMPLEX ARRAY
200 PROCcomplex
210 :
220 PROCcorrelate_complex_arrays
230 :
240 REM GENERATE TIME DOMAIN SEQUENCE(S) NORMALISED TO 0dB
250 A%=0: B%=1: PROCfft
260 A%=0: B%=0: C%=1: mean_signal=mean_signal_1
270 PROCrayleigh_sequence
280 :
290 A%=2: B%=3: PROCfft
300 A%=1: B%=2: C%=3: mean_signal=mean_signal_2
310 PROCrayleigh_sequence
320 :
330 STOP
340 :
350 DEF PROCdoppler_array
360 REM GENERATE DOPPLER ARRAY
370 F%=sample_sequence_length%*DOPPLER%/1024
380 FOR I%=1 TO F%: P=SQR(1-((I%-1)/F%)^2)
390 X1(I%)=1/SQR(P): NEXT
400 R%=F%+1: P=2*F%-1: P=(F%-1)/SQR(P)
410 P=F%*(PI/2-ATN(P)): X1(R%)=SQR(P)
420 ENDPROC
430 :
440 DEFPROCcomplex
450 FOR I%=2 TO R%
460 PROCrnd: X(I%,0)=X1(I%)*T
470 PROCrnd: X(I%,1)=X1(I%)*T
480 PROCrnd: X(I%,2)=X1(I%)*T
490 PROCrnd: X(I%,3)=X1(I%)*T: NEXT
500 ENDPROC
```

```
510 :
520 DEFPROCfft
530 LOCAL C%,D%,E%,F%,G%,K%
540 C%=sample_sequence_length%/2
550 D%=sample_sequence_length%-1: J%=1
560 FOR I%=1 TO D%
570 IF I%<J% THEN
580 T1=X(J%,A%): T2=X(J%,B%)
590 X(J%,A%)=X(I%,A%): X(J%,B%)=X(I%,B%)
600 X(I%,A%)=T1: X(I%,B%)=T2: K%=C%
610 ENDIF
620 K%=C%
630 WHILE K%<J%
640 J%=J%-K%: K%=K%/2
650 ENDWHILE
660 J%=J%+K%: NEXT I%
670 FOR L%=1 TO M%
680 E%=2^L%: F%=E% DIV 2: U1=1: U2=0
690 W1=COS(PI/F%): W2=-SIN(PI/F%)
700 FOR J%=1 TO F%
710 FOR I%=J% TO sample_sequence_length% STEP E%
720 G%=I%+F%
730 V1=X(G%,A%)*U1-X(G%,B%)*U2
740 V2=X(G%,B%)*U1+X(G%,A%)*U2
750 X(G%,A%)=X(I%,A%)-V1: X(G%,B%)=X(I%,B%)-V2
760 X(I%,A%)=X(I%,A%)+V1: X(I%,B%)=X(I%,B%)+V2
770 NEXT I%
780 U3=U1: U4=U2: U1=U3*W1-U4*W2: U2=U4*W1+U3*W2
790 NEXT J%: NEXT L%
800 ENDPROC
810 :
820 DEFPROCrayleigh_sequence
830 S=0: FOR I%=1 TO sample_sequence_length%
840 X(I%,A%)=X(I%,B%)^2+X(I%,C%)^2: S=S+X(I%,A%)
850 NEXT
860 S=S/sample_sequence_length%
870 FOR I%=1 TO sample_sequence_length%
880 X(I%,A%)=10*LOG(X(I%,A%)/S)+mean_signal
890 NEXT
900 ENDPROC
910 :
920 DEFPROCrnd
930 REM PROCEDURE RETURNS NORMALISED RANDOM SAMPLES
940 REM WITH ZERO MEAN & UNITY VARIANCE
950 T=0: FOR J%=1 TO 12: T=T+RND(1): NEXT: T=T-6
960 ENDPROC
970 :
980 DEFPROCcorrelate_complex_arrays
990 FOR I%=2 TO R%
1000 X(I%,2)=X(I%,2)+((X(I%,0)-X(I%,2))*COR)
1010 X(I%,3)=X(I%,3)+((X(I%,1)-X(I%,3))*COR): NEXT
1020 ENDPROC
```
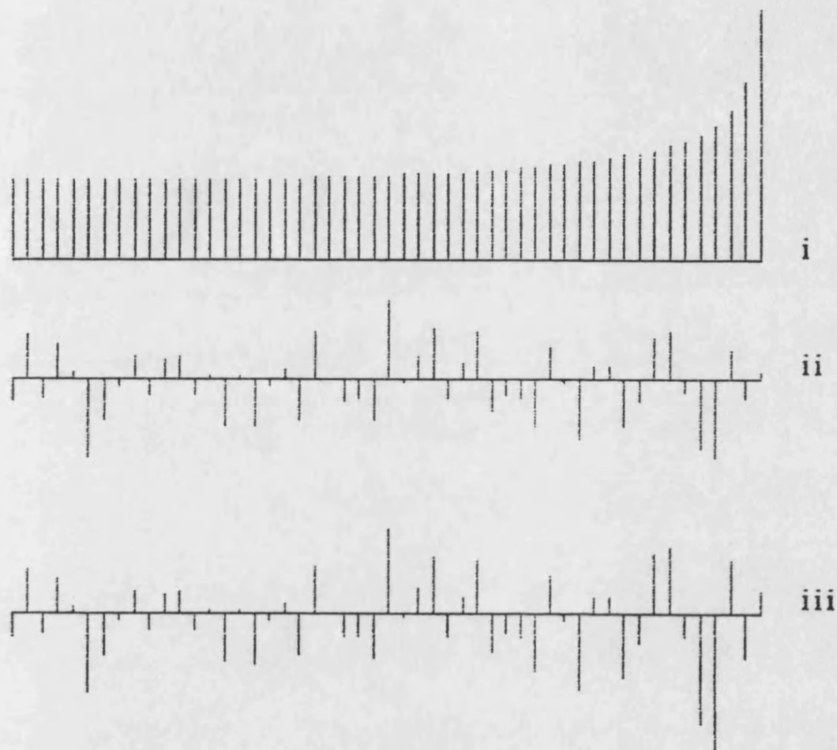
Figure A2.1   Fourier coefficients (iii) generated by multiplying discrete fourier spectrum of the z-directional electric field components (i) by Gaussian distributed random numbers (ii)

```
┌─────────────────────────────┐
│  Generate Doppler array     │
│                             │
│    PROCdoppler_array        │
└─────────────────────────────┘
              │
              │
┌─────────────────────────────────────┐
│  Multiply two identical Doppler      │
│  arrays by random numbers to         │
│  produce complex array               │
│                                      │
│         PROCcomplex                  │
└─────────────────────────────────────┘
              │
              │
┌─────────────────────────────────────┐
│  Fast Fourier transform complex array│
│                                      │
│              PROCfft                 │
└─────────────────────────────────────┘
              │
              │
┌─────────────────────────────────────┐
│  Add components in quadrature and    │
│         normalise to 0dB             │
│                                      │
│      PROCrayleigh_sequence           │
└─────────────────────────────────────┘
```
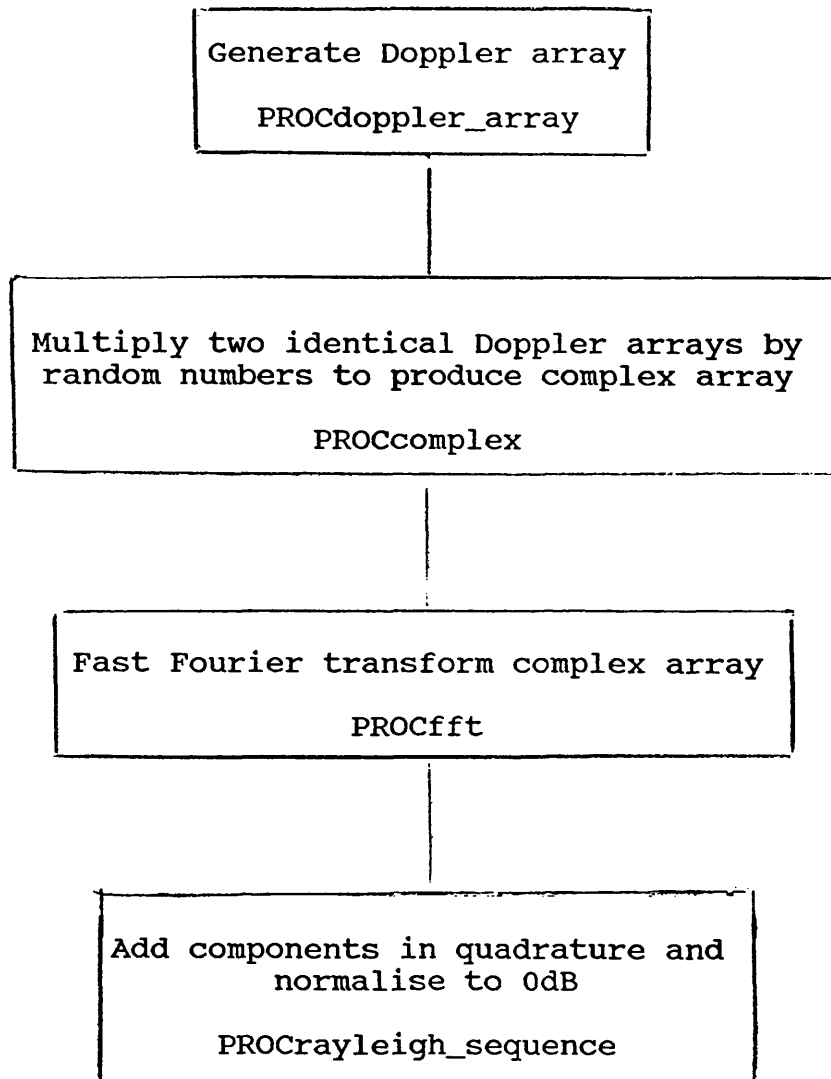
Figure A2.2   Overview of procedures used to generate a Rayleigh fading sequence.
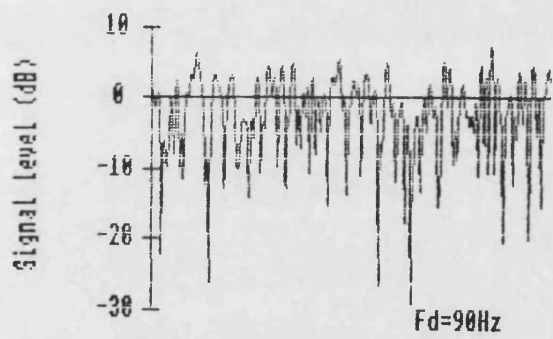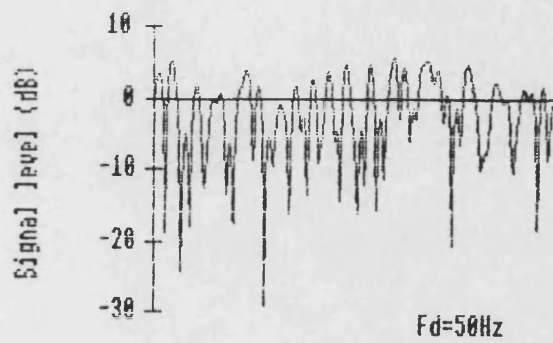
Figure A2.3 Simulated Rayleigh signals with Doppler frequencies of 50 Hz and 90 Hz using Arredondo type simulator. The horizontal scale corresponds to one second in time.
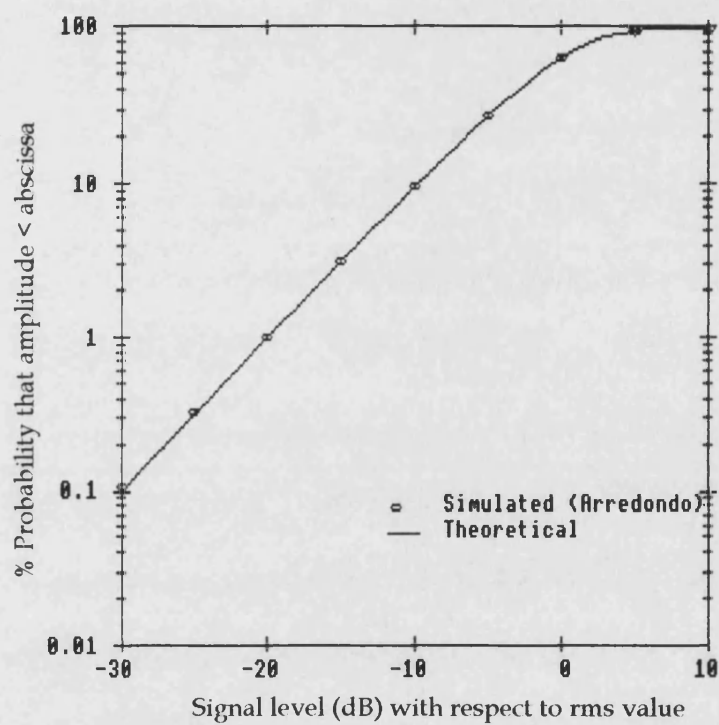
Figure A2.4   Cumulative   distribution of theoretical
and simulated Rayleigh signals.

195
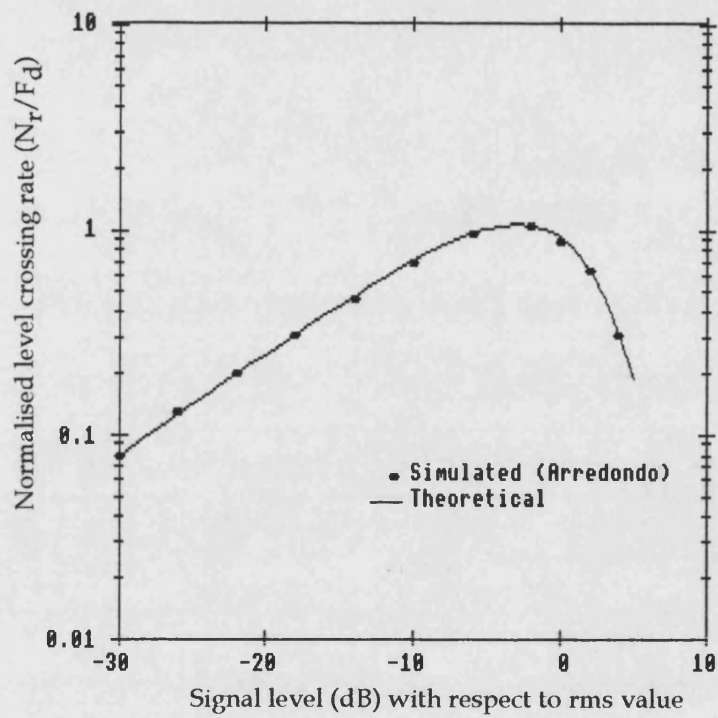
Figure A2.5 Normalised level crossing rates using Arredondo simulator.

196
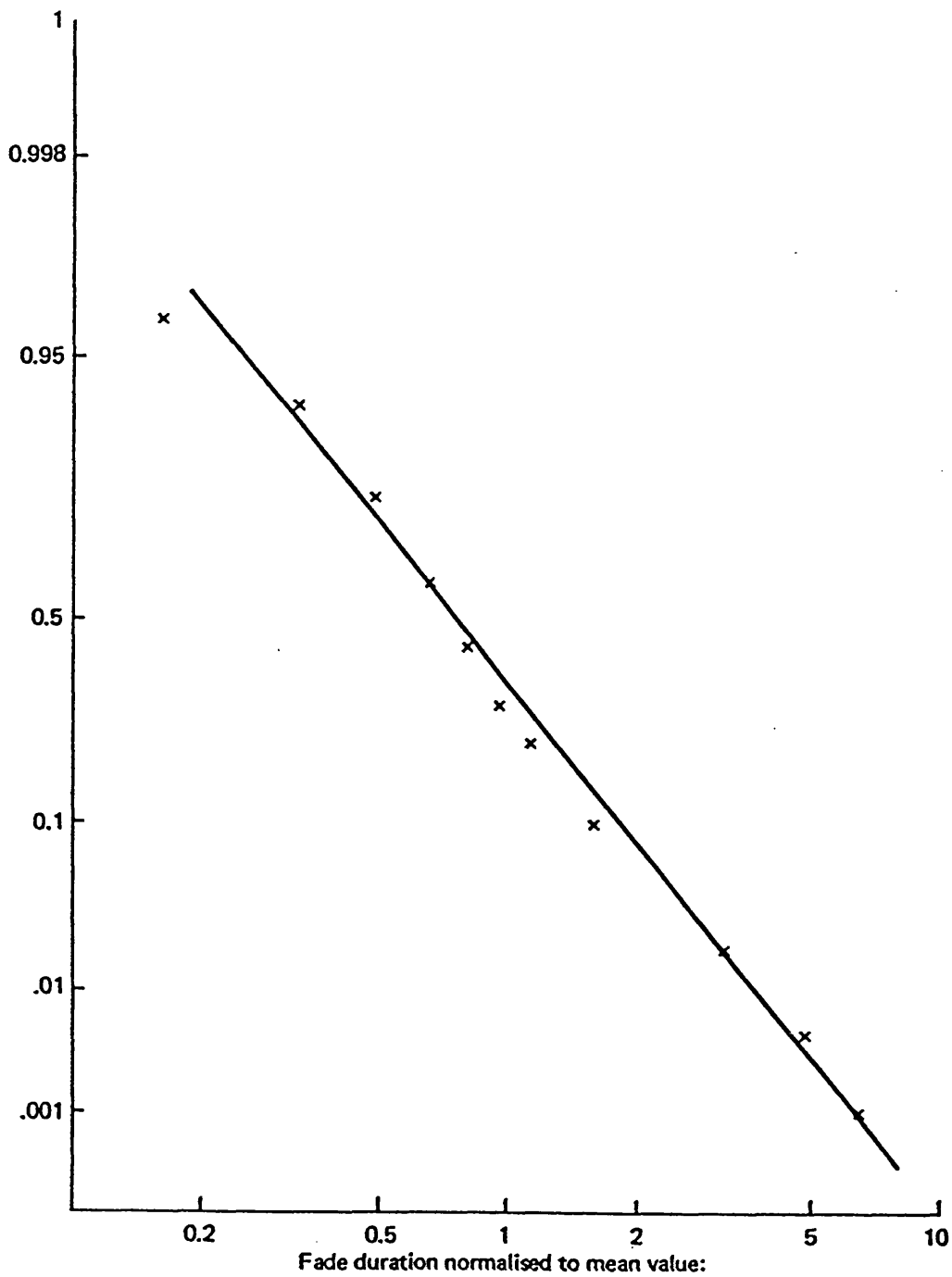
Figure A2.6 Probability of simulated Rayleigh signal fades exceeding given duration.
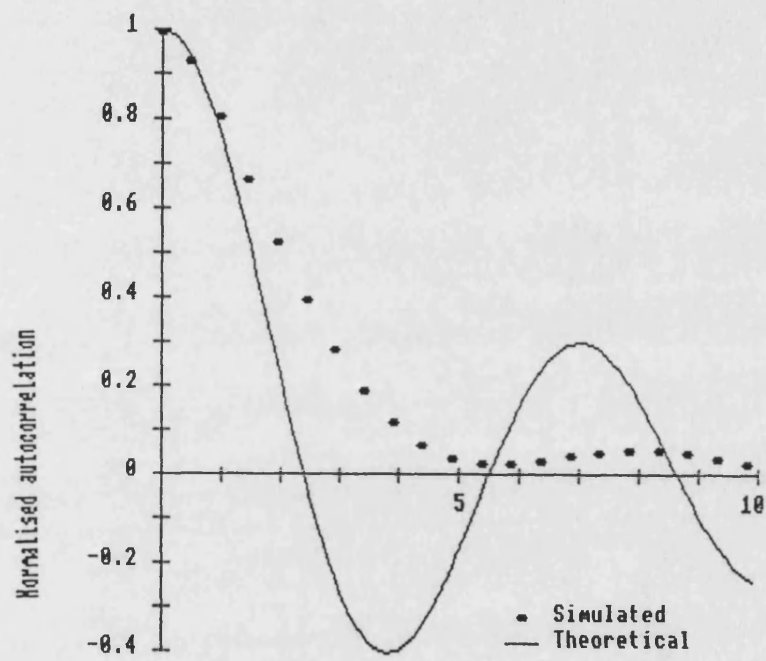
Figure A2.7 Computed auto-correlation of simulated Arredondo simulator.
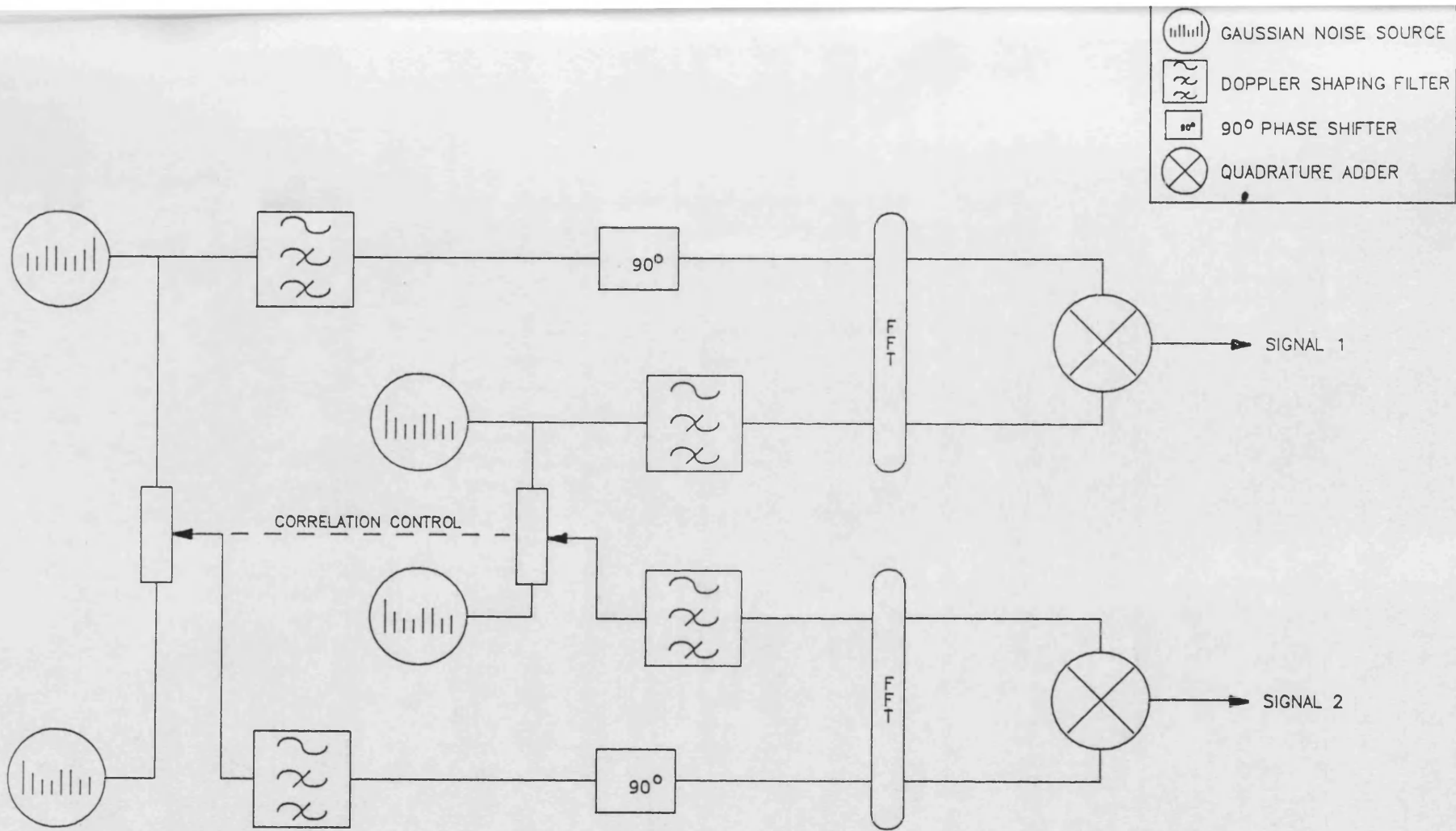
Figure A2.8   Schematic diagram of Arredondo Rayleigh fading simulator with diversity.
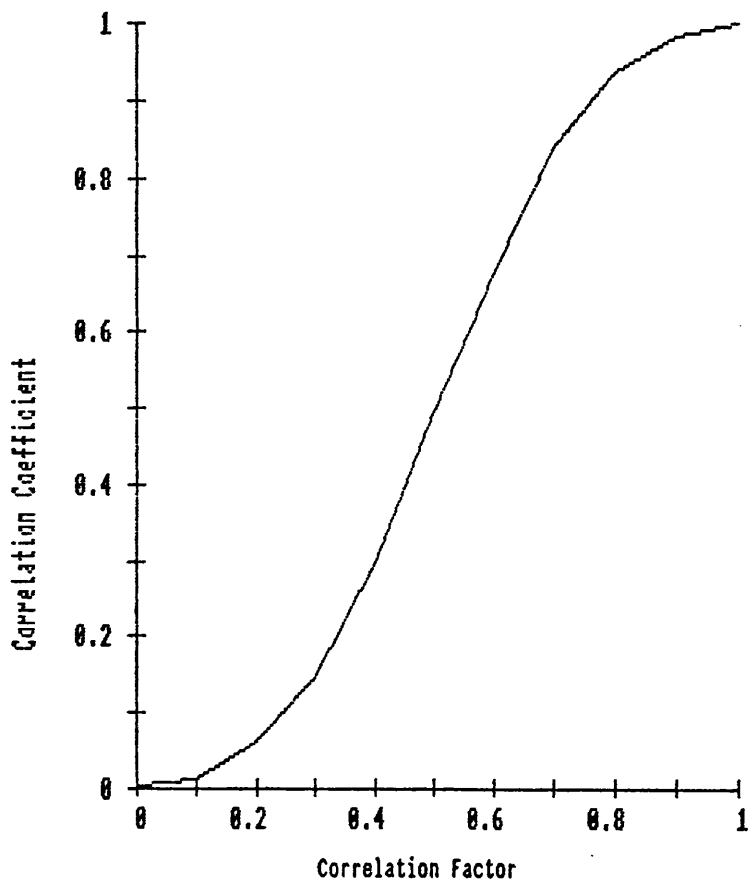
Figure A2.9 Relationship between correlation factor and correlation coefficient (Arredondo model).

BASIC procedures for simulating Rayleigh signal with Jakes model.

```
 10 REM PROGRAM USES JAKES SIMULATION MODEL TO GENERATE
 20 REM RAYLEIGH SIGNAL AND STORE IN FILE CALLED "RAYOUT":
 30 :
 40 DIM R(8),S(8)
 50 A=OPENOUT "RAYOUT"
 60 INPUT"DOPPLER FREQUENCY=";Fd%
 70 INPUT "NO OF SECONDS=";NO_OF_SECONDS
 80 Z=RND(-TIME)
 90 :
100 No%=8: N%=2*(2*No%+1)
110 F%=NO_OF_SECONDS*Fd%/2: M%=20*F%
120 Wm=2*PI*F%
130 :
140 REM GENERATE RAYLEIGH SIGNAL
150 FOR I%=1 TO No%: Q1=PI*RND(1): Q2=PI*RND(1)
160 R(I%)=COS(Q1): S(I%)=SIN(Q1): NEXT
170 FOR I%=1 TO M%: t=I%/M%
180 Z=0:Y=0
190 FOR n%=1 TO No%
200 Wn=Wm*COS(2*PI*n%/N%)
210 Z=Z+R(n%)*COS(Wn*t): Y=Y+S(n%)*COS(Wn*t)
220 NEXT
230 X0=(2*Z)+(SQR2)*COS(Wm*t): X1=(2*Y)
240 X=X0^2+X1^2
250 :
260 REM NORMALISE TO 0dB AND STORE SEQUENCE
270 Xout=10*LOG(X/17): PRINT# A, Xout: NEXT
280 CLOSE#A
290 :
300 STOP
```

The following program generates two partially correlated Rayleigh signals.

```
  10 REM PROGRAM GENERATES TWO PARTIALLY CORRELATED
  20 REM RAYLEIGH SIGNALS AND STORES IN FILES "BRANCH1"
  30 REM AND "BRANCH2"
  40 DIM R(8),S(8),R1(8),S1(8)
  50 INPUT "DOPPLER FREQUENCY=";Fd%
  60 INPUT "NO OF SECONDS=";NO_OF_SECONDS
  70 Z=RND(-TIME)
  80 :
  90 No%=8: N%=2*(2*No%+1)
 100 F%=NO_OF_SECONDS*Fd%/2: M%=20*F%
 110 Wm=2*PI*F%: COR=.7
 120 :
 130 FOR I%=1 TO No%: Q1=PI*(2*RND(1)-1)
 140 Q2=PI*(2*RND(1)-1): Q3=(COR*Q1)+(1-COR)*Q2
 150 R(I%)=COS(Q1): S(I%)=SIN(Q1)
 160 R1(I%)=COS(Q3): S1(I%)=SIN(Q3): NEXT
 170 :
 180 REM GENERATE FIRST RAYLEIGH SIGNAL
 190 A=OPENOUT "BRANCH1"
 200 PROCjakes
 210 CLOSE#A
 220
 230 REM GENERATE SECOND RAYLEIGH SIGNAL
 240 A=OPENOUT "BRANCH2"
 250 PROCjakes
 260 CLOSE#A
 270 STOP
 280 :
 290 DEFPROCjakes
 300 FOR I%=1 TO M%: t=I%/M%
 310 Z=0:Y=0
 320 FOR n%=1 TO No%
 330 Wn=Wm*COS(2*PI*n%/N%)
 340 Z=Z+R1(n%)*COS(Wn*t): Y=Y+S1(n%)*COS(Wn*t)
 350 NEXT
 360 X0=(2*Z)+(SQR2)*COS(Wm*t): X1=(2*Y)
 370 X=X0^2+X1^2
 380 Xout=10*LOG(X/17): PRINT #A, Xout: NEXT
 390 ENDPROC
```

The following program uses a development of the Jakes model

```
10 REM PROGRAM USES A MODIFIED JAKES SIMULATION
20 REM MODEL TO GENERATE RAYLEIGH SIGNAL AND
30 REM STORE IN FILE CALLED "RAYOUT"
40 DIM R(8),S(8),B(30),THETA_n(12)
50 A=OPENOUT "RAYOUT"
60 INPUT "DOPPLER FREQUENCY=";Fd%
70 INPUT "NO OF SECONDS=";NO_OF_SECONDS
80 Z=RND(-TIME)
90 :
100 No%=12: N%=4*No%
110 F%=NO_OF_SECONDS*Fd%/2: M%=20*F%: DIM X(M%,1)
120 Wm=2*PI*F%
130 :
140 REM GENERATE RAYLEIGH SIGNAL
150 :
160 FOR I%=1 TO No%: THETA_n(I%)=PI*(2*RND(1)-1): NEXT
170 FOR I%=1 TO M%: t=I%/M%
180 Z=0:Y=0
190 FOR n%=1 TO No%: BETA=PI*n%/No%: ALPHA_n=2*PI*(n%-.5)/No%
200 Wn=Wm*COS(ALPHA_n)
210 Z=Z+(COS(BETA))*COS((Wn*t)+THETA_n(n%)):
220 Y=Y+SIN(BETA)*COS((Wn*t)+THETA_n(n%))
230 NEXT
240 X(I%,0)=SQR(2/No%)*Z: X(I%,1)=SQR(2/No%)*Y
250 NEXT
260 :
270 REM NORMALISE TO 0dB AND STORE SEQUENCE
280 S=0: FOR I%=1 TO M%: X(I%,0)=X(I%,0)^2+X(I%,1)^2
290 S=S+X(I%,0): NEXT
300 S=S/M%: FOR I%=1 TO M%: Xout=10*LOG(X(I%,0)/S)
310 PRINT # A, Xout: NEXT
320 CLOSE#A
330 :
340 STOP
```

Basic procedures used for combining/selecting signals.

```
 10 DEF PROCselection_combining
 20 FOR I%=1 TO sample_sequence_length%
 30 IF X(I%,0)<X(I%,1) THEN X(I%,0)=X(I%,1)
 40 NEXT
 50 ENDPROC
 60 :
 70 :
 80 DEF PROCequal_gain_combining
 90 FOR I%=1 TO sample_sequence_length%
100 X(I%,0)=10^(X(I%,0)/10): X(I%,1)=10^(X(I%,1)/10)
110 X(I%,0)=0.25*(SQR(X(I%,0))+SQR(X(I%,1)))^2
120 X(I%,0)=10*LOG(X(I%,0)): NEXT
130 ENDPROC
140 :
150 :
160 DEF PROCmaximal_ratio_combining
170 FOR I%=1 TO sample_sequence_length%
180 X(I%,0)=10^(X(I%,0)/10): X(I%,1)=10^(X(I%,1)/10)
190 X(I%,0)=0.5*(X(I%,0)+X(I%,1))
200 X(I%,0)=10*LOG(X(I%,0)): NEXT
210 ENDPROC
```

Bit error probabilities due to impulsive noise.

Impulsive noise consists of bursts of energy which can be regarded as impulses if the duration of each noise pulse is short compared with the reciprocal of the receiver bandwidth. Measurements of the amplitude and time statistics have been made at VHF and UHF in various urban and suburban locations[94-95]. It is recognised that impulsive noise impairs data transmission and work on predicting and measuring bit error rates has been reported[96-98]. Unlike thermal noise impulsive noise is very difficult to model. A CCIR recommendation[99] provides median values of impulsive noise power expressed in terms of dB above thermal noise at T=288K for business, residential and rural areas in the USA.

The median values of the impulsive noise power, for frequencies between 0.3 and 250MHz, is of the form:-

$$F_{am}=c-d \log f_c \qquad A5.1$$

where f_c is the frequency in MHz and c and d are constants, the values of which are provided in CCIR Recomendation 258-4 and are listed below. At 150 Mhz the median value of impulsive noise based on A5.1 are estimated as follows.

	c	d	F_{am} (dB)
Business	76.8	27.7	16.5
Inter-state highway	73.0	27.7	12.7
Residential	72.5	27.7	12.2
Rural	67.2	27.7	6.93

By adding F_{am} to the thermal noise level input into the DMRCS an allowance can be made for the effects of impulsive noise at the frequency and in the type of environment under consideration.

The simulation presented in Chapter 6 were based on a UHF mobile-base path where the base receiver would be clear of local noise sources.

ANNEX 6

DATA BIT ERROR RATE MEASUREMENTS

Measurements have been carried out with several modems typical of those used for the transmission of data over mobile radio networks. The three modems used supported the following data modulation and bit rates.

i) Fast Frequency Shift Keying (FFSK) at 1200 bits/sec.

ii) Bipolar Coded FM (BFM) at 4800 bits/sec.

iii) Gaussian filtered Minimum Shift Keying (GMSK) at 8000 bits/sec

Fast Frequency Shift Keying (FFSK) of an audio sub-carrier (also referred to as Minimum Shift Keying (MSK)) is accepted as an international standard[100-101]. It can be considered either as a version of FSK with the carrier deviation equal to half the bit rate, giving smooth phase transistions between the bit boundaries[102] or as a version of Quadrature PSK in which the phase change from bit to bit is a linear function of time, changing by +/-90 degrees during each bit period[103]. It offers a superior spectrum efficiency compared with other traditional constant envelope types, e.g Octave FSK and DPSK. A binary "0" is represented by one and a half cycles of 1800Hz and a binary "1" by one cycle of 1200Hz. To ensure phase continuity each binary "0" and "1" subcarrier waveform

starts with either 0 or 180 degrees, FFSK can be coherently demodulated[102,104], such detection requires a reference signal that is in phase synchronisation with the audio sub-carrier. This signal is usually obtained by deriving a reference from the data signal. The fading experienced on a mobile radio channel results in sharp phase transactions having large instantaneous frequency changes which carrier recovery circuits have difficulty tracking due to their narrow bandwidth. An alternative method of generating a reference signal is by the transmission of an adjacent tone reference[105-106]. Bandwidth limitations prohibit this approach and modems for land mobile radio use invariably utilise non-coherent differential[107-108], zero crossing[109] or frequency discriminator[110] demodulation.

Whilst FFSK of an audio sub-carrier is recognised as a standard for indirect modulation Bipolar signalling is an established method of directly representing digital symbols on an RF carrier. In this particular scheme, (also refered to as Alternate-Mark-Inversion (AMI) coding), binary "1"'s are encoded as marks which are alternatively positive and negative,while binary "0"'s are encoded as spaces. An example of this is shown in Figure A6.1. Because three levels are distinguished in the demodulator, compared with two for binary signalling, higher signal/noise ratios are required for given bit error probabilities.

One advantage of bipolar signalling stems from the fact that the information is higher than that of binary signalling. A bipolar code is a pseudo-ternary code in that unlike ternary codes the extra information is unused. It follows that many of the +1, 0, -1 combinations will be unused as n baud have to represent 2^n rather than 3^n states. The combinations of +1, 0 and -1 which are not utilised enable the DC and low frequency components to be eliminated. This condition is particularly important with direct modulation implemented on commonly used phased modulated radios. This is because the frequency modulating voltage must not contain any DC component since otherwise its integral, the phase modulating voltage would increase infinitely. Furthermore it is desirable to exclude DC errors due to transmitter and receiver oscillator drift and to avoid the need for DC coupling. A further advantage of the unused +1, 0 and -1 combinations is that they can be used for error monitoring as an error can form one of these unused combinations.

Bipolar coding is only one of a number of pseudo ternary codes[111] and although its performance can be improved upon[112] it offers the advantage of requiring simple coding and circuitry. 4800 baud bipolar coded FM/PM is widely used around the world in mobile data terminals[113-114] and has been recommended as a standard[100].

Premodulation Gaussian filtered Minimum Shift Keying is commonly used to achieve higher data transmission rates over mobile radio channels. In this modulation technique, the digital binary data is filtered by a Gaussian low-pass filter prior to being modulated by the FM modulator.

In order to simulate reception from a single tranmitter the test equipment configured as shown in Figure A6.2 was used. A binary data test set generated 2047-bit pseudo random binary sequences of 10^6 bits. This data and a clock signal were passed to the transmit modem. The modems were transparent in that neither additional channel coding nor a frame supplement was used. The output of the modem was connected via a filter and attenuator to the external modulation input of the RF signal generator, the attenuator being adjusted to set the peak RF deviation to +/- 2.5KHz. This value was used because it ensured firstly that out of band radiation both with the signal generators and more importantly with typical commercial base and mobile transmitters were within the limits required of mobile and fixed station transmitters[115]. Secondly, it did not provide significant distortion in the radio receivers. The output from the signal generator sourced a mobile radio receiver that was typical of those used for mobile communications, this particular one utilised a quadrature discriminator. In order to

recover the data, interfaces were made electrically close to the demodulators. The signals were demodulated in a modem receiver and the recovered data clock signals were returned to the data test set where a mod-2 addition of the transmitted and received data enabled bit errors to be detected and counted.

The signal level at the input of the radio receiver was adjusted and measurements of bit error rates recorded. The results for 1200 baud FFSK are shown in Figure A6.3, for 4800 baud bipolar coded FM in Figure A6.4 and for 8000 baud GMSK in Figure A6.5. In all cases, without fading the bit error rate was highly dependent on the received signal level, falling rapidly as the signal level was increased. The noise floor was measured and found to be -20.5dBuV.

Some measurements were made with a multipath fading simulator similar to those proposed elsewhere[79-80].
When the signals were subject to fading the bit error rates decreased inversely with signal level before becoming irreduceable. This latter effect being due to the random FM noise arising from the phase fluctuations of the RF signal.

Relationship between signal to noise levels and probability of bit error.

For non-coherent demodulation of FFSK the probability of bit error can be given by[116]:-

$$Pe(\gamma) = 0.5 \ e^{-\frac{\gamma}{2}} \qquad A6.1$$

Intuitively from equation A5.1 the bit error probability for the FFSK modem is given by:-

$$Pe(\gamma) = \frac{1}{2} e^{-a\gamma^b} \qquad A6.2$$

where γ is the received signal to noise ratio and a and b are constants. Using a curve fitting algorithm for the non-faded signal in Figure A6.3 and a measured noise floor of -20.5dBuV it can be shown that:-

$$Pe(\gamma) = \frac{1}{2} e^{-0.73\gamma^{1.61}} \qquad A6.3$$

Similarly for bipolar FM the probability of bit error is given by[116]:-

$$Pe(\gamma) = \frac{1}{2} erfc\sqrt{\frac{\gamma}{2}} \qquad A6.4$$

Assuming the probability of bit error is of the form:-

$$Pe(\gamma) = \frac{1}{2} erfc(a\gamma^b) \qquad A6.5$$

and applying a curve fitting algorithm to the non-fading signal in Figure A6.4 it can be shown that:-

$$Pe(\gamma) = \frac{1}{2} erfc(6.53\gamma^{0.58}) \qquad A6.6$$

For the GMSK modem a curve fitting program was applied to A6.5 and the following relationship was found:-

$$Pe(\gamma) = \frac{1}{2} e^{-(0.503\gamma^{.724})} \qquad A6.7$$

Relationship between Doppler frequency and irreducible probability of bit error.

In order to provide an accurate simulation of

irreducible bit error probability for the different data modulations empirical formulae based on the measured results have been deduced. For FFSK the relationship is given by:-

$$Pe_{IBER}=1.3x10^{F_d/48-5} \qquad 6.8$$

and for GMSK:-

$$Pe_{IBER}=7.9 \ x \ 10^{-6} \ 10^{.0325F_d} \qquad A6.9$$
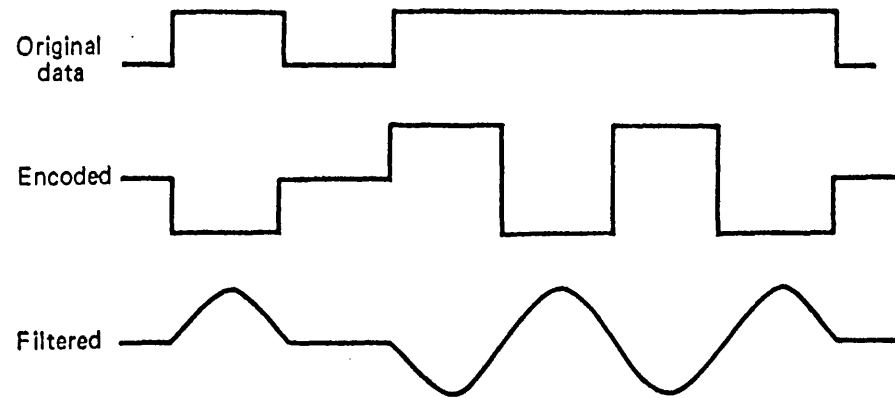
Figure A6.1 Bipolar (or alternate-mark-inversion) signalling.
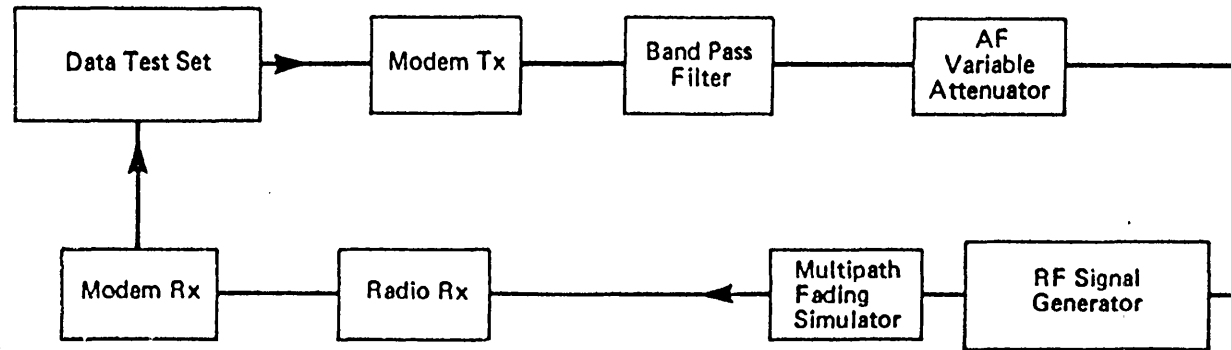
Figure A6.2 Configuration of test equipment used to determine dependance of measured bit error rates on received rf signal level.
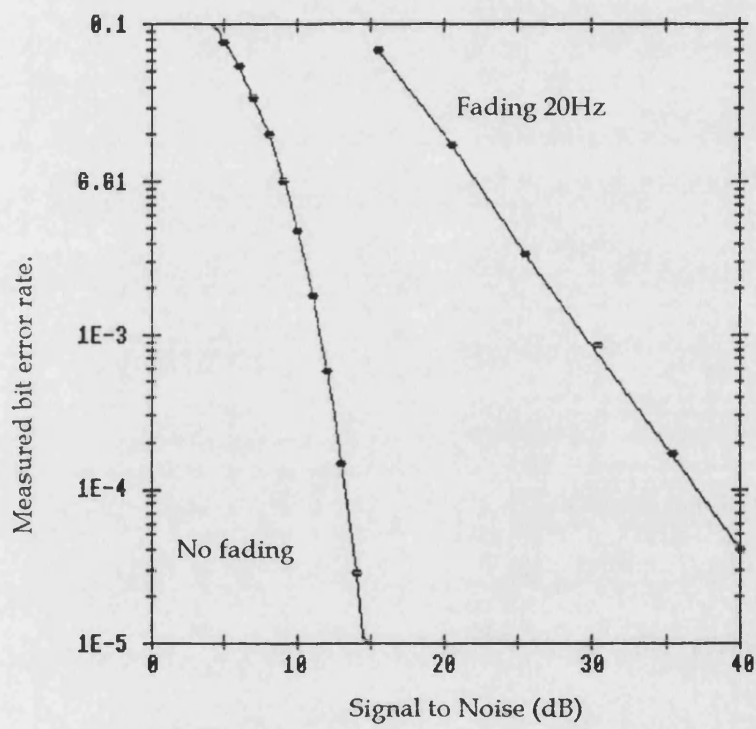
Figure A6.3 Measured bit error rates for 1200 bits/sec
FFSK over VHF FM mobile radio.
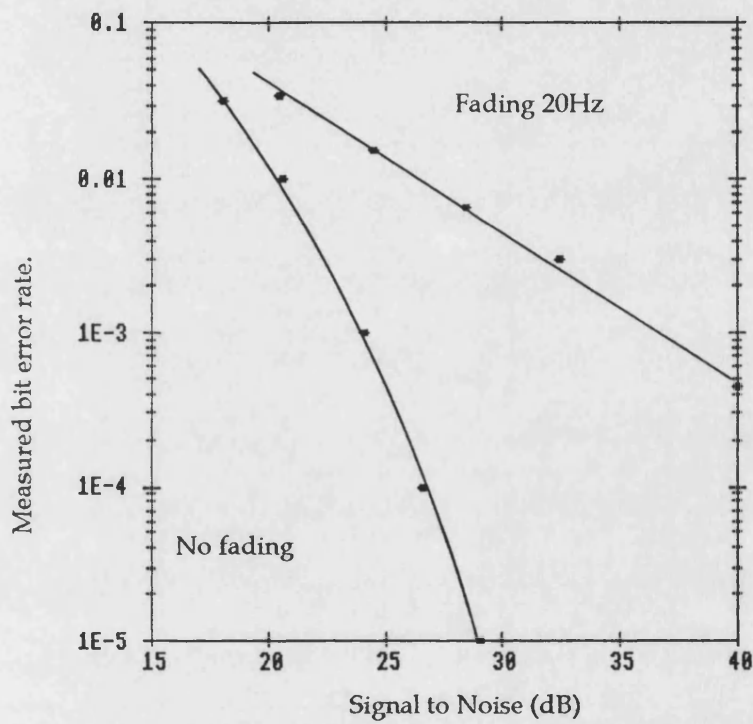
Figure A6.4 Measured bit error rates for 4800 bits/sec bipolar FM over VHF mobile radio.
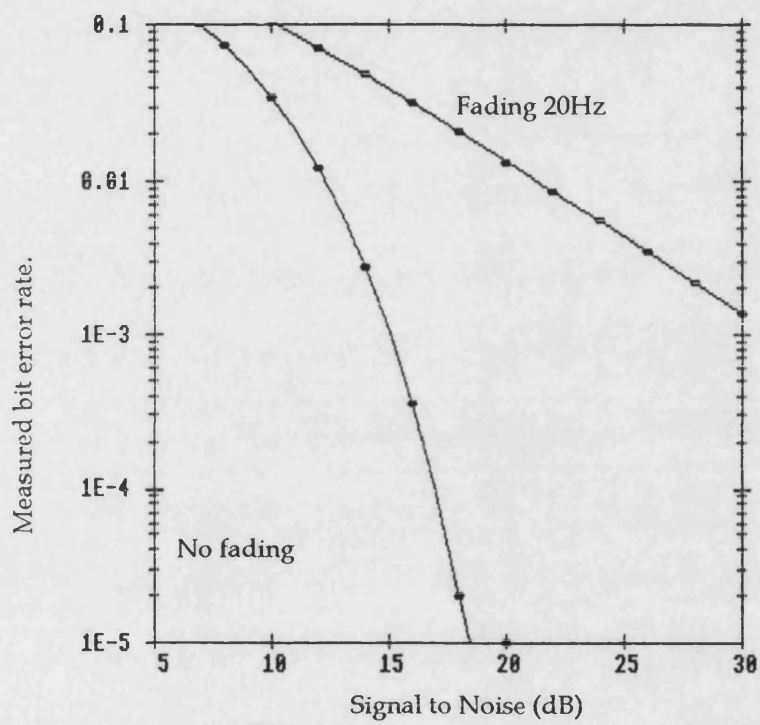
Figure A6.5 Measured bit error rates for 8000 bits/sec
GMSK over VHF mobile radio.

Procedure for removing slow fading component from received signal strength composed of fast and slow components.

```
  10 REM PROGRAM TO REMOVE THE SHADDOWING FROM A RAYLEIGH
  11 REM SIGNAL SUPERIMPOSED ON A SHADDOWING SIGNAL.
  20 CLOSE #0
  30 M%=40000:         REM TOTAL NO OF SAMPLES
  40 WINDOW%=2001: REM DURATION OVER WHICH SIGNAL IS AVERAGED.
  50 DIM MEAN(M%), X(M%)
  60 K%=(WINDOW%-1)/2
  70 :
  80 REM READ SIGNAL AND CONVERT TO LINEAR FORM
  90 A=OPENIN "SIGNAL1"
 100 FOR I%=1 TO M%
 110 INPUT #A,X
 120 X(I%)=10^(X/10)
 130 NEXT
 140 CLOSE #A
 150 :
 160 REM CALCULATE "MOVING AVERAGE"
 170 B=OPENOUT "SIGNAL_MEAN"
 180 FOR I%=K% TO M%-K%
 190 MEAN=0
 200 FOR J%=-K% TO K%
 210 MEAN=MEAN+X(I%+J%)
 220 NEXT J%
 230 MEAN(I%)=10*LOG(MEAN/WINDOW%)
 240 PRINT #B, MEAN(I%)
 250 NEXT
 260 :
 270 REM SUBTRACT MOVING AVERAGE FROM SIGNAL
 280 A=OPENIN "SIGNAL1"
 281 C=OPENOUT "SIGNAL2"
 290 FOR I%=1 TO M%
 300 INPUT #A,X
 310 X(I%)=X
 320 NEXT
 330 :
 340 FOR I%=K% TO M%-K%
 350 Z=X(I%)-MEAN(I%)
 360 PRINT #C,Z
 361 NEXT
 362 CLOSE #0
 363 STOP
 370
```

REFERENCES

1 Ahern B H, Data based command and control system. Conference Proceeding of Communications 1974, pp 3.3/1-3.3/8.

2 Hollis J B, The engineering of a mobile data system for the London Fire Brigade. Electronic Technology, Vol 22, January 1988, pp 13-15.

3 Morris J, Creative resources management using digital communications. Proceedings of the IEEE 33rd Vehicular Technology Conference, 25-27 May 1983, Toronto, Ontario, pp 427-431.

4 Lodde R C, Experiences gathered during the development and operation of a nationwide mobile digital communications system. Proceedings of the IEEE 32nd Vehicular Technology Conference, May 1982, pp 384-391.

5 Morris J, MDTs give mobiles direct access to digital computer data bases. Mobile Radio Technology, December 1983, pp 24-31.

6 Owen P L T, Operational requirement for automatic

vehicle location (AVL) in the UK police and fire services. Nav 85 Conference on Land Navigation and Location for Mobile Applications, York University, 1985.

7 Yang T T and Yan Yip K, Use of wireless area packet data networks as a solution to land-based positioning and navigation. Differential Satellite Navigation Systems Conference 1994.

8 Wilkinson G, Mobile data a Fire Service perspective. Blenheim Online Conference:- Business Opportunities and Technical Developments in Mobile Data, London September 1992 pp 103-113.

9 Pearce J, Mobile Data: The practical realities. Mobile Radio Users Association Annual Conference, Cambridge April 1990.

10 Proceedings of the Blenheim Online conference on Business opportunities and technical developments in Mobile Data. Held in London, September 1992.

11 Proceedings of the IBC Technical services Conference on Mobile Data Services - communications and computing on the move. Held in London 26th September 1991.

12 Haine J L, Air interface protocol for mobile packet data. IEE Colloquium on Future Mobile Radio Trunking and Data Systems. Digest 1991/051 27 February 1991, pp4/1-4/10.

13 Hollis J B, Air interface protocols for a national mobile data network. IEE Coloquium on Cordless Computing - Systems and Users Experience Digest 1993/003. 12 January 1993, pp 1/1-1/5.

14 Davie M C and Smith J B, A cellular packet radio data nework. Electronics & Communication Engineering Journal June 1991, pp 137-143.

15 Handford R, Ericsson's Mobitex is Europe's top mobile data technology. Mobile Communications, (Published by Financial Times Business Enterprises Ltd), Issue No 123, April 7 1993, pp 123/2 & 123/9.

16 French R C, Mobile radio data transmission in the urban environment. Proceedings of the International Conference on Communications. Philadelphia, Pennsylvania, USA June 14-16 1976, pp 27-15 to 27-20.

17 Arredondo G A and Smith J I, Voice and data transmission in a mobile radio channel at 850 MHz. IEEE

Transactions on Vehicular Technology, vol VT-26, No 1, February 1977, pp 88-93.

18 RAM Mobile Data, Mobitex System Overview, Version 2.0 3 May 1994.

19 Jakes W C, A comparison of specific space diversity techniques for reduction of fast fading in UHF mobile radio systems. IEEE Transactions on Vehicular Technology, Vol VT-20, No 4, November 1971, pp 81-92.

20 Parsons J D, Henze M, Ratcliff P A and Withers M J, Diversity techniques for mobile radio reception. The Radio and Electronic Engineer, Vol 45, No 7, July 1975, pp 357-367.

21 Comroe R A and Costello D J, ARQ schemes for data transmission in mobile radio systems. IEEE Transactions on Vehicular Technology, Vol VT-33, August 1984, pp 88-97.

22 DaSilva J S, Hefez H M and Mahmoud S A, Optimal packet length for fading land mobile data channels. IEEE International Conference on Communications 1980 pp 61.3.1-61.3.5.

24 Jakes W C and Reudink D O, Comparison of mobile radio transmission of UHF and X band. IEEE Transactions   on Vehicular Technology, Vol VT-16, No 1, October 1986, pp 10-14.

25   Clarke R H, A statistical theory of mobile-radio reception. Bell System Technical Journal, Vol 47, July-August 1968, pp 957-1000.

26   Nylund H W, Characteristics of small-area signal fading on mobile circuits in the 150 MHz band. IEEE Transactions on Vehicular Technology, Vol VT-17, No 1, October 1968, pp 24-30.

27 Gans M J, A power spectral theory of propagation in the mobile radio environment. IEEE Transactions on Vehicular Technolgy, Vol VT-21, No 1, February 1972, pp 27-38.

28 Rice S O, Mathematical analysis of random noise. Bell System Technical Journal, Vol 23, July 1944, pp 282-332 and Vol 24, January 1945, pp 46-156.

29 Rice S O, Statistical properties of a sine wave plus random noise. Bell System Technical Journal, Vol 27, January 1948, pp 109-159.

30   Lee W C Y, Statistical analysis of the level crossings and duration of fades of the signal from an energy density mobile radio antenna. Bell System Technical Journal, February 1967, pp 417-448.

31 Blake I F and Linsey W C, Level-crossing problems for random processes. IEEE Transactions on Information Theory, Vol IT-19, No 3, May 1973, pp 295-315.

32 Vigants A, Number and duration of fades at 6 and 4 GHz. Bell System Technical Journal, Vol 50, March 1971, pp 815-841.

33 Nielson D L, Microwave propagation measurements for mobile digital radio application. IEEE Transactions on Vehicular Technology, Vol VT-27, No 3, August 1978, pp 117-132.

34   Freeburg T A, An accurate simulation of multi-path fading. Proceedings of the National Electronics Conference, Vol 32, October 1978, pp 140-142.

35 Bodtmann W F and Arnold H W, Fade duration statistics of a Rayleigh-distributed wave. IEEE Transactions on Communications, Vol COM-30, No 3, March 1982, pp 549-553.

36   Arnold H W and Bodtmann W F, Interfade interval
statistics of a Rayleigh-distributed wave. IEEE
Transactions on Communications, Vol COM-31, No 9,
September 1983, pp 1114-1116.

37   Cox D C, Delay Doppler characteristics of multipath
propagation at 910 MHz in a suburban mobile radio
environment. IEEE Transactions on Antennas and
Propagation, Vol AP-20, No 5, September 1972, pp 625-
635.

38   Cox D C, 910 MHz urban mobile radio propagation:
multipath characteristics in New York City. IEEE
Transactions on Communications, Vol COM-21, November
1973, pp 1188-1194.

39   Cox D C, Multipath delay spread and path loss
correlation for 910 MHz urban mobile radio propagation.
IEEE Transactions on Vehicular Technology, Vol VT-26,
November 1977, pp 340-344.

40   Bajwa A S and Parsons J D, Small-area
characterisation of UHF urban and suburban mobile radio
propagation. IEE Proceedings Vol 129 Part F, no 2, April
1982, pp 102-109.

41   Bajwa A S and Parsons J D, Large area characterisation of urban UHF multipath propagation and its relevance to the performance bounds of mobile radio systems. IEE Proceedings Vol 132, Part F, No 2, April 1985, pp 99-106.

42   Cox D C and Leak R P, Correlation bandwidth and delay spread multipath propagation statistics for 910 MHz urban mobile radio channels. IEEE Transactions on Communications, Vol COM-23, November 1975, pp 1271-1280.

44   Meno F I, Mobile radio fading in Scandinavian terrain. IEEE Transactions on Vehicular Technology, Vol VT-26, no 4, November 1977, pp 335-340.

45   Reudink D O, Properties of mobile radio propagation above 400 MHz. IEEE Transactions on Vehicular Technology, Vol VT-23, no 4, November 1974, pp 143-160.

46   Lee W C Y and Yeh Y S, On the estimation of the second order statistics of log-normal fading in mobile radio environment. IEEE Transactions on Communications, Vol COM-22, No 6, June 1974, pp 869-873.

47   French R C, Radio propagation in London at 462 MHz. The Radio and Electronic Engineer, Vol 46, No 7, July

1976, pp 333-336.

48   Low K, UHF field-strength measurements for
determination of the influence of buildings and
vegetation in the land mobile radio service. IEEE
Vehicular Technology Conference Proceedings, Dallas,
Texas, USA, 20-22 May 1986, pp 40-45.

49 Rubinstein T N, The standard deviations of the local
means of land mobile radio signals in flat   suburban
terrain.   IEEE   Vehicular   Technology   Conference
Proceedings, Dallas, USA, 20-22 May 1986, pp 52-56.

50 Adachi F, Hattori T; Hirade K, Kamata T, A periodic
switching diversity technique for a digital FM land
mobile radio. IEEE Transactions on Vehicular Technology,
Vol VT-27, No 4, November 1978, pp 211-219.

51 Lee W C Y, A study of the antenna array configuration
of an m-branch diversity combining mobile radio receiver.
IEEE Transactions on Vehicular Technology, Vol VT-20, No
4, November 1971, pp 93-104.

52 Adachi F, Ohno K and Ikura M, Postdetection selection
diversity reception with correlated, unequal average power
Rayleigh signals for $\pi/4$-shift QDPSK mobile radio. IEEE

Transactions on Vehicular Technology. Vol VT-41, No 2, May 1992, pp 199-210.

53   Lee W C Y, Antenna spacing requirement for a mobile radio base-station diversity. The Bell System Technical Journal, Vol 50, No 6, July-August 1971, pp 1859-1876.

54   Lee W C Y, Effects on correlation between two mobile radio base-station antennas. IEEE Transactions on Communications, Vol COM-21, No 11, November 1973, pp 1214-1224.

55   Rhee S and Zysman G I, Results of suburban base station spatial diversity measurements in the UHF band. IEEE Transactions on Communications, Vol COM-22, No 10, October 1974, pp 1630-1636.

56   Lee W C Y, Mobile radio signal correlation versus antenna height and spacing. IEEE Transactions on Vehicular Technology, Vol 25, August 1977, pp 290-292.

57   Adachi F, Feeney M T, Williamson A G and Parsons J D, Crosscorrelation between the envelopes of 900 MHz signals received at a mobile radio base station site. IEE Proceedings, Vol 133, Pt F, No 6, October 1986, pp 506-512.

58   Kozono S, Tsuruhara T and Sakamoto M, Base station polarisation diversity reception for mobile radio. IEEE Transactions on Vehicular Technology, Vol VT-33, No 4, November 1984, pp 301-306.

59   Brennan D G, Linear diversity combining techniques. Proceedings of the IRE, Vol 47, June 1959, pp 1075-1102.

60   Lee W C Y, Mobile Communication Engineering, McGraw Hill 1982. Section 10.3.

61   Kahn L R, Ratio squarer. Proceedings of the IRE, Vol 42, November 1954 p 1704.

62   Jakes W C Microwave mobile communications, Wiley, New York, 1974, page 319-

63   Lee W C Y, Mobile radio performance for a two-branch equal-gain combining receiver with correlated signals at the land site. IEEE Transactions on Vehicular Technology, Vol VT-27, No 4, November 1978, pp 239-243.

64   Granlund J, Topics in the design of antennas for scatter. MIT Lincoln Lab., Lexington, Mass., USA. Technical Report No 135, November 1956, pp 105-113.

65   Parsons J D and Feeney M T, Comparison of selection and switched diversity systems for error-rate reduction at base-station sites in digital mobile radio systems. IEEE Vehicular Technology Conference Proceedings 1987,pp 393-398.

66   Eastmond B C and Pautler J A, Performance of a two-branch radiotelephone selection diversity receiver. IEEE Vehicular Technology Conference Proceedings 1979, pp 164-171.

67   Leung C, Bit error rates of selection diversity systems in Rayleigh fading channels. International Communication Conference Proceedings 1981, pp 23.5.1-23.5.5.

68   Shortall W E, A switched diversity receiving system for mobile radio. IEEE Transactions on Vehicular Technology, Vol VT-22, No 4, November 1973, pp 185-191.

69   Rustako A J, Yeh Y S and Murray R R, Performance of feedback and switch space diversity 900 MHz FM mobile radio systems with Rayleigh fading. IEEE Transactions on Vehicular Technology, Vol VT-22, No 4, November 1973, pp 173-184.

70   Feeney M T and Adachi F, The performance of various diversity combiners on signals received at a base-station site. IERE Third International Conference on Land Mobile Radio, Cambridge 10-13 December 1985, Publication no 65, pp 55-62.

71   Booker H G, Ratcliffe J A and Shinn D H, Phil. Trans. Roy. Soc. (London) Vol 242, September 1950, pp 579-607.

72   Pierce J N and Stein, Multiple diversity with non-independent fading, Proceedings of the IRE, Vol 48, January 1960, pp 89-104.

73   Jakes W C, Microwave mobile communications, Wiley, New York, 1974.

74   Okumura Y, Ohmori E, Kawano T and Fukuda K, Field strength and its variability in VHF and UHF land mobile service. Review of the Electronic Communications Laboratory, Vol 16, September-October 1968, pp 825-873.

75   Lee W C Y, Studies of base-station antenna height effects on mobile radio. IEEE Transactions on Vehicular Technology, Vol 29, May 1980, pp 252-260.

76   Longley A G and Rice P L, Prediction of tropospheric

radio transission loss over irregular terrain, a computer method. ESSA Tech. Rep., ERL-79-ITS 67, Institute for Telecommunications Sciences, Boulder, CO, page 11. (Alternatively see Durkin J, Computer prediction of service areas for VHF and UHF land mobile radio services. IEEE Transactions on Vehicular Technology, Vol VT26, No 4, November 1977, pp323-327).

77 Lee W C Y and Brandt, The elevation angle of mobile radio signal arrival. IEEE Transactions on Communications (Special Joint Issue on Mobile Radio Communications), vol COM-21, November 1973, pp 1194-1197

78 Lee W C Y, Estimate of local average power of a mobile radio signal. IEEE Transactions on Vehicular Technology, Vol VT-34, No 1, February 1985, pp 22-27.

79 Arredondo G A, Chriss W H and Walker E H, A multipath fading simulator for mobile radio. IEEE Transactions on Communications, Vol COM-21, No 11, November 1973, pp 1325-1328.

80 Ball J R, A real-time fading simulator for mobile radio. The Radio and Electronic Engineer, Vol 52, No 10, October 1982, pp 475-478.

81   Caples E L, Massad K E and Minor T R, A UHF channel simulator for digital mobile radio. IEEE Transactions on Vehicular Technology, Vol VT-29, No 2, May 1980, pp 281-289.

82   Arnold H W and Bodtmann W F, A hybrid multichannel hardware simulator for frequency-selective mobile radio paths. IEEE Transactions on Communications, Vol COM-31, No 3, March 1983, pp 370-377.

83   Goubran R A, Hafez H M and Sheikh A U H, Real-time programmable land mobile channel simulator. IEEE Vehicular Technology Conference Proceedings, 1986, pp 215-218.

84   Jakes W C, Microwave mobile communications, Wiley, New York, 1974, pp70-76.

85   Dent P, Bottomley G E and Croft T, Jakes fading model revisited. Electronic Letters Vol 29, No 13, 24 June 1993, pp 1162-1163.

86   Smith J I, A computer generated multipath fading simulation for mobile radio. IEEE Transactions on Vehicular Technology, Vol VT-24, No 3, August 1975, pp

39-40.

87   Comroe R A, Simulate multipath fading in BASIC. EDN, October 1979, pp 120-122.

88   Stremler F G, Introduction to communication systems. Addison-Wesley, 1977.

89   Gans M J, A power-spectral theory of propagation in the mobile-radio environment. IEEE Transactions on Vehicular Technology, Vol VT-21, No 1, February 1972, pp 27-38.

90   Bello P A and Nelin B D, The influence of fading spectrum on the binary error probabilities of incoherent and differentially coherent matched filter receivers. IRE Transactions on Communications Systems, Vol 10, June 1962, pp 160-168.

91   Chadwick H D, The error probability of a wide-band FSK receiver in the presence of multipath fading. IEEE Transactions on Communication Technology, Vol COM-19, October 1971, pp 699-707.

92   Hirade k, Ishizuka M, Adachi F and Ohtani K, Error rate performance of digital FM with differential

detection in land mobile radio channels. IEEE Transactions on Vehicular Technology, Vol VT-28, No 3, August 1979, pp 204-212.

93 Hummels D R and Ratcliffe F W, Calculation of error probability for MSK and OQPSK systems operating in a fading multipath environment. IEEE Transactions on Vehicular Technology, Vol VT-30, No 3, August 1981, pp 112-120.

94 Sheikh A U H and Parsons J D, The frequency dependence of urban man-made radio noise. The Radio and Electronic Engineer, Vol 53, No 3, March 1983, pp 92-98.

95 Parsons J D and Sheikh A U H, Statistical characterization of v.h.f. man-made radio noise. The Radio and Electronic Engineer, Vol 53, No 3, March 1983, pp 99-106.

96 Edwards, J A, Parsons J D and Albert-Osaghae V K I, Error rate prediction in binary FSK communication systems subjected to impulsive noise. IEE Proceedings Part F, Vol 132, No 6, November 1981, pp 337-341.

97 Parsons J D, Edwards J A nd Albert-Osaghae, Error rate prediction in binary FSK communication systems subjected

to impulsive noise: an extended second-order technique. Iee Proceedings Part F, Vol 132, No 6, November 1981, pp 342-346.

98 Parsons J D and Reyhan T, Prediction of bit error rate in the presence of impulsive noise: a numerical approach using measured noise data. IEE Proceedings Part F, Vol 132, No 5, August 1985, pp 334-342.

99   CCIR Report 258-4, Man-made radio noise. Recommendations and reports of the CCIR, 1986. XVIth Plenary Assembly Dubrovnik, 1986, Vol VI Propagation in ionized media.

100 Loberg L and Larsen M, MOBITEX - the new Swedish cellular mobile radio service, 4th International Conference on Radio Receivers and Associated Systems, 1-4 July 1986, University of Bangor, Wales, IERE Conference Publication No 68, pp 77-82.

101 Odmalm C, The development of the Nordic mobile telephone system NMT. Seminar on Land Mobile Services, Beijing, Peoples Republic of China, 17-23 November 1986, pp 385-398.

102 De Buda R, Coherent demodulation of frequency-shift keying with low deviation ratio, IEEE Transactions on Communications, Vol Com-20. June 1972, pp 429-435.

103 Pasupathy S, Minimum shift keying: a spectrally efficient modulation. IEEE Communications Magazine, July 1979, pp 14-22.

104 Suzuki H, Yamao Y and Kikuchi H, A single-chip MSK coherent demodulator for mobile radio transmission. IEEE Transactions on Vehicular Technology, Vol VT-34, No 4, November 1985, pp 157-168.

105 Yokoyama M, BPSK system with sounder to combat Rayleigh fading in mobile radio communication. IEEE Transactions on Vehicular Technology, Vol VT-34, No 1, February 1985, pp 35-40.

106 Davarian F, Comments on "BPSK system with sounder to combat Rayleigh fading in mobile radio communication". IEEE Transactions on Vehicular Technology, Vol VT-34, No 4, November 1985, pp 154-156.

107 Anderson R R, Differential detection of binary FM. Bell System Technical Journal, Vol 44, January 1965, pp 111-159.

108   Gotoh K, Yamamura T, Saito T, Itoh A and Shirato T, A single-chip 1200 bps MSK modem for multi channel access. Proceedings of IEEE Custom Integrated Circuits Conference , Rochester, New York, USA, 21-23 May 1984, pp 255-259.

109 Lucky R W, Salz J and Weldon E J, Principles of data communication. McGraw Hill, New York, Chapter 8.

110 Schilling D L, Hoffman E and Nelson E A, Error rates for digital signals demodulated by an FM discriminator. IEEE Transactions on Communication Technology, Vol COM-15, No 4, August 1967, pp 507-517.

111   Kobayashi H, A survey of coding schemes for transmission or recording of digital data.   IEEE Transactions on Communication Technology, Vol COM-19, No 6, December 1971, pp 1087-1100.

112   Buchner J B, Ternary line codes. Philips Telecommunications Review, Vol 34, No 2, June 1976, pp 72-86.

113   Kaspersen S, A mobile data network for the Oslow area. IERE Third International Conference on Land Mobile Radio, Cambridge, England, December 1985, IEE Conference

Publication No 65, pp 77-82.

114   Maddison M S, The application of packet techniques
for spectrum efficient data networking by radio. IEE
Colloquium on Modems for Radio Communication. Digest
1986/67, pp 8/1-8/4.

115   MPT1301 Performance Specification. Angle modulated
VHF and UHF radio equipment for use at base and mobile
stations in the private mobile radio service. Department
of Trade and Industry Radio Regulatory Division, June
1983.

116   Edwards J R, A comparison of modulation schemes for
binary data transmission. The Radio and Electronic
Engineer, Vol 43, No 9, September 1973, pp 562-568.